MICRORNAS AND TYPE I INTERFERON ARE CRITICAL IMMUNE MODULATORS IN LYME ARTHRITIS

by

Robert Bruce Lochhead, Jr.

A dissertation submitted to the faculty of
The University of Utah
in partial fulfillment of the requirements for the degree of

Doctor of Philosophy

in

Microbiology and Immunology

Department of Pathology

The University of Utah

August 2014

The University of Utah Graduate School

STATEMENT OF DISSERTATION APPROVAL

The following faculty members served as the supervisory committee chair and members for the dissertation of **Robert Bruce Lochhead, Jr.**

Dates at right indicate the members' approval of the dissertation.

Janis J. Weis, Chair	5/7/2014	Date Approved
Brenda Bass, Member	5/7/2014	Date Approved
Robert Fujinami, Member	5/7/2014	Date Approved
Matthew Mulvey, Member	5/7/2014	Date Approved
Ryan O'Connell, Member	5/7/2014	Date Approved
Dean Tantin, Member	5/7/2014	Date Approved

The dissertation has also been approved by **Peter E. Jensen**, Chair of the Department/School/College of **Pathology**, and by David B. Kieda, Dean of The Graduate School.

ABSTRACT

Lyme arthritis is the result of dysregulated immune response to infection by *Borrelia burgdorferi,* a tick-borne spirochete. Several immune modulators have been shown to be important to host defense and Lyme arthritis susceptibility, including toll-like receptor signaling, NF-κB activation, and various cytokines and chemokines, including type I IFN. Here we show that type I IFN and microRNAs play critical roles in modulating Lyme arthritis development.

C3H mice exhibit an early, preclinical upregulation of type I IFN-responsive genes, which is associated with increased arthritis severity. Using C3H IFNAR$^{-/-}$ knockout mice, we showed that C3H mice lacking type I IFN signaling have a partial reduction in arthritis severity. Radiation chimeras showed that IFN signaling in both radiation sensitive and radiation resistant cells within the joint are required for maximal arthritis. *Ex vivo* cell sorting of cells isolated from joint tissue also showed that hematopoietic cells were the only cell types capable of initiating a type I IFN response after stimulation with *B. burgdorferi,* but both hematopoietic and resident cells were involved in amplification of the type I IFN response. Endothelial cells and fibroblasts were also major producers of IFN-responsive genes and inflammatory cytokines.

MicroRNAs have been shown to be important immune regulators, and have been associated with several inflammatory diseases, including rheumatoid arthritis and lupus. Here we show that several microRNAs were differentially expressed in B6, C3H, and B6

IL10$^{-/-}$ mice infected with *B. burgdorferi.* MicroRNA-146a, a repressor of TLR signaling and NF-κB activation, was upregulated in all three strains, suggesting it plays an important role in the immune response to infection. B6 miR-146a$^{-/-}$ mice infected with *B. burgdorferi* developed more severe arthritis, had elevated myeloid infiltration, upregulation of inflammatory cytokines, and had fewer numbers of bacteria in joint tissue at 4 weeks postinfection, indicating that miR-146a-mediated regulation of NF-κB activation modulated immune response and arthritis development. Similar patterns of dysregulation were observed in B6 miR-146a$^{-/-}$ macrophages, which produced excessive cytokines, exhibited increased phagocytosis, and had elevated protein levels of TRAF6. Together, these data show that miR-146a is a critical regulator of NF-κB activation and arthritis development during infection with *B. burgdorferi.*

To Colleen, my rock

TABLE OF CONTENTS

LIST OF FIGURES

Figure

LIST OF TABLES

Table

ACKNOWLEDGEMENTS

Many individuals contributed to this thesis, and this work would not have been possible without their help. First and foremost, I would like to thank Dr. Janis Weis, my mentor, who is a paragon of scientific mentorship. Her passion for the research, keen intellect, wise counsel, undying patience, and dedication to her role as mentor have been central to my success these four years. I am grateful for her guidance and friendship, and hope to emulate her in my future career as a mentor.

I would also like to thank the members of my thesis advisory committee, Drs. Brenda Bass, Robert Fujinami, Matthew Mulvey, Ryan O'Connell, and Dean Tantin, for their guidance, suggestions, and encouragement during my graduate career. Ryan O'Connell, in particular, was key to my success. Not only did he provide essential advice and guidance, he also took me under his wing and treated me almost as if I were one of his own graduate students, and inspired me to continue to pursue a career in academic research. John Weis and his lab members were like a second thesis committee, and helped me polish my talks and were great people to bounce ideas off of during lab meetings.

The current and former members of the Weis lab were instrumental in my research. My bay fellow and companion KC Bramwell has been an example of determination and fortitude, and was a calming force in my sometimes-hectic world. Lynn Sonderegger taught me everything I know about immunology, IL-10, flow cytometry, and Led

Zeppelin. Ying Ma, the “secret weapon” of the Weis lab, had her hands on every phase of this research. I wish to particularly acknowledge her assistance on the dozens of mouse infection experiments and the K/BxN arthritis experiment. Lab technicians and undergraduate students made life so much easier in the lab. Jake Thompson, in particular, was of great assistance with the IL-10 mouse work, and came in every day for 3 weeks to give mice antibiotics. One of the most rewarding parts of my graduate career was mentoring other students, including undergraduate Hector Zumeta; visiting scholar Lu Dalla Rosa, who did much of the DKO and IL-10 work; and rotation students Marah Hoel, Sarah Saffran, Jackie Paquette, and Sarah Whiteside, who helped with various aspects of my microRNA work. I’d also like to acknowledge former work done by Mark Wooten, Devin Bolz, Jennifer Miller, Hillary Crandall, Lynn Sonderegger, and others, which provided a scientific foundation upon which my research was built; and Jackie Paquette and Sarah Whiteside, to whom I now pass the torch.

I would like to thank the Microbial Biology graduate program, Dr. Sandy Parkinson, and members of the Dale lab, during the first years of my graduate career; and the Microbial Pathogenesis Training Grant for financial support during the last years of my graduate career.

Finally, I’d like to thank my two daughters, Meri and Lily, and my beloved wife, Colleen, for their love and support.

CHAPTER 1

INTRODUCTION

Lyme Borreliosis

Lyme borreliosis, or Lyme disease, is an inflammatory disorder caused by infection of tick-borne spirochetes belonging to the genus *Borrelia* [1]. In Europe, most cases are caused by infection with *Borrelia garinii* and *Borrelia afzelii*, while *Borrelia burgdorferi* is the principal cause of Lyme borreliosis in North America [2]. The first documented case of infection with *B. burgdorferi* was in a 5,300 year-old ice mummy discovered in the Italian Alps [3]. Today, Lyme borreliosis is endemic to temperate regions in the northern hemisphere containing infected *Ixodes* ticks, the arthropod vector of *Borrelia spp.,* which in the United States includes the Pacific north-west, upper mid-west and the Atlantic seaboard from Maine to Virginia [4,5].

Lyme borreliosis is the most common vector-borne disease in the United States, with an estimated 300,000 cases per year [6]. Lyme disease was first identified because of an unusually high incidence of juvenile idiopathic arthritis that occurred in Lyme, Connecticut [7]. It was later discovered by Burgdorfer et al., that this disease was in fact caused by a spirochete infection transmitted through the deer tick *Ixodes scapularis* [1]. Since its identification, the geographic endemic area and number of cases has steadily increased [4]. This is believed to be due to a number of factors, including reforestation [8] and expansion of deer and host populations [9], part of which may be contributed to climate change [10].

Lyme disease in humans occurs in three stages [2]. The first, early localized disease, occurs days or weeks following exposure to the pathogen and is often characterized by a bulls-eye rash, or erythema migrans, that spreads from the site of a tick bite. The second stage, early-disseminated disease, occurs weeks to months after

infection when spirochetes spread from the transmission site to distal sites of infection. Symptoms include neuropathy, facial palsy, episodes of acute arthritis, and carditis. Although rare, Lyme carditis has been implied as the cause of several deaths [11]. The third stage, late-disseminated disease, occurs months to years after infection, and may result in persistent or recurrent Lyme arthritis, as well as neurologic Lyme disease.

Lyme disease is usually resolved with effective antibiotic treatment, although symptoms may persist for months or years following successful treatment [12]. Persistence of symptoms following successful treatment remains enigmatic and several hypotheses have been proposed to explain this phenomenon. One is that bacterial antigens remain, even after antibiotic treatment [13]. Another is that the immune response to infection is unable to fully resolve after treatment [12]. A third is that low numbers of spirochetes persist, even after antibiotic treatment [14,15]. This posttreatment Lyme disease syndrome, sometimes called "chronic Lyme disease," remains controversial both within the medical community and within the public at large [16,17]. Long-term antibiotic treatment of chronic Lyme disease syndrome patients continues to be administered by some medical professionals, despite NIH studies showing no therapeutic benefit over placebo controls [18].

Biology of *Borrelia burgdorferi*

Borrelia burgdorferi is an obligate anaerobe and, like other spirochetes, is characterized by their unique spiral morphology and planar wave motility, due to the flagella being within the periplasm [19]. *B. burgdorferi* is also unique in its genomic architecture. Its genome consists of an AT-rich 1 Mbp linear chromosome and at least 17 linear and circular plasmids [20-22]. This genome architecture is one of the most

complex of all bacteria, and may play an important role in diversification of vector and host specificity [23], as well as virulence [24]. This genome lacks many genes essential for metabolism of fatty acids, amino acids, and nucleotides, nutrients which are acquired from their host [25]. Interestingly, *B. burgdorferi* is one of only a few organisms that does not require iron, an adaptation believed to be in response to the unavailability of accessible iron within their hosts and evasion of innate defense mechanisms [26].

The reproductive cycle of *B. burgdorferi* involves transmission between their two hosts, ticks and small vertebrates such as mice and birds [27]. Larval and nymphal ticks become infected as they take a blood meal from an infected small vertebrate [5], and infected ticks remain infectious during molting [28]. Reservoir hosts include *Paromyscus* spp. mice, birds, and squirrels, which remain infectious until the next cycle of tick feeding [5]. White-tailed deer are also infected by feeding adult ticks, but are not part of the transmission cycle. Nevertheless, deer are important hosts for tick ecology, and expansion of deer populations in endemic regions is linked to the spread of Lyme disease [8].

Transmission from ticks to mammals occurs via tick salivary glands during a blood meal [29]. Replicating, nonmotile spirochetes remain in the mid-gut of ticks until the tick takes a blood meal. *B. burgdorferi* then become motile and move into salivary glands, enabling transmission to a new host [30]. As spirochetes move from tick to mammal host, a temperature-sensitive transcriptional change in genes encoding for surface proteins, among others, is required for successful transmission and continuation of the enzootic cycle [31,32]. Humans are incidental hosts, and are infected by both nymphal and adult ticks [33]. In addition to humans, domesticated animals, such as dogs and horses, are also

susceptible to infection and disease [34].

B. burgdorferi is not transmitted vertically from mother to egg; therefore it must persist within their hosts for many months until the next transmission cycle begins [35]. *Borrelia* contain many genes encoding for a large number of surface lipoproteins and adhesins, many of which are required for transmission and evasion of host immune response [36]. Furthermore, these bacteria are capable of varying antigenic regions of surface proteins through homologous recombination [37], inactivating complement [38], and downregulating target antigens [39], thus evading the host response.

Host Defense

While *B. burgdorferi* are able to persistently infect immunocompetent mice for at least a year [40], innate and adaptive immune responses are required for proper control of infection and spirochetemia [41,42]. Early in infection, numerous cells of the innate immune system are involved in host response, including endothelial cells [43], neutrophils [44], macrophages [45], and NK cells [46]. Toll-like receptors (TLRs) recognize and respond to pathogen-associated molecular patterns (PAMPs), and are critical for host defense, and mice lacking key TLR proteins have 10-100-fold higher bacterial numbers in joint, skin, and heart tissue [47-50]. The role of Toll-like receptors in Lyme arthritis is discussed in more detail below. Nod-like receptors are also involved in recognition of *B. burgdorferi,* although their roles in host defense are less clear [51,52].

B cell response to infection is critical in management of infections, and both T-cell-dependent and T-cell-independent antibody production are important in host defense [41,53]. Nevertheless, bacterial-mediated modulation of the B cell response is believed to

impair antibody production and kinetics, highlighted by a lack of germinal center formation, which may be important for persistence [54]. Interestingly, *B. burgdorferi* can be detected inside lymph nodes, causing lymphadenopathy associated with Lyme borreliosis [55]. How the presence of bacteria within lymph nodes affects antibody production and host response is unknown, although the strong B-cell mitogenic activity of *B. burgdorferi* likely plays a role [56].

Lyme Arthritis

Lyme arthritis is one of the most common manifestations of Lyme disease, and has been reported in as many as 60% of untreated individuals [57]. Lyme arthritis is characterized by edema, synovial hyperplasia, neutrophil infiltration, and swelling, and arthritis severity varies among individuals, from chronic persistent arthritis to episodic acute arthritis to mild joint pain [57]. Arthritis is self-limiting, and is usually resolved upon successful antibiotic treatment [58]. In approximately 10% of cases, however, symptoms fail to fully resolve [58], which can develop into autoimmunity [59].

Manifestations of disease vary greatly amongst individuals both in terms of symptoms and severity, suggesting host genetic factors play a role in disease severity. Rheumatoid arthritis-associated HLA alleles (DRB1*0401, *0101, and *0404) have been linked to susceptibility to treatment-refractory Lyme arthritis [60] and production of anti-endothelial cell growth factor (ECGF) autoantibodies [59]. Variations in abundance and activity of regulatory T cells have also been associated with disease severity [61]. A recently identified polymorphism in Toll-like receptor 1 has been linked with excessive cytokine and chemokine production, although the functional relevance of this polymorphism is unknown [62].

Differences in pathogenicity and arthritis severity have also been linked to certain clinical isolates [63]. These isolates can either be disseminating (RST1) or non-disseminating (RST2 and RST3) strains [64]. One group of isolates, in particular (RST1, OspC type A), has been linked with more severe arthritis [24]. Furthermore, individuals infected with this strain were more likely to develop treatment-refractory arthritis, and exhibited a pronounced Th1 response in synovial tissue [65]. There is evidence to suggest that HLA haplotype influences bacterial strain-specific susceptibility [66], although it is unknown how this influences infectivity and disease severity.

Mouse Models of Lyme Disease

Since mice are natural hosts for *B. burgdorferi*, the mouse model is an excellent system to study disease pathogenesis. While wild strains of mice are asymptomatic upon infection, inbred mouse strains exhibit a spectrum of disease severity for a given spirochete burden, implicating genetic factors involving host response to infection playing an important role in pathogenesis [67,68]. For example, C57BL/6 mice develop mild arthritis and show little evidence of carditis, whereas C3H mice develop severe arthritis, despite having similar bacterial numbers in joint tissue; and have higher numbers of spirochetes in heart tissue and are susceptible to Lyme carditis [67].

Lyme arthritis in mice develops 2-4 weeks following infection with *B. burgdorferi,* and is characterized by edema, inflammatory lesions in joint tissue, remodeling of bone and cartilage tissue, inflammatory cell infiltration, and synovial hyperplasia [69]. These symptoms are also observed in human patients, who exhibit a wide range of disease severity, suggesting that murine Lyme arthritis faithfully recapitulates elements of human Lyme disease [12]. Several mouse strains are also susceptible to Lyme carditis in a strain-

specific manner [70], but unlike humans and nonhuman primates, do not develop erythema migrans or neuroborreliosis [71].

Because the mouse model is genetically tractable, several genetic approaches have been used to study Lyme arthritis in mice. Forward genetics has been utilized to identify arthritis-susceptibility genomic loci in the murine model of Lyme arthritis [72]. Congenic mouse lines containing arthritis-associated quantitative trait genetic loci were developed which led to the discovery of a novel arthritis susceptibility gene, *Gusb* [73], involved in lysosomal degradation of complex carbohydrates. Interestingly, this *Gusb* polymorphism also influenced arthritis severity in the K/BxN serum transfer model of rheumatoid arthritis, suggesting that host factors influencing Lyme arthritis severity may also influence other inflammatory diseases.

Reverse genetic approaches have also been used to identify immune genes that impact disease severity, such as interleukin-10 [74,75] and Cxcl1 [76], as well as host defense, such as toll-like receptor 2 (TLR2) [48] and myeloid differentiation factor 88 (MyD88) [47]. Other knockout studies have examined the role of dozens of immune genes and their role in a variety of immunological processes [77]. This approach has also been utilized to identify cell types that are involved in exacerbation of disease severity, such as neutrophils [78], and cell types that are not required for arthritis development, such as T and B cells [79].

A third genetic approach has been used recently taking advantage of genetic screen tools. This enables simultaneously examining a very large number of genes in an unbiased manner. This approach was used to identify a previously unrecognized preclinical interferon profile associated with arthritis susceptibility [80]. Subsequent

experiments showed that dysregulation of type I interferon exacerbated disease severity [81]. The role of type I interferon in Lyme arthritis is discussed further below and is the subject of Chapter 2. A genetic screen approach was also used to identify microRNAs associated with Lyme arthritis severity, and is the subject of Chapter 3.

Toll-like Receptors in Lyme Arthritis

Toll-like receptors recognize and respond to a number of pathogen molecular products, such as lipopolysaccharide, nucleic acid, and lipoproteins [82]. Recognition of *B. burgdorferi* lipoproteins by TLR2 is an important mechanism of host response to infection [49,83,84], and is a key element of the innate immune response [42]. TLRs signaling is divided into two pathways; the first dependent on the adaptor protein MyD88 which leads to NF-κB and MAP kinase activation, and the second TRIF-dependent, leading to upregulation of type I interferon [82]. Signaling through TLRs leads to transcriptional upregulation or downregulation of thousands of genes through activation of several transcription factor families, including IRF3/IRF7, which upregulate type I interferon [85], and NF-κB family of transcription factors, which regulate many cellular functions, including inflammation, host defense, leukocyte function, and hematopoiesis [86].

The importance of TLR signaling in clinical Lyme arthritis was validated in a recent patient study, which identified a polymorphism in TLR1 associated with a heightened Th1 response and increased Lyme arthritis severity [62]. TLR1/TLR2 heterodimers have been shown to be important in *B. burgdorferi* recognition [87] and host immune response [88]. It is unknown what effect this polymorphism has on TLR signaling, but two hypotheses are that either it amplifies the immune response, leading to

elevated inflammation and arthritis, or it impairs host defense, resulting in greater numbers of bacteria and increased arthritis severity.

Type I Interferon in Lyme Arthritis

Type I interferons (IFNs) are a family of proinflammatory cytokines important for host defense through activation of an antimicrobial state in a cell-intrinsic and cell-extrinsic manner, and is critical in protection against viral pathogens [89]. Dysregulation of type I IFNs are also associated with increased disease severity. In certain bacterial infections, induction of type I IFN can lead to impaired host defense, in part through suppression of pathways important for bactericidal function, including IFN-γ signaling [90]. In addition, type I IFN-based therapy is associated with development of autoimmunity [91]. A hallmark feature of systemic lupus erythematosus (SLE) is constitutive type I IFN production by plasmacytoid dendritic cells, leading to immune activation and autoantibody production [92].

As mentioned earlier, the role of type I IFN in Lyme arthritis development was first identified through microarray expression analysis [80]. Subsequent research by Miller et al. showed that abrogation of this IFN signature at 1 week postinfection led to a partial decrease in Lyme arthritis severity at 4 weeks postinfection [81]. TLRs, especially those that recognize nucleic acids, are important activators of type I IFN [82], and *B. burgdorferi* RNA has been shown to initiate a type I IFN response [93]. TLR2, traditionally associated with MyD88-dependent signaling, is also able to activate type I IFN upon *B. burgdorferi* stimulation in a TRIF-dependent manner [94]. In addition to TLRs, NOD2, an intracellular pattern recognition receptor, is also capable of inducing a type I IFN signature in response to *B. burgdorferi* [95]. Further elucidation into joint cell

types associated with induction and amplification of the arthritogenic type I IFN response is the subject of Chapter 2.

NF-κB Activation in Lyme Arthritis

Infection with *B. burgdorferi* leads to TLR-mediated NF-κB activation [43], and has been shown to play a critical role in host defense during *B. burgdorferi* infection, since mice lacking CD14, TLR2, or the adapter protein MyD88 are unable to control infection [48,96,97]. Not surprisingly, these mice also develop severe arthritis, probably due to the very high bacterial burden in joint tissue.

While NF-κB activation is essential in controlling infection, downregulation and return to homeostasis is also important in order to prevent persistent inflammation, tissue damage, and autoimmunity [98]. Failure to downregulate NF-κB-activated cytokines can lead to increased Lyme arthritis severity and development of treatment-refractory arthritis [62,99]. This failure to down-modulate NF-κB is also observed in synovial cells and peripheral blood mononuclear cells from patients with other inflammatory disorders, such as rheumatoid arthritis and lupus [100]. While evidence suggests that proper regulation of TLR/NF-κB signaling is important in limiting Lyme arthritis development in both mice and humans, decoupling its role in host defense from arthritis development has remained difficult.

Many CXC chemokines are regulated by NF-κB, and influence inflammation and host defense through recruitment of neutrophils (CXCL1, CXCL2), T cells (CXCL9, CXCL10), and B cells (CXCL12, CXCL13) [101]. Neutrophil chemokines, particularly CXCL1, are important for arthritis development [76]. CXCL1 is tightly regulated at the transcriptional and posttranscriptional level [102]; TLR, IL-1, or TNFα stimulation

results in Cxcl1 upregulation, which is dependent on two NF-κB binding sites [103], and is further regulated by the presence of multiple 3' UTR AU-rich elements [104].

In addition to arthritis, TLR signaling also plays an important role in neuroborreliosis in humans and nonhuman primates [105]. In humans, elevated levels of IL-6 and CXCL13 in serum and cerebral spinal fluid correlate with active neuroborreliosis [106], and elevated levels of IL-6 and IL-1β are speculated to be associated with neuropsychiatric symptoms observed in some patients [107]. Furthermore, failure to upregulate TNFα in nervous tissue early in infection is correlated with development of chronic Lyme neuroborreliosis, suggesting that this cytokine is important for early elimination of bacteria [108]. Although mice do not develop neuroborreliosis, studying the role of TLR/NF-κB signaling in murine Lyme arthritis may shed light on mechanisms of other clinical manifestations of Lyme disease. Because of the central role of TLR signaling in host defense and disease pathogenesis, understanding TLR regulation is critical in elucidating mechanisms of arthritis and inflammation.

MicroRNAs in TLR Signaling and Autoimmunity

MicroRNAs are small, noncoding regulators of translation [109]. Since their discovery, microRNAs have been shown to play important roles in many biological processes, including immune response and inflammation and autoimmunity [110,111]. MicroRNAs act as translational inhibitors by recognizing and binding to 3' UTR of target mRNAs [112]. Over 1,000 microRNAs have been identified in humans and mice, and many microRNAs are capable of targeting many different genes [109]. Because of this, it is believed that as many protein-coding genes are regulated by microRNAs [113,114].

A number of microRNAs are upregulated by TLR/NF-κB activation, including the

anti-inflammatory microRNA miR-146a and the proinflammatory microRNA miR-155 [115]. These microRNAs are important in providing feedback regulation of NF-κB signaling, and are required for maintaining immune homeostasis [115]. Because NF-κB is a key node in many cellular responses, these microRNAs have been shown to modulate a number of inflammatory responses [116].

Several microRNAs are differentially expressed in rheumatoid arthritis (RA) synovial tissue, including miR-146a and miR-155 [117,118]. Overexpression of miR-146a in RA patients is highly correlated with elevated levels of the arthritogenic cytokine TNFα and disease severity [119,120], although it is not known whether this is a marker of sustained inflammation or points to functional inability of miR-146a to modulate the inflammatory response. In support of the latter, a polymorphism in the 3'-UTR of IRAK1, a target of miR-146a [121], was identified to be positively associated with RA susceptibility. In a mouse study, addition of exogenous miR-146a was able to partially reduce pathology in the mouse collagen induced arthritis model [122]. Mouse studies have also shown that absence of miR-155 was able to reduce arthritis severity in both collagen-induced arthritis and K/BxN serum transfer arthritis, two models for RA [123]. Similarly, microRNA-182 was shown to be an important regulator of T cell clonal expansion in the ovalbumin-induced model of RA [124].

MicroRNAs miR-146a and miR-155 have also been associated with systemic lupus erythematosus (SLE) [125,126]. Unlike in RA, there appears to be an inverse relationship between miR-146a expression and the type I IFN signature, a marker for increased disease severity [127]. Furthermore, polymorphisms within the promoter region of miR-146a are associated with susceptibility to SLE [128,129]. In mice, several microRNAs,

including miR-155, share similar expression patterns in different lupus models [130].

MicroRNAs are also required for regulation of other inflammatory and autoimmune diseases [131]. For example, miR-155 expression is an important component of experimental autoimmune encephalitis (EAE), a mouse model for multiple sclerosis [132], through miR-155-dependent regulation of Th17 cell activation [133]. Conversely, microRNA-124 is a suppressor of EAE severity through its function in macrophages [134]. In the NOD mouse model of type 1 diabetes, miR-21, another TLR-induced microRNA, is an important modulator of pancreatic beta cell death through suppression of the proapoptotic gene *Pdcd4* [135].

The studies and findings, both in humans and in mouse models, strongly support the notion that microRNAs are important regulators of inflammation and autoimmunity. However, no studies have been done examining the role of microRNAs in regulating Lyme arthritis. Chapter 3 of this dissertation examines microRNA expression in Lyme arthritis and discusses how miR-146a modulates arthritis severity.

Preview of Thesis Research

The focus of this dissertation is examining the roles of type I interferon and microRNAs in modulating Lyme arthritis severity. Chapter 2 builds on previous studies by Crandall et al. and Miller et al., showing the importance of type I interferon in arthritis development in the C3H mouse model of Lyme disease [80,81]. This study focuses on cellular sources of arthritogenic type I interferon response, as well as cell types involved in initiation of this response.

Chapter 3 contains the results of a study researching the role of microRNAs in Lyme arthritis development. This study focuses on one microRNA, miR-146a, and its

critical role as a suppressor of inflammation and arthritis. MicroRNA-146a was identified in a microRNA microarray screen as being highly induced during infection with *B. burgdorferi.*

Included in Appendix A are data from another microRNA identified in the microarray, miR-155. This microRNA was uniquely upregulated in the B6 $IL10^{-/-}$ mouse model of Lyme arthritis, and its upregulation is consistent with a previous report showing that IL-10 is a negative regulator of miR-155 [136]. Also included (Appendix B) are results on the role of IL-10 in regulating persistent Lyme arthritis development and T cell activation, an extension of previous work performed by Sonderegger et al. [75]. Appendix C includes results showing that miR-146a also influences the K/BxN serum transfer model of rheumatoid arthritis.

References

1. Burgdorfer W, Barbour AG, Hayes SF, Benach JL, Grunwaldt E, et al. (1982) Lyme disease-a tick-borne spirochetosis? Science 216: 1317-1319.

2. Steere AC, Coburn J, Glickstein L (2004) The emergence of Lyme disease. J Clin Invest 113: 1093-1101.

3. Keller A, Graefen A, Ball M, Matzas M, Boisguerin V, et al. (2012) New insights into the Tyrolean Iceman's origin and phenotype as inferred by whole-genome sequencing. Nat Commun 3: 698.

4. Bacon RM, Kugeler KJ, Mead PS, Centers for Disease C, Prevention (2008) Surveillance for Lyme disease--United States, 1992-2006. MMWR Surveill Summ 57: 1-9.

5. Kurtenbach K, Hanincova K, Tsao JI, Margos G, Fish D, et al. (2006) Fundamental processes in the evolutionary ecology of Lyme borreliosis. Nat Rev Microbiol 4: 660-669.

6. Kuehn BM (2013) CDC estimates 300,000 US cases of Lyme disease annually. JAMA 310: 1110.

7. Steere AC, Malawista SE, Snydman DR, Shope RE, Andiman WA, et al. (1977) Lyme arthritis: an epidemic of oligoarticular arthritis in children and adults in three connecticut communities. Arthritis Rheum 20: 7-17.

8. Barbour AG, Fish D (1993) The biological and social phenomenon of Lyme disease. Science 260: 1610-1616.

9. Levi T, Kilpatrick AM, Mangel M, Wilmers CC (2012) Deer, predators, and the emergence of Lyme disease. Proc Natl Acad Sci U S A 109: 10942-10947.

10. Ogden NH, Mechai S, Margos G (2013) Changing geographic ranges of ticks and tick-borne pathogens: drivers, mechanisms and consequences for pathogen diversity. Front Cell Infect Microbiol 3: 46.

11. Centers for Disease C, Prevention (2013) Three sudden cardiac deaths associated with Lyme carditis - United States, November 2012-July 2013. MMWR Morb Mortal Wkly Rep 62: 993-996.

12. Steere AC, Schoen RT, Taylor E (1987) The clinical evolution of Lyme arthritis. Ann Intern Med 107: 725-731.

13. Bockenstedt LK, Gonzalez DG, Haberman AM, Belperron AA (2012) Spirochete antigens persist near cartilage after murine Lyme borreliosis therapy. J Clin Invest 122: 2652-2660.

14. Embers ME, Barthold SW, Borda JT, Bowers L, Doyle L, et al. (2012) Persistence of Borrelia burgdorferi in rhesus macaques following antibiotic treatment of disseminated infection. PLoS One 7: e29914.

15. Hodzic E, Feng S, Holden K, Freet KJ, Barthold SW (2008) Persistence of Borrelia burgdorferi following antibiotic treatment in mice. Antimicrob Agents Chemother 52: 1728-1736.

16. Halperin JJ, Baker P, Wormser GP (2013) Common misconceptions about Lyme disease. Am J Med 126: 264 e261-267.

17. Stricker RB, Johnson L (2013) Chronic Lyme disease: liberation from Lyme denialism. Am J Med 126: e13-14.

18. Klempner MS, Baker PJ, Shapiro ED, Marques A, Dattwyler RJ, et al. (2013) Treatment trials for post-Lyme disease symptoms revisited. Am J Med 126: 665-669.

19. Charon NW, Goldstein SF, Marko M, Hsieh C, Gebhardt LL, et al. (2009) The flat-ribbon configuration of the periplasmic flagella of Borrelia burgdorferi and its relationship to motility and morphology. J Bacteriol 191: 600-607.

20. Casjens S, Huang WM (1993) Linear chromosomal physical and genetic map of Borrelia burgdorferi, the Lyme disease agent. Mol Microbiol 8: 967-980.

21. Fraser CM, Casjens S, Huang WM, Sutton GG, Clayton R, et al. (1997) Genomic sequence of a Lyme disease spirochaete, Borrelia burgdorferi. Nature 390: 580-586.

22. Casjens S, Palmer N, van Vugt R, Huang WM, Stevenson B, et al. (2000) A bacterial genome in flux: the twelve linear and nine circular extrachromosomal DNAs in an infectious isolate of the Lyme disease spirochete Borrelia burgdorferi. Mol Microbiol 35: 490-516.

23. Qiu WG, Martin CL (2014) Evolutionary genomics of Borrelia burgdorferi sensu lato: Findings, hypotheses, and the rise of hybrids. Infect Genet Evol.

24. Strle K, Jones KL, Drouin EE, Li X, Steere AC (2011) Borrelia burgdorferi RST1 (OspC type A) genotype is associated with greater inflammation and more severe Lyme disease. Am J Pathol 178: 2726-2739.

25. Casjens S (2000) Borrelia genomes in the year 2000. J Mol Microbiol Biotechnol 2: 401-410.

26. Posey JE, Gherardini FC (2000) Lack of a role for iron in the Lyme disease pathogen. Science 288: 1651-1653.

27. Tilly K, Rosa PA, Stewart PE (2008) Biology of infection with Borrelia burgdorferi. Infect Dis Clin North Am 22: 217-234, v.

28. Mather TN, Mather ME (1990) Intrinsic competence of three ixodid ticks (Acari) as vectors of the Lyme disease spirochete. J Med Entomol 27: 646-650.

29. Ribeiro JM, Mather TN, Piesman J, Spielman A (1987) Dissemination and salivary delivery of Lyme disease spirochetes in vector ticks (Acari: Ixodidae). J Med Entomol 24: 201-205.

30. Dunham-Ems SM, Caimano MJ, Pal U, Wolgemuth CW, Eggers CH, et al. (2009) Live imaging reveals a biphasic mode of dissemination of Borrelia burgdorferi within ticks. J Clin Invest 119: 3652-3665.

31. Schwan TG, Piesman J, Golde WT, Dolan MC, Rosa PA (1995) Induction of an outer surface protein on Borrelia burgdorferi during tick feeding. Proc Natl Acad Sci U S A 92: 2909-2913.

32. Revel AT, Talaat AM, Norgard MV (2002) DNA microarray analysis of differential gene expression in Borrelia burgdorferi, the Lyme disease spirochete. Proc Natl Acad Sci U S A 99: 1562-1567.

33. Piesman J, Mather TN, Sinsky RJ, Spielman A (1987) Duration of tick attachment and Borrelia burgdorferi transmission. J Clin Microbiol 25: 557-558.

34. Wagner B, Erb HN (2012) Dogs and horses with antibodies to outer-surface protein C as on-time sentinels for ticks infected with Borrelia burgdorferi in New York State in 2011. Prev Vet Med 107: 275-279.

35. Radolf JD, Caimano MJ, Stevenson B, Hu LT (2012) Of ticks, mice and men: understanding the dual-host lifestyle of Lyme disease spirochaetes. Nat Rev Microbiol 10: 87-99.

36. Coburn J, Leong J, Chaconas G (2013) Illuminating the roles of the Borrelia burgdorferi adhesins. Trends Microbiol 21: 372-379.

37. Wilske B, Barbour AG, Bergstrom S, Burman N, Restrepo BI, et al. (1992) Antigenic variation and strain heterogeneity in Borrelia spp. Res Microbiol 143: 583-596.

38. Hellwage J, Meri T, Heikkila T, Alitalo A, Panelius J, et al. (2001) The complement regulator factor H binds to the surface protein OspE of Borrelia burgdorferi. J Biol Chem 276: 8427-8435.

39. Schwan TG, Piesman J (2000) Temporal changes in outer surface proteins A and C of the lyme disease-associated spirochete, Borrelia burgdorferi, during the chain of infection in ticks and mice. J Clin Microbiol 38: 382-388.

40. Barthold SW, de Souza MS, Janotka JL, Smith AL, Persing DH (1993) Chronic Lyme borreliosis in the laboratory mouse. Am J Pathol 143: 959-971.

41. LaRocca TJ, Benach JL (2008) The important and diverse roles of antibodies in the host response to Borrelia infections. Curr Top Microbiol Immunol 319: 63-103.

42. Berende A, Oosting M, Kullberg BJ, Netea MG, Joosten LA (2010) Activation of innate host defense mechanisms by Borrelia. Eur Cytokine Netw 21: 7-18.

43. Wooten RM, Modur VR, McIntyre TM, Weis JJ (1996) Borrelia burgdorferi outer membrane protein A induces nuclear translocation of nuclear factor-kappa B and inflammatory activation in human endothelial cells. J Immunol 157: 4584-4590.

44. Morrison TB, Weis JH, Weis JJ (1997) Borrelia burgdorferi outer surface protein A (OspA) activates and primes human neutrophils. J Immunol 158: 4838-4845.

45. Montgomery RR, Booth CJ, Wang X, Blaho VA, Malawista SE, et al. (2007) Recruitment of macrophages and polymorphonuclear leukocytes in Lyme carditis. Infect Immun 75: 613-620.

46. Brown CR, Reiner SL (1998) Activation of natural killer cells in arthritis-susceptible but not arthritis-resistant mouse strains following Borrelia burgdorferi infection. Infect Immun 66: 5208-5214.

47. Bolz DD, Sundsbak RS, Ma Y, Akira S, Kirschning CJ, et al. (2004) MyD88 plays a unique role in host defense but not arthritis development in Lyme disease. J Immunol 173: 2003-2010.

48. Wooten RM, Ma Y, Yoder RA, Brown JP, Weis JH, et al. (2002) Toll-like receptor 2 is required for innate, but not acquired, host defense to Borrelia burgdorferi. J Immunol 168: 348-355.

49. Hirschfeld M, Kirschning CJ, Schwandner R, Wesche H, Weis JH, et al. (1999) Cutting edge: inflammatory signaling by Borrelia burgdorferi lipoproteins is mediated by toll-like receptor 2. J Immunol 163: 2382-2386.

50. Hawley KL, Martin-Ruiz I, Iglesias-Pedraz JM, Berwin B, Anguita J (2013) CD14 targets complement receptor 3 to lipid rafts during phagocytosis of Borrelia burgdorferi. Int J Biol Sci 9: 803-810.

51. Chauhan VS, Sterka DG, Jr., Furr SR, Young AB, Marriott I (2009) NOD2 plays an important role in the inflammatory responses of microglia and astrocytes to bacterial CNS pathogens. Glia 57: 414-423.

52. Sterka D, Jr., Rati DM, Marriott I (2006) Functional expression of NOD2, a novel pattern recognition receptor for bacterial motifs, in primary murine astrocytes. Glia 53: 322-330.

53. Belperron AA, Dailey CM, Booth CJ, Bockenstedt LK (2007) Marginal zone B-cell depletion impairs murine host defense against Borrelia burgdorferi infection. Infect Immun 75: 3354-3360.

54. Hastey CJ, Elsner RA, Barthold SW, Baumgarth N (2012) Delays and diversions mark the development of B cell responses to Borrelia burgdorferi infection. J Immunol 188: 5612-5622.

55. Tunev SS, Hastey CJ, Hodzic E, Feng S, Barthold SW, et al. (2011) Lymphoadenopathy during lyme borreliosis is caused by spirochete migration-induced specific B cell activation. PLoS Pathog 7: e1002066.

56. Yang L, Ma Y, Schoenfeld R, Griffiths M, Eichwald E, et al. (1992) Evidence for B-lymphocyte mitogen activity in Borrelia burgdorferi-infected mice. Infect Immun 60: 3033-3041.

57. Steere AC, Glickstein L (2004) Elucidation of Lyme arthritis. Nat Rev Immunol 4: 143-152.

58. Steere AC, Levin RE, Molloy PJ, Kalish RA, Abraham JH, 3rd, et al. (1994) Treatment of Lyme arthritis. Arthritis Rheum 37: 878-888.

59. Drouin EE, Seward RJ, Strle K, McHugh G, Katchar K, et al. (2013) A novel human autoantigen, endothelial cell growth factor, is a target of T and B cell responses in patients with Lyme disease. Arthritis Rheum 65: 186-196.

60. Steere AC, Dwyer E, Winchester R (1990) Association of chronic Lyme arthritis with HLA-DR4 and HLA-DR2 alleles. N Engl J Med 323: 219-223.

61. Vudattu NK, Strle K, Steere AC, Drouin EE (2013) Dysregulation of CD4+CD25(high) T cells in the synovial fluid of patients with antibiotic-refractory Lyme arthritis. Arthritis Rheum 65: 1643-1653.

62. Strle K, Shin JJ, Glickstein LJ, Steere AC (2012) Association of a Toll-like receptor 1 polymorphism with heightened Th1 inflammatory responses and antibiotic-refractory Lyme arthritis. Arthritis Rheum 64: 1497-1507.

63. Wang G, Ojaimi C, Wu H, Saksenberg V, Iyer R, et al. (2002) Disease severity in a murine model of lyme borreliosis is associated with the genotype of the infecting Borrelia burgdorferi sensu stricto strain. J Infect Dis 186: 782-791.

64. Dolan MC, Piesman J, Schneider BS, Schriefer M, Brandt K, et al. (2004) Comparison of disseminated and nondisseminated strains of Borrelia burgdorferi sensu stricto in mice naturally infected by tick bite. Infect Immun 72: 5262-5266.

65. Jones KL, McHugh GA, Glickstein LJ, Steere AC (2009) Analysis of Borrelia burgdorferi genotypes in patients with Lyme arthritis: High frequency of ribosomal RNA intergenic spacer type 1 strains in antibiotic-refractory arthritis. Arthritis Rheum 60: 2174-2182.

66. Wormser GP, Kaslow R, Tang J, Wade K, Liveris D, et al. (2005) Association between human leukocyte antigen class II alleles and genotype of Borrelia burgdorferi in patients with early lyme disease. J Infect Dis 192: 2020-2026.

67. Barthold SW, Beck DS, Hansen GM, Terwilliger GA, Moody KD (1990) Lyme borreliosis in selected strains and ages of laboratory mice. J Infect Dis 162: 133-138.

68. Wright SD, Nielsen SW (1990) Experimental infection of the white-footed mouse with Borrelia burgdorferi. Am J Vet Res 51: 1980-1987.

69. Barthold SW, Persing DH, Armstrong AL, Peeples RA (1991) Kinetics of Borrelia burgdorferi dissemination and evolution of disease after intradermal inoculation of mice. Am J Pathol 139: 263-273.

70. Armstrong AL, Barthold SW, Persing DH, Beck DS (1992) Carditis in Lyme disease susceptible and resistant strains of laboratory mice infected with Borrelia burgdorferi. Am J Trop Med Hyg 47: 249-258.

71. Pachner AR, Gelderblom H, Cadavid D (2001) The rhesus model of Lyme neuroborreliosis. Immunol Rev 183: 186-204.

72. Weis JJ, McCracken BA, Ma Y, Fairbairn D, Roper RJ, et al. (1999) Identification of quantitative trait loci governing arthritis severity and humoral responses in the murine model of Lyme disease. J Immunol 162: 948-956.

73. Bramwell KK, Ma Y, Weis JH, Chen X, Zachary JF, et al. (2014) Lysosomal beta-glucuronidase regulates Lyme and rheumatoid arthritis severity. J Clin Invest 124: 311-320.

74. Brown JP, Zachary JF, Teuscher C, Weis JJ, Wooten RM (1999) Dual role of interleukin-10 in murine Lyme disease: regulation of arthritis severity and host defense. Infect Immun 67: 5142-5150.

75. Sonderegger FL, Ma Y, Maylor-Hagan H, Brewster J, Huang X, et al. (2012) Localized production of IL-10 suppresses early inflammatory cell infiltration and subsequent development of IFN-gamma-mediated Lyme arthritis. J Immunol 188: 1381-1393.

76. Ritzman AM, Hughes-Hanks JM, Blaho VA, Wax LE, Mitchell WJ, et al. (2010) The chemokine receptor CXCR2 ligand KC (CXCL1) mediates neutrophil recruitment and is critical for development of experimental Lyme arthritis and carditis. Infect Immun 78: 4593-4600.

77. Radolf JD, Samuels DS (2010) Borrelia : molecular biology, host interaction, and pathogenesis. Norfolk, UK: Caister Academic Press. xii, 547 p., 544 p. of plates p.

78. Brown CR, Blaho VA, Loiacono CM (2003) Susceptibility to experimental Lyme arthritis correlates with KC and monocyte chemoattractant protein-1 production in joints and requires neutrophil recruitment via CXCR2. J Immunol 171: 893-901.

79. Barthold SW, Sidman CL, Smith AL (1992) Lyme borreliosis in genetically resistant and susceptible mice with severe combined immunodeficiency. Am J Trop Med Hyg 47: 605-613.

80. Crandall H, Dunn DM, Ma Y, Wooten RM, Zachary JF, et al. (2006) Gene expression profiling reveals unique pathways associated with differential severity of lyme arthritis. J Immunol 177: 7930-7942.

81. Miller JC, Ma Y, Bian J, Sheehan KC, Zachary JF, et al. (2008) A critical role for type I IFN in arthritis development following Borrelia burgdorferi infection of mice. J Immunol 181: 8492-8503.

82. Akira S, Takeda K (2004) Toll-like receptor signalling. Nat Rev Immunol 4: 499-511.

83. Aliprantis AO, Yang RB, Mark MR, Suggett S, Devaux B, et al. (1999) Cell activation and apoptosis by bacterial lipoproteins through toll-like receptor-2. Science 285: 736-739.

84. Brightbill HD, Libraty DH, Krutzik SR, Yang RB, Belisle JT, et al. (1999) Host defense mechanisms triggered by microbial lipoproteins through toll-like receptors. Science 285: 732-736.

85. Taniguchi T, Ogasawara K, Takaoka A, Tanaka N (2001) IRF family of transcription factors as regulators of host defense. Annu Rev Immunol 19: 623-655.

86. DiDonato JA, Mercurio F, Karin M (2012) NF-kappaB and the link between inflammation and cancer. Immunol Rev 246: 379-400.

87. Oosting M, Ter Hofstede H, Sturm P, Adema GJ, Kullberg BJ, et al. (2011) TLR1/TLR2 heterodimers play an important role in the recognition of Borrelia spirochetes. PLoS One 6: e25998.

88. Alexopoulou L, Thomas V, Schnare M, Lobet Y, Anguita J, et al. (2002) Hyporesponsiveness to vaccination with Borrelia burgdorferi OspA in humans and in TLR1- and TLR2-deficient mice. Nat Med 8: 878-884.

89. Ivashkiv LB, Donlin LT (2014) Regulation of type I interferon responses. Nat Rev Immunol 14: 36-49.

90. Trinchieri G (2010) Type I interferon: friend or foe? J Exp Med 207: 2053-2063.

91. Biggioggero M, Gabbriellini L, Meroni PL (2010) Type I interferon therapy and its role in autoimmunity. Autoimmunity 43: 248-254.

92. Jego G, Palucka AK, Blanck JP, Chalouni C, Pascual V, et al. (2003) Plasmacytoid dendritic cells induce plasma cell differentiation through type I interferon and interleukin 6. Immunity 19: 225-234.

93. Miller JC, Maylor-Hagen H, Ma Y, Weis JH, Weis JJ (2010) The Lyme disease spirochete Borrelia burgdorferi utilizes multiple ligands, including RNA, for interferon regulatory factor 3-dependent induction of type I interferon-responsive genes. Infect Immun 78: 3144-3153.

94. Petnicki-Ocwieja T, Chung E, Acosta DI, Ramos LT, Shin OS, et al. (2013) TRIF mediates Toll-like receptor 2-dependent inflammatory responses to Borrelia burgdorferi. Infect Immun 81: 402-410.

95. Petnicki-Ocwieja T, DeFrancesco AS, Chung E, Darcy CT, Bronson RT, et al. (2011) Nod2 suppresses Borrelia burgdorferi mediated murine Lyme arthritis and carditis through the induction of tolerance. PLoS One 6: e17414.

96. Bockenstedt LK, Liu N, Schwartz I, Fish D (2006) MyD88 deficiency enhances acquisition and transmission of Borrelia burgdorferi by Ixodes scapularis ticks. Infect Immun 74: 2154-2160.

97. Benhnia MR, Wroblewski D, Akhtar MN, Patel RA, Lavezzi W, et al. (2005) Signaling through CD14 attenuates the inflammatory response to Borrelia burgdorferi, the agent of Lyme disease. J Immunol 174: 1539-1548.

98. Ruland J (2011) Return to homeostasis: downregulation of NF-kappaB responses. Nat Immunol 12: 709-714.

99. Shin JJ, Glickstein LJ, Steere AC (2007) High levels of inflammatory chemokines and cytokines in joint fluid and synovial tissue throughout the course of antibiotic-refractory lyme arthritis. Arthritis Rheum 56: 1325-1335.

100. Gabay C, Lamacchia C, Palmer G (2010) IL-1 pathways in inflammation and human diseases. Nat Rev Rheumatol 6: 232-241.

101. Rot A, von Andrian UH (2004) Chemokines in innate and adaptive host defense: basic chemokinese grammar for immune cells. Annu Rev Immunol 22: 891-928.

102. Hamilton T, Li X, Novotny M, Pavicic PG, Jr., Datta S, et al. (2012) Cell type- and stimulus-specific mechanisms for post-transcriptional control of neutrophil chemokine gene expression. J Leukoc Biol 91: 377-383.

103. Ohmori Y, Fukumoto S, Hamilton TA (1995) Two structurally distinct kappa B sequence motifs cooperatively control LPS-induced KC gene transcription in mouse macrophages. J Immunol 155: 3593-3600.

104. Datta S, Biswas R, Novotny M, Pavicic PG, Jr., Herjan T, et al. (2008) Tristetraprolin regulates CXCL1 (KC) mRNA stability. J Immunol 180: 2545-2552.

105. Bernardino AL, Myers TA, Alvarez X, Hasegawa A, Philipp MT (2008) Toll-like receptors: insights into their possible role in the pathogenesis of lyme neuroborreliosis. Infect Immun 76: 4385-4395.

106. Cerar T, Ogrinc K, Lotric-Furlan S, Kobal J, Levicnik-Stezinar S, et al. (2013) Diagnostic value of cytokines and chemokines in lyme neuroborreliosis. Clin Vaccine Immunol 20: 1578-1584.

107. Bransfield RC (2012) The psychoimmunology of lyme/tick-borne diseases and its association with neuropsychiatric symptoms. Open Neurol J 6: 88-93.

108. Widhe M, Grusell M, Ekerfelt C, Vrethem M, Forsberg P, et al. (2002) Cytokines in Lyme borreliosis: lack of early tumour necrosis factor-alpha and transforming growth factor-beta1 responses are associated with chronic neuroborreliosis. Immunology 107: 46-55.

109. Yates LA, Norbury CJ, Gilbert RJ (2013) The long and short of microRNA. Cell 153: 516-519.

110. Hu R, O'Connell RM (2013) MicroRNA control in the development of systemic autoimmunity. Arthritis Res Ther 15: 202.

111. Boldin MP, Baltimore D (2012) MicroRNAs, new effectors and regulators of NF-kappaB. Immunol Rev 246: 205-220.

112. Meijer HA, Kong YW, Lu WT, Wilczynska A, Spriggs RV, et al. (2013) Translational repression and eIF4A2 activity are critical for microRNA-mediated gene regulation. Science 340: 82-85.

113. Bartel DP (2004) MicroRNAs: genomics, biogenesis, mechanism, and function. Cell 116: 281-297.

114. Lewis BP, Burge CB, Bartel DP (2005) Conserved seed pairing, often flanked by adenosines, indicates that thousands of human genes are microRNA targets. Cell 120: 15-20.

115. O'Neill LA, Sheedy FJ, McCoy CE (2011) MicroRNAs: the fine-tuners of Toll-like receptor signalling. Nat Rev Immunol 11: 163-175.

116. O'Connell RM, Rao DS, Baltimore D (2012) microRNA regulation of inflammatory responses. Annu Rev Immunol 30: 295-312.

117. Nakasa T, Miyaki S, Okubo A, Hashimoto M, Nishida K, et al. (2008) Expression of microRNA-146 in rheumatoid arthritis synovial tissue. Arthritis Rheum 58: 1284-1292.

118. Stanczyk J, Pedrioli DM, Brentano F, Sanchez-Pernaute O, Kolling C, et al. (2008) Altered expression of MicroRNA in synovial fibroblasts and synovial tissue in rheumatoid arthritis. Arthritis Rheum 58: 1001-1009.

119. Abou-Zeid A, Saad M, Soliman E (2011) MicroRNA 146a expression in rheumatoid arthritis: association with tumor necrosis factor-alpha and disease activity. Genet Test Mol Biomarkers 15: 807-812.

120. Li J, Wan Y, Guo Q, Zou L, Zhang J, et al. (2010) Altered microRNA expression profile with miR-146a upregulation in CD4+ T cells from patients with rheumatoid arthritis. Arthritis Res Ther 12: R81.

121. Chatzikyriakidou A, Voulgari PV, Georgiou I, Drosos AA (2010) The role of microRNA-146a (miR-146a) and its target IL-1R-associated kinase (IRAK1) in psoriatic arthritis susceptibility. Scand J Immunol 71: 382-385.

122. Nakasa T, Shibuya H, Nagata Y, Niimoto T, Ochi M (2011) The inhibitory effect of microRNA-146a expression on bone destruction in collagen-induced arthritis. Arthritis Rheum 63: 1582-1590.

123. Bluml S, Bonelli M, Niederreiter B, Puchner A, Mayr G, et al. (2011) Essential role of microRNA-155 in the pathogenesis of autoimmune arthritis in mice. Arthritis Rheum 63: 1281-1288.

124. Stittrich AB, Haftmann C, Sgouroudis E, Kuhl AA, Hegazy AN, et al. (2010) The microRNA miR-182 is induced by IL-2 and promotes clonal expansion of activated helper T lymphocytes. Nat Immunol 11: 1057-1062.

125. Wang G, Tam LS, Kwan BC, Li EK, Chow KM, et al. (2012) Expression of miR-146a and miR-155 in the urinary sediment of systemic lupus erythematosus. Clin Rheumatol 31: 435-440.

126. Wang H, Peng W, Ouyang X, Li W, Dai Y (2012) Circulating microRNAs as candidate biomarkers in patients with systemic lupus erythematosus. Transl Res 160: 198-206.

127. Tang Y, Luo X, Cui H, Ni X, Yuan M, et al. (2009) MicroRNA-146A contributes to abnormal activation of the type I interferon pathway in human lupus by targeting the key signaling proteins. Arthritis Rheum 60: 1065-1075.

128. Luo X, Yang W, Ye DQ, Cui H, Zhang Y, et al. (2011) A functional variant in microRNA-146a promoter modulates its expression and confers disease risk for systemic lupus erythematosus. PLoS Genet 7: e1002128.

129. Lofgren SE, Frostegard J, Truedsson L, Pons-Estel BA, D'Alfonso S, et al. (2012) Genetic association of miRNA-146a with systemic lupus erythematosus in Europeans through decreased expression of the gene. Genes Immun 13: 268-274.

130. Dai R, Zhang Y, Khan D, Heid B, Caudell D, et al. (2010) Identification of a common lupus disease-associated microRNA expression pattern in three different murine models of lupus. PLoS One 5: e14302.

131. O'Connell RM, Rao DS, Chaudhuri AA, Baltimore D (2010) Physiological and pathological roles for microRNAs in the immune system. Nat Rev Immunol 10: 111-122.

132. O'Connell RM, Kahn D, Gibson WS, Round JL, Scholz RL, et al. (2010) MicroRNA-155 promotes autoimmune inflammation by enhancing inflammatory T cell development. Immunity 33: 607-619.

133. Hu R, Huffaker TB, Kagele DA, Runtsch MC, Bake E, et al. (2013) MicroRNA-155 confers encephalogenic potential to Th17 cells by promoting effector gene expression. J Immunol 190: 5972-5980.

134. Ponomarev ED, Veremeyko T, Barteneva N, Krichevsky AM, Weiner HL (2011) MicroRNA-124 promotes microglia quiescence and suppresses EAE by deactivating macrophages via the C/EBP-alpha-PU.1 pathway. Nat Med 17: 64-70.

135. Ruan Q, Wang T, Kameswaran V, Wei Q, Johnson DS, et al. (2011) The microRNA-21-PDCD4 axis prevents type 1 diabetes by blocking pancreatic beta cell death. Proc Natl Acad Sci U S A 108: 12030-12035.

136. McCoy CE, Sheedy FJ, Qualls JE, Doyle SL, Quinn SR, et al. (2010) IL-10 inhibits miR-155 induction by toll-like receptors. J Biol Chem 285: 20492-20498.

CHAPTER 2

ENDOTHELIAL CELLS AND FIBROBLASTS AMPLIFY THE ARTHRITOGENIC TYPE I IFN RESPONSE IN MURINE LYME DISEASE AND ARE MAJOR SOURCES OF CHEMOKINES IN *BORRELIA BURGDORFERI*-INFECTED JOINT TISSUE

Originally published in *The Journal of Immunology*. Robert B Lochhead, F. Lynn Sonderegger, Ying Ma, James E. Brewster, Doug Cornwall, Heather Maylor-Hagen, Jennifer C. Miller, James F. Zachary, John H. Weis, and Janis J. Weis. 2012. Endothelial Cells and Fibroblasts Amplify the Arthritogenic Type I IFN Response in Murine Lyme Disease and Are Major Sources of Chemokines in *Borrelia burgdorferi*-Infected Joint Tissue. J. Immunol. 189(5): 2488-501.

The Journal of Immunology

Endothelial Cells and Fibroblasts Amplify the Arthritogenic Type I IFN Response in Murine Lyme Disease and Are Major Sources of Chemokines in *Borrelia burgdorferi*-Infected Joint Tissue

Robert B. Lochhead,*,[1] F. Lynn Sonderegger,*,[1] Ying Ma,*,[1] James E. Brewster,* Doug Cornwall,* Heather Maylor-Hagen,* Jennifer C. Miller,*,[2] James F. Zachary,† John H. Weis,* and Janis J. Weis*

Localized elevation in type I IFN has been uniquely linked to the severe Lyme arthritis that develops in C3H mice infected with the spirochete *Borrelia burgdorferi*. In this study, the dynamic interactions that result in generation of these responses were further examined in C3H mice carrying the type I IFN receptor gene ablation, which effectively blocks all autocrine/paracrine signaling crucial to induction of downstream effectors. Reciprocal radiation chimeras between C3H and IFNAR1$^{-/-}$ mice implicated both radiation-sensitive and radiation-resistant cells of the joint tissue in the proarthritic induction of type I IFN. Ex vivo analysis of cells from the naive joint revealed CD45^{+} cells residing in the tissue to be uniquely capable of initiating the type I IFN response to *B. burgdorferi*. Type I IFN responses were analyzed in real time by lineage sorting of cells from infected joint tissue. This demonstrated that myeloid cells, endothelial cells, and fibroblasts were responsible for propagating the robust IFN response, which peaked at day 7 postinfection and rapidly resolved. Endothelial cells and fibroblasts were the dominant sources of IFN signature transcripts in the joint tissue. Fibroblasts were also the major early source of chemokines associated with polymorphonuclear leukocyte and monocyte/macrophage infiltration, thus providing a focal point for arthritis development. These findings suggest joint-localized interactions among related and unrelated stromal, endothelial, and myeloid cell lineages that may be broadly applicable to understanding the pathogeneses of diseases associated with type I IFN signature, including systemic lupus erythematosus and some rheumatoid arthritides. ***The Journal of Immunology*****, 2012, 189: 2488–2501.**

Lyme disease in humans is caused by infection with the tick-borne spirochete *Borrelia burgdorferi* and results in clinical arthritis in up to 30% of infected individuals (1, 2). Lyme arthritis has been extensively studied in the C3H mouse, which replicates many of the features of acute human disease, including edema, synovial hyperplasia, inflammatory cell infiltration, and reactive/reparative changes associated with joint tissue (3). A range of arthritis severity has been observed in humans and in different inbred strains of mice, as initially reported by Steere and Barthold et al. (2, 4). Additionally, numerous studies in mice have suggested that characteristics of the *B. burgdorferi*-induced inflammatory cascade determine the severity of arthritis that develops (5, 6). For example, ablation of the anti-inflammatory gene IL-10$^{-/-}$ results in greater severity of Lyme arthritis in both B6 and C3H mice (7, 8).

Previous global gene expression analysis in the joint tissue of C3H mice revealed an early inflammatory response at 1 wk of infection, weeks prior to the development of arthritic lesions (9). This early transcriptional event was characterized by robust but transient induction of IFN-responsive transcripts, and was absent from the mildly arthritic B6 mice. Innate immune production of type I IFNs (IFN-α,β) was suspected, as type II IFN (IFN-γ) is not required for Lyme arthritis development in C3H mice (10). Additionally, the peak of IFN-inducible transcript induction was prior to infiltration of lymphocytes into joint tissue likely to be required for IFN-γ production (11, 12). The involvement of type I IFN in Lyme arthritis was subsequently confirmed through the systemic administration of a type I IFN receptor (IFNAR1)-blocking mAb that was capable of disrupting signaling by all type I IFNs. This treatment suppressed the spike in IFN-inducible transcripts in the joint tissue at 1 wk of infection and the subsequent development of arthritis at 4 wk postinfection (13). In contrast, blocking IFN-γ suppressed expression of many of the overlapping IFN-inducible transcripts, but did not result in reduced arthritis severity.

The unique contribution of type I IFN to the development of severe Lyme arthritis in C3H mice implies specialized targets for this IFN in the infected joint tissue that cannot be compensated with IFN-γ. The potential importance of this finding is underscored by the pathological role of type I IFNs in systemic lupus erythematosus (SLE) and in the injurious side effects associated with IFN-αβ–based therapies for multiple sclerosis and hepatitis C

*Division of Microbiology and Immunology, Department of Pathology, University of Utah, Salt Lake City, UT 84112; and †University of Illinois at Urbana-Champaign, Urbana, IL 61802

[1]R.B.L., F.L.S., and Y.M. contributed equally to this manuscript.

[2]Current address: Department of Microbiology, North Carolina State University, Raleigh, NC.

Received for publication April 13, 2012. Accepted for publication July 1, 2012.

This work was supported by Public Health Services Grants AI-32223 and AI-43521 (to J.J.W.), AI-24158 and AI-088451 (to J.H.W.), the Training Program in Microbial Pathogenesis 5T32-AI-055434 (to J.C.M. and F.L.S.), and an Arthritis Foundation award (to J.C.M.).

Address correspondence and reprint requests to Dr. Janis J. Weis, Department of Pathology, University of Utah, 15 North Medical Drive East, Room 2100, Salt Lake City, UT 84112-5650. E-mail address: janis.weis@path.utah.edu

Abbreviations used in this article: BMDM, bone marrow-derived macrophage; PMN, polymorphonuclear leukocyte; RA, rheumatoid arthritis; SLE, systemic lupus erythematosus.

www.jimmunol.org/cgi/doi/10.4049/jimmunol.1201095

infection (14–16). Even more relevant to Lyme arthritis pathogenesis are recent studies implicating type I IFN in a subgroup of rheumatoid arthritis (RA) patients who fail to respond to therapeutic TNF blockade (17–19). Thus, studies with Lyme arthritis may broadly improve our understanding of immune-mediated inflammatory diseases by providing insight for patient groups currently not well served by existing therapies.

To further our understanding of the contribution of type I IFN signaling in the development of Lyme arthritis, the IFN receptor 1 gene ablation (IFNAR1$^{-/-}$) was crossed onto the C3H background (C3H IFNAR1$^{-/-}$). Arthritis severity was reduced in the absence of IFNAR1. The development of radiation chimeras between C3H and IFNAR1$^{-/-}$ mice allowed assessment of contributions of both myeloid lineage and parenchymal cells to the proarthritic IFN response: both developmental lineages were involved. Ex vivo recovery of sorted cells from the joint tissue revealed dynamic contributions of various cell lineages to the arthritis-promoting IFN response. Resident myeloid cells of the joint tissue were identified as the initiators of type I IFN production upon encounter with *B. burgdorferi*, whereas endothelial cells and joint fibroblasts expressing adhesion/activation markers were found to amplify the response and served as the major source of disease-promoting chemokines. The development of severe arthritis was determined to be orchestrated by a cascade of events initiated by interaction of *B. burgdorferi* with myeloid, stromal, and endothelial cells at 1 wk postinfection.

Materials and Methods

Mice, bacterial cultures and infections, and assessment of arthritis severity

C3H/HeN mice were obtained from Charles River Breeding Laboratories or from National Cancer Institute, and C57BL/6 mice were from National Cancer Institute. The IFNAR1 gene ablation from the C57BL/6 mouse (20) (provided by M.-K. Kaja, University of Washington, Seattle, WA) was crossed six generations onto the C3H background. Filial mating was performed to generate C3H/HeN IFNAR1$^{-/-}$. All mice were housed in the University of Utah Animal Research Center (Salt Lake City, UT) following all institutional guidelines for the care and use of mice in biomedical research. Mice were infected with 2×10^4 bacteria of the clonal *B. burgdorferi* strain N40 by intradermal injection into the skin of the back (3). Infected and control C57BL/6 mice received 5×10^4 U universal type I IFN (PBL) on day 1 and 10^4 U every other day for 28 d by i.p. injection, or received an equivalent volume of PBS (21). Ankle measurements were obtained using a metric caliper before and at 4 wk of infection. Rear ankle joints were prepared for assessment of histopathology by removal of skin and fixation of the tissue in 10% neutral buffered formalin, as described (8). Decalcified joints were embedded in paraffin, sectioned at 3 μm, and stained with H&E. Each slide was scored from 1 to 5 for various aspects of disease, including severity and extent of the lesion, polymorphonuclear leukocyte (PMN) and mononuclear cell (e.g., monocytes, macrophages) infiltration, tendon sheath thickening (e.g., synoviocyte and fibroblast hyperplasia), and reactive/reparative responses (e.g., periosteal hyperplasia and new bone formation and remodeling), with 5 representing the most severe lesion, and 0 representing no lesion. Ankle measurements and arthritic lesions were assessed in coded samples. Infection was confirmed in mice euthanized prior to 14 d postinfection by culturing bladder tissue in BSK II media containing 6% rabbit serum, phosphomycin, and rifampicin. ELISA quantification of *B. burgdorferi*-specific IgM and IgG concentrations was used to confirm infection in mice euthanized at and after 14 d postinfection, as described (22).

Preparation of single-cell suspensions from mouse tissue

Single-cell suspensions were prepared from the rear ankle joint tissue, following removal of skin. Joint tissue was partially removed from bone using 20-gauge syringe needles to facilitate digestion by incubation in RPMI 1640 containing 0.2 mg/ml endotoxin-free Liberase TM (Roche) and 100 μg/ml DNase I (Sigma-Aldrich) for 1 h at 37°C. After incubation, gentle pipetting further disrupted tissue and intact tissue was broken apart using the end of a 5-ml syringe. The single-cell suspension was filtered through a 100 μm cell strainer and centrifuged, and the RBCs were lysed using ammonium-chloride-potassium lysing buffer. Blood was collected in Eppendorf tubes containing acid citrate dextrose, and leukocyte populations were analyzed, as described (23).

Flow cytometry

All flow cytometry data were analyzed using BD CellQuest Pro software. Sorting experiments were performed using a BD FACSAria II. All other FACS data were collected on a BD FACS Canto II flow cytometer or BD LSRII flow cytometer. The 7-aminoactinomycin D (eBioscience) or DAPI (Invitrogen) was used in all experiments, and dead cells were excluded from analyses, as were doublet cells. All Abs used for flow cytometry were purchased from either BioLegend or eBioscience. Unconjugated F_c blocking Ab (clone 93; BioLegend) was included in all Ab-labeling experiments. Position of gates for sorting and analysis was based on analysis of appropriate isotype controls. Fluorochrome-conjugated Abs and isotype controls used in this study were as follows: FITC-conjugated anti-CD11b (M1/70) and anti-B220 (RA3-6B2); PerCP/Cy5.5-conjugated anti-Ly6c (HK1.4) and anti-CD31 (390); PE-conjugated anti-CD54 (YN1/1.7.4), anti-CD31 (390), anti-IFNAR1 (MAR1-583), and anti-CD29 (HMβ1-1); PE/Cy-7–conjugated anti-CD11b (M1/70), anti-CD90.2 (30-H12), and anti-CD45.2 (104); allophycocyanin-conjugated anti-F4/80 (BM8), anti-TCR β (H57-597), anti-CD29 (HMβ1-1), anti-CD45 (30-F11), and anti-CD106 (429); Alexa Fluor 700-conjugated anti-Ly6G/Ly6C (RB6-8C5) and anti-CD45.2 (104); Pacific Blue-conjugated anti-TCRβ (H57-597) and anti-B220 (RA3-6B2); and biotin-conjugated anti-PE (PE001) and PE-conjugated streptavidin.

Injection of mAbs

The following Abs were used in vivo for cytokine neutralization: anti–IFN-γ (XMG1.2), anti–TNF-α (XT3.11), and rat IgG1 (HPRN) isotype control, and were aggregate, endotoxin free, and sterile (Bio X Cell). Groups of five to six mice received 1 mg indicated Ab 1 d prior to infection, followed by 0.5 mg of the same Ab every 4–5 d thereafter, all by i.p. injection (11, 13).

Isolation of RNA and quantitative RT-PCR

For all experiments examining gene expression in joint tissue, mice were killed, and the skin was removed from the tibiotarsal joints. Ankle joints were excised, frozen immediately in dry ice/ethanol, and stored at −80°C. Total RNA from joint tissue and cultured cells was performed using TRIzol reagent (Invitrogen) (24). RNA from FACS-sorted cell populations was purified with the RNAeasy kit (Qiagen). RNA recovered from tissue and cells was reverse transcribed, and transcripts were quantified using a Roche LC-480 according to our previously described protocols (24). Primer sequences used in this study were as follows: *Ccl2* forward (5′-CCCAATGAGTAGGCTGGAGAGC-3′), reverse (5′-GGTGGTTGTGGAAAAGGTAGTGG-3′); *Ccl8* forward (5′-GCTTCTTTGCCTGCTGCTCATAG-3′), reverse (5′-CATCTGCTTGTAACATCTCTCTGCC-3′); *Cxcl1* forward (5′-ATGGCTGGGATTCACCTC-3′), reverse (5′-CTTCAGGGTCAAGGCAAG-3′); *Cxcl2* forward (5′-CCCACTGCGCCCAGACAG-3′), reverse (5′-AGGTCAGTTAGCCTTGCCTT-3′); *Fn1* forward (5′-GCAGTGGTCATTTCAGATGCG-3′), reverse (5′-TCTCCCTTTCCATTCCCGAG-3′); *Icam1* (CD54) forward (5′-AGGGCTGGCATTGTTCTCTA-3′), reverse (5′-CTTCAGAGGCAGGAAACAGG-3′); *Pecam1* (CD31) forward (5′-TCCTTCACCATCAACAGCATCC-3′), reverse (5′-TTTTGTCCAGTGTCACCTTGGG-3′); *Ptprc* (CD45) forward (5′-GGGTCCACCTACATAAATGCCAG-3′), reverse (5′-GTTCCTGTTTCCTTCTTCACATCG-3′); *Thy1* (CD90) forward (5′-GGATGAGGGCGACTACTTTTGTG-3′), reverse (5′-TTCTGAACCAGCAGGCTTATGC-3′); *Vcam1* (CD106) forward (5′-CCCGTCATTGAGGATATTGG-3′), reverse (5′-GGTCATTGTCACAGCACCAC-3′). Primer sequences for *β-actin*, *Igtp*, *Iigp*, *Mmp3*, *Stat1*, *Cxcl13* (9), *Cxcl9*, *Cxcl10*, *Oasl2* (13), *Ifit*, *Gbp2* (25), *Tnfα*, and *Ifnβ* (26) can be found in the indicated citations.

Isolation of DNA and quantification of joint spirochetes

For quantification of joint spirochetes at 4 wk postinfection, total DNA was isolated from joint tissue, as described. PCR quantification of spirochetes was performed by amplification of the *B. burgdorferi recA* gene and normalized to the mouse *Nidogen* gene using a Roche LC-480 (27).

Generation of reciprocal radiation chimeras

The diminished severity of Lyme arthritis in mice 10 wk and older required the development of a protocol allowing rapid reconstitution of irradiated mice with high numbers of hematopoietic cells (11). C3H and C3H IFNAR1$^{-/-}$ mice 5 wk of age were lethally irradiated with 2 doses of 525 cGy 3 h apart using a GE Isovolt Titan. Twenty-four hours following irradiation, splenocytes were harvested from C3H or C3H IFNAR1$^{-/-}$ donor mice, and 2×10^7 splenocytes in a 200 μl volume were injected i.v.

into each irradiated recipient. Chimerism was determined at 6 wk postirradiation by flow cytometry assessment of mAb anti-IFNAR1 expression by blood leukocytes (28). Staining required sequential treatment with PE-conjugated anti-IFNAR1, biotin-conjugated anti-PE, and PE-conjugated streptavidin, which allowed sufficient fluorescence intensity to readily distinguish wild-type from IFNAR1$^{-/-}$ cells. Peripheral blood B cells and monocytes were found to be >90% donor derived, whereas T cells were ~60% donor derived. Total blood leukocyte counts were comparable to those from nonirradiated control mice 7 wk posttransplantation. Mice were infected at 3 wk postirradiation and transplantation, 7–8 wk of age and, therefore, allowing Lyme arthritis to be assessed.

Cell culture

Bone marrow-derived macrophages (BMDM) were isolated from the femurs and tibias of mice, as previously described (29). Macrophage cultures were plated in 12-well dishes at a density of 6×10^5/ml in media containing the serum replacement Nutridoma (Roche) and stimulated with live *B. burgdorferi* cN40 (7.4×10^6/ml), 10 U/ml IFN-γ (Sigma-Aldrich), or PBS. Macrophage cultures were stimulated at 37°C, 5% CO_2, and harvested either at 6 h for RNA extraction or at 24 h for assessment of type I IFN in supernatants by bioassay.

Magnetic separation of leukocytes and stromal cells from naive joint tissue

Single-cell suspensions of joint tissue were labeled with biotinylated anti-CD45.2 (BioLegend), followed by labeling with streptavidin magnetic beads (Miltenyi Biotec). Labeled cells were loaded onto MS columns (Miltenyi Biotec), and magnetic separation was performed according to the manufacturer's instructions, with sequential application to a second column. Relative purity of the CD45.2$^+$ and CD45.2$^-$ populations was determined by flow cytometry using allophycocyanin-conjugated anti-CD45 (clone 30-F11), which recognizes an epitope distinct from the Ab used in magnetic bead sorting (anti-CD45.2, clone 104). Unfractionated and fractionated populations were incubated in 2% FBS containing RPMI 1640 in the presence or absence of *B. burgdorferi*, 100 U mouse rIFN-β (PBL), or both for 6 h, conditions found to maintain cell viability and permit IFN-inducible responses to be detected. Samples were collected in TRIzol for RNA recovery (24).

Type I IFN bioassay

Bioactive type I IFN was detected in culture supernatants from BMDM incubated for 24 h with *B. burgdorferi* in the presence or absence of rIFN-γ (eBioscience) by bioassay with B16-Blue IFN-αβ cells (InvivoGen), following manufacturer's directions. Standard curve was generated with mouse rIFN-β (PBL).

Data and statistical analyses

All graphical data represent the mean ± SEM. Statistical analysis was performed using Prism 5.0c software. Multiple-sample data sets were analyzed by one-way ANOVA with appropriate post hoc test for pairwise comparisons (Figs. 2–6, Tables II, III). Two-sample data sets were analyzed by Student *t* test (Figs. 1, 8, Table I). Categorical data for histopathology was assessed by the Mann–Whitney *U* test (Figs. 1, 3, Table I). Statistical significance ($p < 0.05$) is indicated by *.

Results

Lyme arthritis severity can be modulated by augmentation or ablation of type I IFN signaling

We previously demonstrated that administration of a blocking mAb to the type I IFN receptor resulted in a significant diminution of arthritis severity in *B. burgdorferi*-infected C3H mice, implicating the type I IFN autocrine/paracrine pathway in arthritis development (13). As this pathway is not upregulated in the joint tissue of arthritis-resistant B6 mice, we tested the effect of supplementation of *B. burgdorferi*-infected B6 mice with type I IFN throughout *B. burgdorferi* infection. Treatment of B6 mice with daily injections of IFN-α for 4 wk following infection resulted in significantly greater ankle swelling than observed in the control group, receiving daily injections of PBS (Table I). Histopathologically assessed lesion scores suggested a trend toward increased arthritis in the group receiving IFN-α; however, this did not achieve statistical significance. Importantly, the increase in ankle swelling in treated B6 mice (Table I) did not reach the degree of severe arthritis seen in the genetically susceptible C3H mice (Fig. 1). This finding may further indicate the presence of IFN regulatory mechanisms inherent to the B6, but not the C3H genetic background.

As the previous assessment of type I IFN in Lyme arthritis was performed in vivo using a mAb to prevent signaling though the cognate receptor, a more rigorous approach was used by crossing the IFNAR1 gene disruption onto the susceptible C3H genetic background. Marker-assisted protocols were employed for rapid and complete crossing and to ensure that none of the quantitative trait loci associated with Lyme arthritis severity were lost from the recipient C3H mice (30). Infection of C3H IFNAR1$^{-/-}$ mice with *B. burgdorferi* revealed a significant reduction in arthritis severity relative to wild-type C3H mice, as demonstrated by the traits of ankle swelling, overall lesion score, and neutrophil infiltration (Fig. 1), with less robust differences in tendon sheath thickness and reactive/reparative abnormalities also observed (data not shown). These results mirror the significant but incomplete reduction in arthritis severity previously reported in C3H mice treated with IFNAR receptor-blocking Ab prior to infection, thus indicating that the observed partial reduction in arthritis was not reflective of incomplete neutralization by the Ab (13). Three lines of experimental evidence now support the unique involvement of type I IFN in arthritis development in C3H mice, as follows: 1) arthritis can be partially suppressed with receptor-blocking mAb; 2) arthritis is similarly reduced by genetic ablation of the IFN signaling pathway; and 3) ankle swelling can be partially restored in B6 mice by administration of exogenous IFN-α. A modest increase in *B. burgdorferi* levels in joint tissue of IFNAR1$^{-/-}$ mice was observed, and demonstrated that the decreased arthritis seen in the mutant mice was not secondary to reduced numbers of spirochetes in the tissue (Fig. 1).

Effect of type I IFN receptor ablation on B. burgdorferi*-induced IFN profile in joint tissue and in macrophage cultures*

The contribution of type I IFN signaling to the previously reported robust upregulation of IFN-responsive transcripts was assessed in C3H IFNAR1$^{-/-}$ mice at 1 wk *of B. burgdorferi* infection. Interestingly, several of the IFN-inducible transcripts previously found to be reduced but not eliminated by receptor-blocking mAb also displayed residual induction in the joint tissue of *B. burg-*

Table I. Effect of IFN-α administration on arthritis development in *B. burgdorferi*-infected B6 mice

Infection Status	IFN Treatment	Change in Ankle Measurement[a]	Overall Lesion
Mock infected	PBS	0.01 ± 0.01[a]	0 ± 0
B. burgdorferi		0.04 ± 0.04	1.0 ± 0.71
Mock infected	IFN-α	0 ± 0	0 ± 0
B. burgdorferi		0.25* ± 0.15	1.6 ± 0.55

Assessed at 4 wk of infection.
[a]Values represent mean ± SD.
*Statistical significance between PBS- and IFN-α–treated group, $p < 0.05$.

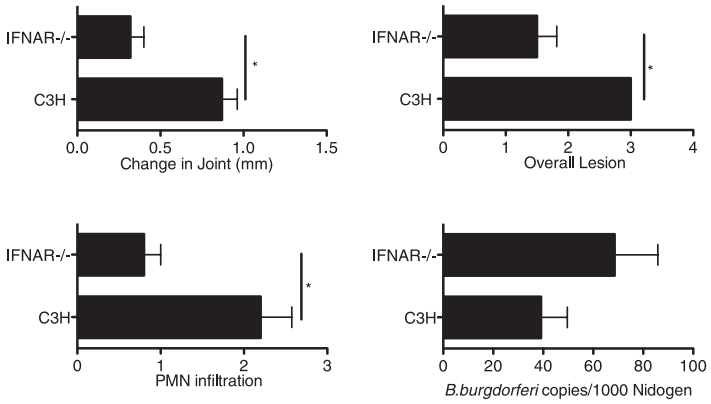

FIGURE 1. IFNAR1 gene ablation results in reduced Lyme arthritis severity in C3H mice. C3H or C3H-IFNAR1$^{-/-}$ mice were infected with *B. burgdorferi* by intradermal injection, and arthritis was assessed at 4 wk, as described in *Materials and Methods*. Arthritis traits included the following: change in ankle joint measurement, PMN infiltration, and overall lesion severity. *B. burgdorferi* number in joint tissue was determined by quantitative PCR and normalized to the single copy mouse gene *Nidogen*. Statistical significance was determined by Student *t* test for ankle swelling and bacterial number in joint tissue, whereas the Mann–Whitney *U* test was used for PMN infiltration and overall lesion. All categories were negative for uninfected control C3H and C3H-IFNAR1$^{-/-}$ mice, injected with BSK media, and are not shown in the figure. $n \geq 9$ mice for each group, pooled from two independent experiments. $*p < 0.05$.

dorferi-infected C3H IFNAR1$^{-/-}$ mice, shown for *Cxcl10*, *Oasl2*, *Igtp*, and *Gbp2* in Fig. 2A, although at much lower levels than previously reported in wild-type C3H mice (9, 13, 24).

Recent reports in other infection models have identified modifying effects of type I IFN on IFN-γ production (31, 32) as well as MyD88-dependent modulation of IFN-β production (33). The identification of low levels of transcripts for both IFN-γ and TNF-α in the joint tissue of infected C3H IFNAR1$^{-/-}$ mice (data not shown) suggested that one or both might be responsible for induction of the IFN profile in absence of type I IFN signaling. Injecting infected C3H IFNAR1$^{-/-}$ mice with neutralizing Abs for IFN-γ or TNF-α allowed testing of this possibility. Treatment with anti-TNF resulted in detectable, but not significant, reduction in the expression of several IFN-inducible transcripts in infected joint tissue when compared with mice treated with an isotype control mAb (Fig. 2A). In contrast, treatment with IFN-γ neutralizing mAb resulted in complete suppression of the expression of IFN-inducible genes to levels found in uninfected mice (Fig. 2A). Thus, the residual profile of IFN-inducible transcripts in infected IFNAR1$^{-/-}$ mice can be attributed to compensatory effects of IFN-γ, possibly reflecting an enhanced effect permitted by the absence of type I IFN modulatory activity.

IFN-γ partially compensates for type I IFN signaling ablation in the BMDM response to B. burgdorferi*, but does not substitute for type I IFN in arthritis development*

The *B. burgdorferi*-induced upregulation of IFN-inducible transcripts in BMDM was previously shown to be dependent on IFN receptor-mediated autocrine/paracrine signaling in B6 mice (13). BMDM were prepared from C3H and C3H IFNAR1$^{-/-}$ mice, and the presence of the receptor was again shown to be necessary for upregulation of IFN-inducible transcripts in response to *B. burgdorferi*, shown for *Cxcl10*, *Oasl2*, *Igtp,* and *Gbp2* (Fig. 2B). Importantly, C3H IFNAR1$^{-/-}$ BMDM were able to respond to *B. burgdorferi* by other sensing/signaling pathways, as indicated by upregulation of *Tnfα* transcripts at concentrations similar to C3H BMDM (Fig. 2C).

The mAb results in Fig. 2A suggested that IFN-γ might compensate for type I IFN signaling in induction of the IFN transcriptional response to *B. burgdorferi*. To model the potential of IFN-γ to compensate for type I IFN within the joint, exogenous IFN-γ was added to BMDM cultures of C3H and C3H IFNAR1$^{-/-}$ macrophages stimulated with *B. burgdorferi* (Fig. 2B). Treatment with rIFN-γ alone resulted in the induction of most transcripts in both wild-type and IFNAR1$^{-/-}$ macrophages, but with a range of expression, shown for *Cxcl10*, *Oasl2*, *Igtp*, and *Gbp2*. Costimulation with IFN-γ and *B. burgdorferi* resulted in expression of IFN-inducible transcripts in both C3H and C3H IFNAR1$^{-/-}$ macrophages, shown for *Cxcl10*, *Igtp*, and *Gbp2* in Fig. 2B. However, expression of *Oasl2*, a transcript linked to early type I IFN responses, was not upregulated in C3H IFNAR1$^{-/-}$ macrophages costimulated with IFN-γ and *B. burgdorferi.* The reduced expression of *Igtp* and *Gbp2* when stimulated simultaneously with IFN-γ and *B. burgdorferi* may reflect a rapid response to dual stimuli that was missed by the 6-h time point (Fig. 2B).

Interestingly, transcriptional induction of IFN-β was observed at low concentrations in response to *B. burgdorferi* in both wild-type and IFNAR1$^{-/-}$ macrophages and was further upregulated by the addition of IFN-γ (Fig. 2C). The induction of IFN-β transcripts in C3H IFNAR1$^{-/-}$ macrophages defines this early production (6 h) as independent of positive feedback through type I IFN receptors. To ensure that these transcripts reflected the translation and release of type I IFN protein (IFN-α and IFN-β), macrophage supernatants collected at 24 h were subjected to bioassay for type I IFN using the B16-Blue cell line (InvivoGen) (Fig. 2C). Type I IFN secretion was detected in C3H BMDM stimulated with *B. burgdorferi*, whereas IFN-γ alone did not have this effect. Treatment with IFN-γ enhanced production of type I IFN protein in responses to *B. burgdorferi*, in macrophages from both C3H and C3H IFNAR1$^{-/-}$ mice. Of note, bioassay results were confirmed to be specific for type I IFN as these findings were not influenced by the addition of neutralizing Ab to IFN-γ (data not shown).

The observation that the residual IFN profile seen in infected C3H IFNAR1$^{-/-}$ was suppressed by anti–IFN-γ neutralizing mAb (Fig. 2A) clearly implicates IFN-γ in the localized response to *B. burgdorferi* in the joint of C3H IFNAR1$^{-/-}$ mice, and suggests it could contribute to the residual arthritis seen in these mice. To test this hypothesis, groups of five infected C3H IFNAR1$^{-/-}$ mice were administered IFN-γ neutralizing mAb or isotype control mAb by i.p. injection every 5 d for 4 wk. IFN-γ neutralization did not cause further reduction in the severity of arthritis in C3H IFNAR1$^{-/-}$ mice: average ankle swelling for five mice treated with isotype control was 0.80 ± 0.23 mm, whereas mice treated with anti–IFN-γ measured 0.803 ± 0.17 mm. This finding indicates that the IFN-γ–dependent induction of transcripts in the joint tissue of infected IFNAR1$^{-/-}$ mice at 1 wk postinfection does not contribute to the residual arthritis seen at 4 wk postinfection, consistent with our previous published results employing blocking mAbs in C3H mice (13). Therefore, the residual arthritis seen in *B. burgdorferi*-infected C3H IFNAR1$^{-/-}$ mice develops independently of either type I or type II IFN.

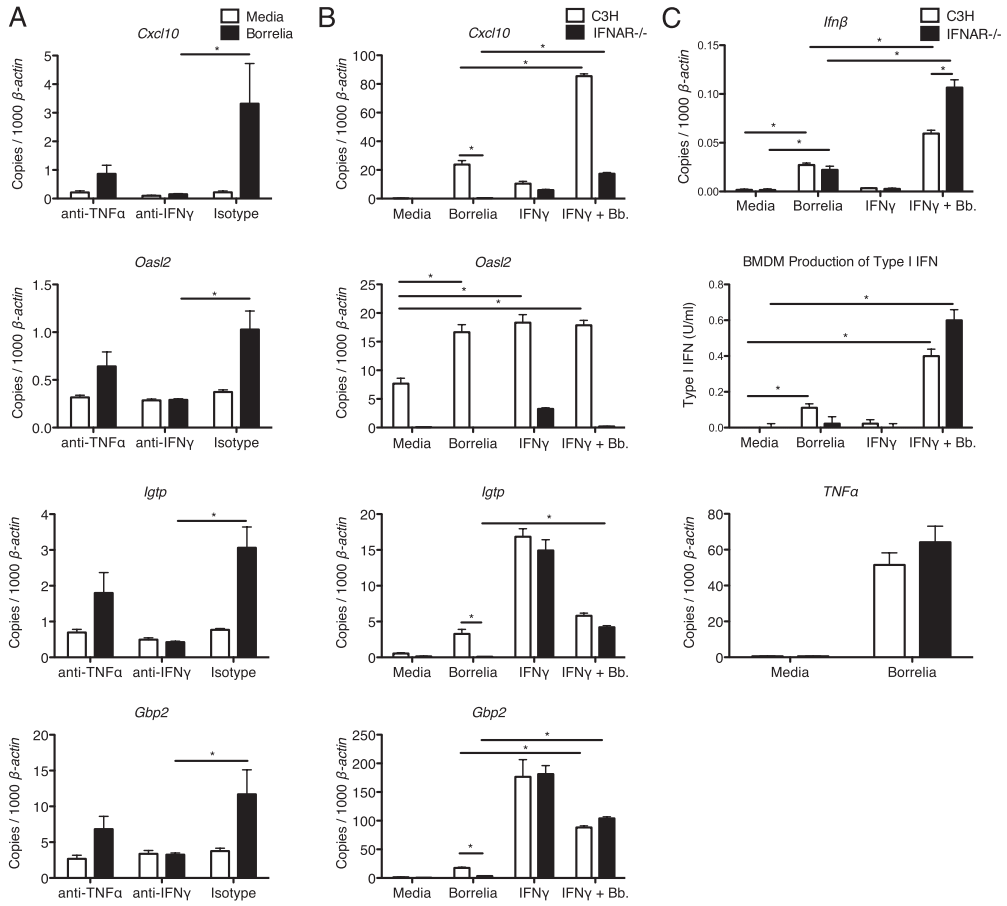

FIGURE 2. IFN-γ provides partial compensation for type I IFN in infected joint tissue and in bone marrow macrophage cultures from C3H IFNAR1$^{-/-}$ mice. (**A**) RT-PCR analysis of transcripts in joint tissue at 7 d postinfection (*Borrelia*) or mock infection of C3H IFNAR1$^{-/-}$ mice (media) treated with anti–TNF-α, anti–IFN-γ, or isotype control IgG1, as described in *Materials and Methods* ($n = 5$). The following transcripts were analyzed and normalized to *β-actin*: *Cxcl10*, *Oasl2*, *Igtp*, and *Gbp2*. (**B**) Effect of exogenous IFN-γ on transcriptional induction of IFN profile in BMDM from C3H and C3H IFNAR1$^{-/-}$ mice incubated with *B. burgdorferi*, IFN-γ, *B. burgdorferi* plus IFN-γ, or media alone for 6 h. RT-PCR analysis of IFN profile transcripts (*Cxcl10*, *Oasl2*, *Igtp*, and *Gbp2*), normalized to *β-actin*. (**C**) *B. burgdorferi*-induced secretion of bioactive type I IFN protein in culture supernatants of C3H and C3H IFNAR1$^{-/-}$ BMDM, collected at 24 h. Supernatants were applied to type I IFN reporter cell line for IFN bioassay, as described in *Materials and Methods*. Transcription analysis of *Ifnβ* at 6 h from same experiment is shown for comparison, and *Tnfα* transcripts are included as viability and responsiveness control. Data are representative of two independent experiments. Statistical significance among groups (transcript analysis) or between experimental and control groups (IFN bioassay) is shown ($*p < 0.05$).

Relative contribution of radiation-sensitive and resistant cells to the type I IFN-dependent development of Lyme arthritis

The results of Fig. 2 suggest that a mixture of cell lineages in the joint tissue may determine both the magnitude and breadth of the IFN response to *B. burgdorferi* and the severity of subsequent arthritis in C3H mice. To address the relative contribution of resident cells of the joint, such as endothelial cells and fibroblasts, and infiltrating hematopoietic cells to the type I IFN-dependent development of arthritis, we developed reciprocal radiation chimeras between C3H and C3H IFNAR1$^{-/-}$ mice, using rapid reconstitution protocol to allow *B. burgdorferi* infection of mice <8 wk of age. The efficiency of reconstitution of hematopoietic cells in the chimeras was determined by staining for IFNAR1 (28), described in *Materials and Methods*. Reconstitution of irradiated C3H mice with syngeneic splenocytes (C3H⇒C3H) resulted in severe arthritis following infection by *B. burgdorferi*, whereas infection of irradiated C3H IFNAR1$^{-/-}$ mice reconstituted with syngeneic splenocytes (IFNAR1$^{-/-}$⇒IFNAR1$^{-/-}$) displayed less severe arthritis (Fig. 3), and similar to nonirradiated mice in Fig. 1. Reconstitution of C3H mice with splenocytes from IFNAR1$^{-/-}$ mice or reconstitution of IFNAR1$^{-/-}$ mice with C3H splenocytes resulted in arthritis of intermediate severity following infection, shown for joint measurement and overall lesion score (Fig. 3). Control of *B. burgdorferi* was not significantly different in the treated animals, demonstrating that reconstitution was adequate for host defense (Fig. 3). That arthritis severity in the chimeras was intermediate compared with that observed for wild-type or IFNAR1$^{-/-}$ mice implies that both radiation-resistant cells of the joint and radiation-sensitive hematopoietic cells contribute to the IFN receptor-dependent autocrine/paracrine effect that drives the severe arthritis of C3H mice.

Ex vivo identification of cell lineages in the joint tissue of naive mice capable of initiating and responding to the type I IFN response

The radiation chimera experiment of Fig. 3 implicated both hematopoietic and resident cells of the joint in the type I IFN-

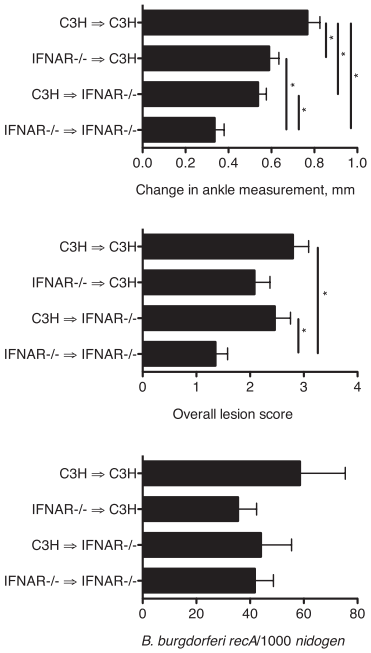

FIGURE 3. Radiation chimeras between C3H and IFNAR1$^{-/-}$ mice reveal contribution of both resident cells and cells of hematopoietic origin to proarthritic IFN response. Reciprocal radiation chimeras between C3H and C3H IFNAR1$^{-/-}$ mice were generated, as described in *Materials and Methods*. Mice were infected with *B. burgdorferi* 3 wk following reconstitution, and arthritis severity was assessed at 4 wk postinfection, shown for change in ankle measurement and overall lesion score. Direction of transplantation from donor to recipient is indicated on the figure. Results are pooled from two separate experiments, with ≥10 mice in each infected mouse group. *B. burgdorferi* numbers at 4 wk postinfection were similar in all mice. Uninfected chimeras did not display ankle abnormalities or *B. burgdorferi* DNA in tissues. Statistical significance among groups ($*p < 0.05$) is indicated.

dependent development of Lyme arthritis. BMDM and other myeloid cells have been identified as sources of IFN when incubated with *B. burgdorferi* (Fig. 2B) (13, 34–36). Although it is likely that the complex milieu of the joint tissue facilitates cooperation among a variety of cell types, it is also possible that myeloid cells, such as macrophages, are uniquely endowed with the ability to internalize and sense *B. burgdorferi* pathogen-associated molecular patterns, which lead to the initiation of the IFN-responsive transcriptional profile (36–38). To identify the relative ability of hematopoietic cells and nonhematopoietic cells of the joint to initiate the IFN profile, single-cell suspensions were recovered from the joints of naive C3H mice following gentle digestion, and fractionated into CD45$^+$ and CD45$^-$ populations by magnetic bead separation. Approximately 20% of the cells in the unfractionated group were CD45$^+$, and this increased to 75–80% following CD45 enrichment, as determined by flow cytometry (Fig. 4A). Cells from the three populations were cultured for 6 h in the presence of *B. burgdorferi*, IFN-β, or *B. burgdorferi* plus IFN-β. The expression of the NF-κB–dependent transcript *Tnfα* served as a control for viability, as its production has been previously characterized in both myeloid and endothelial cells treated with *B. burgdorferi* (22, 39). By this measure, both CD45$^+$ and CD45$^-$ fractions were viable and capable of responding to *B. burgdorferi* (Fig. 4B). Cell viability was further confirmed by the response to IFN-β alone, as both CD45$^+$ and CD45$^-$ fractions upregulated the early IFN-inducible transcripts *Cxcl10* and *Tyki* following this treatment (Fig. 4C, 4D) (40). This also points to the potential involvement of both fractions in the amplification stage of the IFN response. In contrast, only the CD45$^+$ cells were capable of upregulating *Cxcl10* and *Tyki* in response to *B. burgdorferi* alone (Fig. 4C, 4D), indicating novel contribution of CD45$^+$ cells in triggering the IFN-inducible profile. As we previously demonstrated that the IFN profile at 1 wk postinfection is also observed in infected C3H *scid* mice (13), these results strongly implicate a myeloid lineage cell as initiator of the IFN response resulting in activation of large numbers of resident cells that amplify the response.

Assessment of changes in cellular composition and activation in B. burgdorferi*-infected joint tissue*

The unique ability of CD45$^+$ cells to initiate the IFN profile ex vivo, and the ready induction of this response in BMDM cultures, suggested that infiltrating myeloid cells might be the driving force behind the IFN response to *B. burgdorferi* in vivo.

Ly6C$^+$-expressing inflammatory monocytes have recently been implicated in both the beneficial type I IFN response to viral infection and in its pathological production in chronic disease such as SLE (41, 42). Therefore, the composition and infiltration of Ly6C$^+$ myeloid-lineage cells to the joint tissue of C3H mice were

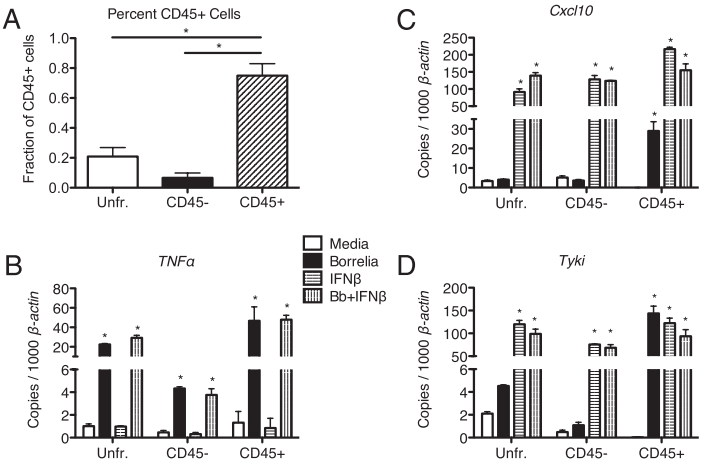

FIGURE 4. Potential contribution of hematopoietic and nonhematopoietic cells to the initial IFN response to *B. burgdorferi* in joints of C3H mice. Enrichment of leukocytes in the CD45$^+$ fraction was confirmed by flow cytometry (**A**) with significant change from unfractionated indicated ($*p < 0.05$). RT-PCR of transcripts for *Tnfα* (**B**), *Cxcl10* (**C**), and *Tyki* (**D**) identified populations responsive to *B. burgdorferi*, IFN-β, and combined treatment, and were normalized to *β-actin*. Only CD45$^+$ cells displayed significant upregulation of the IFN-inducible transcripts *Cxcl10* and *Tyki* in response to *B. burgdorferi* alone, as indicated. Results are representative of three separate experiments, with $n = 3$. Statistical significance between experimental and control groups ($*p < 0.05$) is indicated.

determined by flow cytometry assessment of populations released from the joint tissue over time: PMN leukocytes were defined as $GR1^{high}Ly6C^{dim}CD11b^{high}CD45^{+}$, macrophages were $GR1^{-}Ly6C^{-}F4/80^{+}CD11b^{high}CD45^{+}$, and inflammatory monocytes were $GR1^{dim}Ly6C^{high}CD11b^{high}CD45^{+}$. Increases in all three myeloid lineage populations were seen at days 11 and 14 postinfection relative to uninfected mice, with macrophages and PMNs dominating the inflammatory cell infiltrate (Fig. 5A). The increases in these lineages at day 11 postinfection were similar between C3H and C3H IFNAR1$^{-/-}$ mice, indicating the recruitment or expansion of these cells was not dependent on type I IFN signaling. Importantly, the $Ly6C^{+}$ population showing the greatest increase following infection in both C3H and C3H IFNAR1$^{-/-}$ mice was the inflammatory monocyte; however, this increase was not observed until day 11 of infection and was still elevated at day 14. Of note, there was no increase in any of the myeloid cell populations at day 7 postinfection, the time point previously and in this study associated with the peak of the IFN response (Fig. 5A). This striking result indicated that the induction of the IFN profile was not dependent on recruitment of myeloid cells from the blood or other tissues; rather, it suggested that the initiator of the IFN response might be a myeloid cell endogenous to the joint tissue. This could include macrophages naturally present within in the joint space or synoviocytes of the macrophage lineage.

That $Ly6C^{+}$ myeloid lineage cells contribute to the ultimate development of arthritis is clearly suggested by the dramatic increase in these populations by day 11 postinfection. These cells may also be important in host defense, as their presence at 14 d coincides with our previous identification of upregulation of transcripts associated with host defense at this time point (9). In support of this concept, there was a marked shift in the ratio of PMN to macrophage presence at day 14 postinfection of wild-type mice that did not occur in the absence of IFN signaling (Fig. 5A), consistent with published findings in other experimental models of the role of type I IFN in maturation of the myeloid cells in localized tissues (42). It is interesting to speculate on the possible contribution of this difference to the development of more severe arthritis in C3H mice than in C3H IFNAR1$^{-/-}$ mice.

Changes in cellularity of resident cells of the joint tissue were also found, as shown for the increase in both endothelial cells and fibroblasts in joints of infected mice (Fig. 5B). Endothelial cell ($CD45^{-}CD31^{+}$) and fibroblast ($CD45^{-}CD31^{-}CD90^{+}CD29^{+}$) numbers were increased by days 11 and 14 postinfection in joints from both C3H and C3H IFNAR1$^{-/-}$ mice (Fig. 5B). Increases in these populations were similar in the two mouse strains, indicating lack of dependence on type I IFN. The percentages of endothelial cells and joint fibroblasts that displayed activation markers ($VCAM1^{+}ICAM1^{high}$) were increased by day 11 postinfection, and continued to be elevated through day 14. The similarity in activation marker expression by endothelial cells and joint fibroblasts from C3H and C3H IFNAR1$^{-/-}$ mice indicated that this event was also not dependent on type I signaling (Fig. 5B).

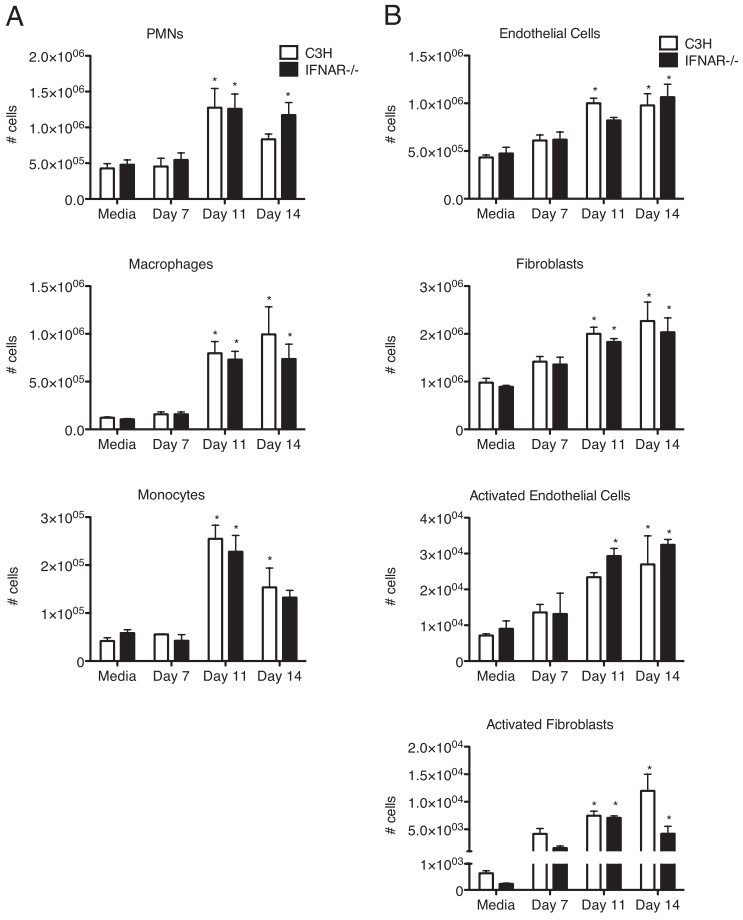

FIGURE 5. Infiltration and expansion of myeloid cells, endothelial cells, and fibroblasts in the joint tissue of *B. burgdorferi*-infected C3H mice. (**A**) Single-cell suspensions were analyzed for the presence of PMNs ($GR1^{+}Ly6C^{+}$ $CD11b^{+}CD45^{+}$), inflammatory monocytes ($Ly6C^{high}GR1^{-}CD11b^{+}$ $CD45^{+}$), and macrophages ($GR1^{-}Ly6C^{dim}$ $F4/80^{+}$ $CD11b^{+}CD45^{+}$) by flow cytometry at days 0 (media), 7, 11, and 14 postinfection with *B. burgdorferi*. Mean ± SEM are indicated, with $n = 3$. (**B**) Single-cell suspensions were analyzed for fibroblasts ($CD45^{-}CD31^{-}CD90^{+}CD29^{+}$) or endothelial cells ($CD45^{-}CD31^{+}$) by flow cytometry at days 0 (media), 7, 11, and 14 of infection. Activated cells were identified as $VCAM1^{+}ICAM1^{high}$. Statistically significant differences were found at 11 and 14 d of infection relative to uninfected mice, for both the C3H and IFNAR$^{-/-}$ mice, but differences were not found between the two mouse genotypes at any time point ($^{*}p < 0.05$) indicated. These results are representative of two separate experiments, $n = 3$.

However, the potential participation of these cells in the amplification of the IFN response and participation in other proinflammatory cascades in C3H mice is clearly supported by the expression of classic activation markers. Thus, the complex environment of the infected joint tissue provides opportunity for activation of multiple cell types that contribute to the IFN-dependent and IFN-independent events associated with the development of Lyme arthritis.

Ex vivo analysis of IFN-responsive cells sorted from the joint tissue of B. burgdorferi-*infected mice*

The presence of activated endothelial cells and fibroblasts in the joint tissue of infected C3H mice suggested that they could be early participants in the response to *B. burgdorferi*, in addition to resident myeloid lineage cells (Figs. 4, 5). To quantitatively analyze the IFN response within the infected joint tissue, single-cell suspensions were prepared by enzymatic digestion, stained with lineage markers, separated by FACS, and RNA recovered for transcript analysis at 0, 7, 11, and 14 d postinfection. The following cell types were identified for cell sorting: myeloid cells were $CD45.2^+Cd11b^+$; lymphoid cells were $CD45.2^+CD11b^-$ ($B220^+$ or $TCR\beta^+$); endothelial cells were $CD45^-CD31^+$ with many of these also expressing high levels of Ly6C; and a final group was comprised of a heterogeneous mixture of stromal cell types, such as fibroblasts, chondrocytes, and smooth muscle cells that were $CD45^-CD31^-$. A subset of this group was $CD90^+CD29^+$, indicative of joint fibroblasts, including synovial fibroblasts, and some of which were also $Ly6C^+$ (data not shown). Pilot studies confirmed that the earliest time to reproducibly capture the IFN profile in cells sorted from the infected joint was day 7 of infection, which coincides with the earliest time point at which *B. burgdorferi* 16S rRNA can be reliably detected in this tissue (data not shown). IFN-inducible transcripts peaked at 7 d postinfection, in both the unfractionated and each of the sorted populations of joint cells, shown for *Cxcl9*, *Iigp*, *Gbp2*, and *Oasl2* (Fig. 6). IFN-induced transcript levels receded dramatically by day 11 postinfection, similar to uninfected levels. In addition to the expected contribution of myeloid cells and lesser contribution of lymphoid cells, endothelial and fibroblast-enriched fractions displayed robust upregulation of the IFN-inducible transcripts. Although the importance of synovial fibroblasts in the pathogenesis of RA is well appreciated (43), the dominating role of endothelial cells and fibroblasts in the tissue response to *B. burgdorferi* infection has not been previously demonstrated. The precise and synchronized timing of the IFN response in all cell lineages further indicates carefully orchestrated expression patterns in the joint tissue.

The results of Fig. 6 implicated both endothelial cells and joint fibroblasts in the early response to *B. burgdorferi* in the joint tissue. An interesting observation from the transcript analysis in Fig. 6 is the finding that both *Iigp* and *Gbp2* were constitutively expressed in endothelial cells at higher concentrations than found in myeloid or fibroblast-enriched cells. This suggested the possibility that endothelial cells of the joint tissue were poised to respond to blood-borne pathogens or inflammatory mediators. Therefore, activation states of endothelial cells and synovial fibroblasts were further dissected with more specific staining reagents, and the FACS separation was repeated for joint tissue from uninfected and day 7 infected C3H mice. Leukocytes were identified as $CD45^+$, endothelial cells were identified as $CD31^+$ $CD45^-$, and in this protocol joint fibroblasts were isolated using the markers $CD45^-$ and $CD31^-$ to remove hematopoietic and endothelial cells, followed by enrichment for fibroblasts, including synovial fibroblasts, using $CD90^+CD29^+$ (Fig. 7A) (44). The fidelity of the sorting protocol was confirmed by lineage-specific transcript analysis and revealed enrichment of CD45 transcripts only in leukocytes, CD31 enrichment in endothelial cells, CD90 (Thy1) enrichment in fibroblasts and leukocytes, and enrichment of fibronectin in joint fibroblasts and other cell types, which were not defined in our analysis, but include epithelial cells, chondrocytes, and smooth muscle cells (Fig. 7B). Transcripts from *Mmp3* were also only identified in the joint fibroblast and other fractions (data not shown), further evidence that this represents a functionally discrete subset in the joint tissue. Similar confirmation of sorting fidelity was obtained for the lineage-sorted fractions used in Fig. 6 (data not shown). The activation status of endothelial cells and fibroblasts in the joint at the critical day 7 time point was studied following FACS recovery of cells stained for VCAM1, ICAM1, and PECAM1. Endothelial cells demonstrated increased staining intensity and transcriptional upregulation for all three activation markers at day 7 postinfection,

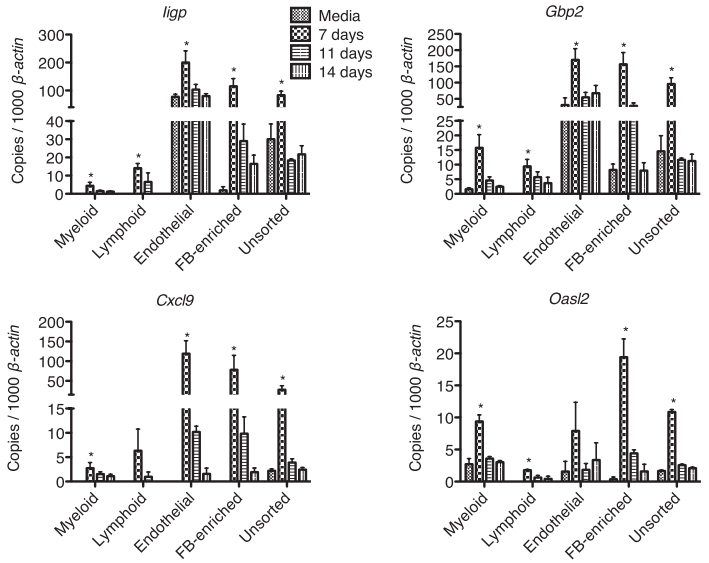

FIGURE 6. Ex vivo identification of endothelial cells and fibroblasts as major contributors to the IFN response of infected C3H joints. FACS analysis of cells released from joint tissue of C3H mice infected for 0 (media), 7, 11, and 14 d. Single-cell suspensions of joint tissue were prepared for lineage staining, and FACS was used to collect and quantify lineages. RT-PCR analysis of sorted lineages at each time point (n = 3). Myeloid cells ($CD45^+CD11b^+$), lymphoid cells ($CD45^+CD11b^-$, $TCR\beta^+$, or $B220^+$), endothelial cells ($CD45^-CD31^+$), and fibroblast-enriched cells ($CD45^-$ $CD31^-$) were sorted simultaneously. Expression of IFN-inducible transcripts, *Gbp2*, *Iigp*, *Cxcl9*, and *Oasl2*, was normalized to *β-actin*. Statistical significance between experimental and control groups ($*p < 0.05$) is indicated.

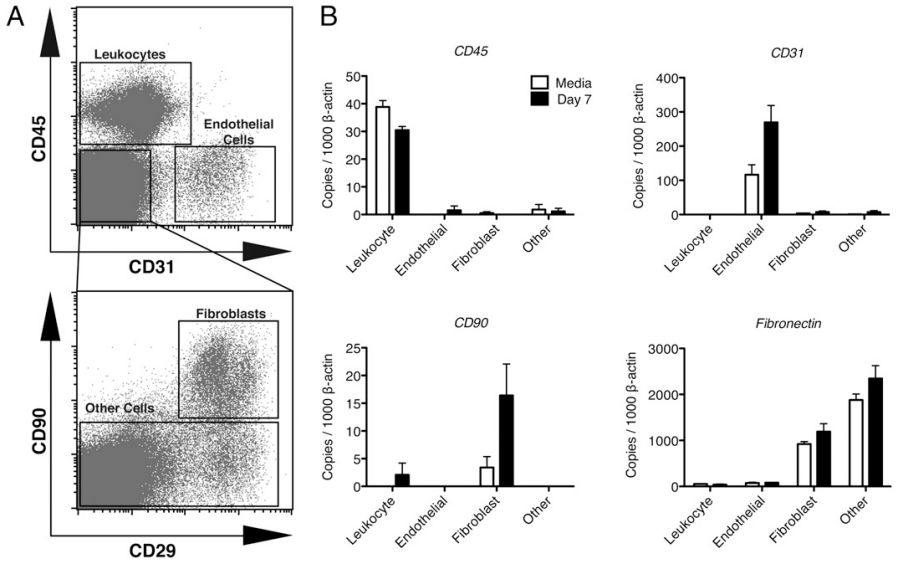

FIGURE 7. Characteristics of endothelial cells and fibroblasts recovered from joints of C3H mice at day 7 postinfection display markers of activation. (**A**) Flow cytometry analysis of single-cell suspensions from joint tissue of uninfected and day 7 infected C3H mice. Fibroblasts were identified as $CD45^-CD31^-CD90^+CD29^+$, whereas endothelial cells were $CD45^-CD31^+$. Cell populations shown for a single mouse, representative of four. (**B**) Accuracy of sorting demonstrated by transcript analysis of lineage-specific markers in indicated FACS-recovered populations: *CD45*, *CD90*, *CD31*, *Fibronectin*, from uninfected (media) and mice infected 7 d earlier with *B. burgdorferi* (day 7).

whereas joint fibroblasts showed increased expression of *Vcam1* and *Icam1* (and do not express *Pecam1*) (Fig. 8A, 8B). These data indicate that cellular activation precedes proliferation of endothelial cells and fibroblasts shown earlier (Fig. 5B), and demonstrate strong correlation between transcript induction and protein expression at day 7 postinfection. Interestingly, these $VCAM1^+ICAM1^+$ fibroblasts were also $Ly6C^+$ (data not shown), and may constitute fibroblast-like synoviocytes implicated in RA (43, 44).

Transcriptional analyses of the highly enriched endothelial and fibroblast fractions from the joint further supported their contribution to the IFN profile at day 7 (Table II). Endothelial cells and fibroblasts were found to be major contributors of the classic IFN-inducible transcripts *Gbp2*, *Iigp*, and *Oasl 2*, as well as the IFN transcriptional activator *Stat1*. The contribution of endothelial cells and fibroblasts to the *B. burgdorferi*-induced IFN response is striking, and previously unrecognized, although human endothelial cell cultures were previously shown to respond to *B. burg-*

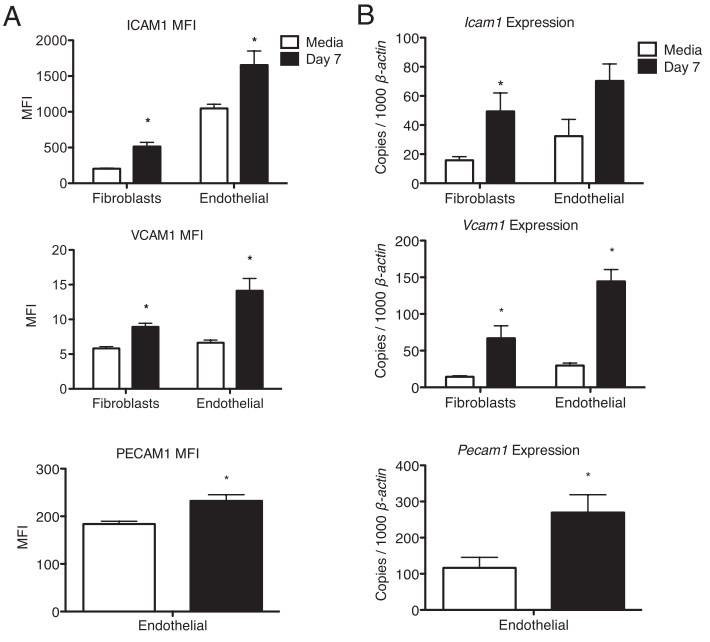

FIGURE 8. Endothelial cells and fibroblasts display activation markers at day 7 of infection. (**A**) Mean fluorescence intensity (MFI) of ICAM1, VCAM1, and PECAM1 on fibroblasts ($CD45^-CD31^-CD90^+CD29^+$) and endothelial cells ($CD45^-CD31^+$) recovered from joint tissue of uninfected mice and mice at day 7 of infection. (**B**) Transcript analysis from cells recovered by FACS analysis of uninfected and day 7 infected mice. RT-PCR performed as described, $n = 4$. Results representative of two independent experiments. Statistical significance between uninfected and infected cell types was determined by Student t test, and is shown ($^*p < 0.05$).

dorferi through a classic NF-κB–dependent signaling cascade (45). Further analyses of the transcriptional response to *B. burgdorferi* revealed both joint fibroblasts and endothelial cells to be the dominant sources of chemokines (Table III), with joint fibroblasts supplying the PMN and monocyte-recruiting *Cxcl1*, *Cxcl2*, *Ccl2*, and *Ccl8*, and endothelial cells serving as the primary source of the CXCR3-interacting chemokines *Cxcl9* and *Cxcl10*, important in recruiting NK and T cells. This coincides with an increase in the expression of the classic activation markers VCAM1, ICAM1, and PECAM1 by fibroblasts and endothelial cells (Fig. 8), which would further contribute to the recruitment of inflammatory cells. Also of note is the production of *Cxcl1* and *Cxcl10* by endothelial cells, important stimulants for neutrophils and activated neutrophils, respectively. The unique contribution of leukocytes to *Cxcl13* recruitment of B lymphocytes may be important in the resolution of infection and disease. It is particularly interesting in light of the strong association of CXCL13 with tissue-specific infection by *B. burgdorferi* in humans (46, 47).

Integration of our ex vivo analysis of the early responses of the infected joint tissue with characteristics of the arthritic lesions at 28 d postinfection has allowed development of a dynamic model for *B. burgdorferi*-induced arthritis development in C3H mice (Fig. 9). Two phases of arthritis development are shown in this model, with the first phase incorporating the initiation of type I IFN production and the upregulation of other proinflammatory molecules, and the second phase depicting the progression to the arthritic lesion. The involvement of myeloid cells, endothelial cells, and fibroblasts is depicted, with upregulation of chemokines by fibroblasts and synoviocytes providing the key stimulus for arthritis development.

Discussion

Previously, we noted a transient and early induction of type I IFN signature transcriptional response in the joint tissue of *B. burgdorferi*-infected C3H mice and determined this to be a predictor of the severity of Lyme arthritis in this mouse strain (9). Subsequently, we discovered that blocking the early type I IFN signaling cascade by systemic administration of mAb muted the arthritic response in C3H mice at 4 wk postinfection, thus formally coupling the induction of type I IFN to Lyme arthritis (13). Together these findings defined a model by which joint-localized bacteria triggered a provocative burst of type I IFN that in turn established an inflammatory cascade that resulted in severe arthritis 2–3 wk later (Fig. 9). The identification of the cellular interactions required to trigger the response in the joint tissue was important in understanding the initiation of this response in C3H mice. A variety of different cell types have been identified as initiators of type I IFN in other infectious and pathological conditions, suggesting that in vivo analysis would be required to characterize the cells responsible for initiating and executing this response in the joint.

To achieve a more rigorous assessment of type I IFN-dependent signaling on the development of Lyme arthritis, the IFNAR1 gene disruption was crossed onto the C3H mouse. Experiments with this mouse strain confirmed the importance of type I IFN signaling in the development of arthritis (Fig. 1), but also confirmed the importance of additional, IFN-independent pathways in the maximal arthritis of infected C3H mice, in line with the documented multigenic nature of this arthritis (24, 30). The development of the C3H IFNAR1$^{-/-}$ mouse permitted the generation of reciprocal radiation chimeras with C3H mice. These experiments revealed contributions of both hematopoietic and mesenchyme-derived cells to the IFN-dependent portion of arthritis development (Fig. 3), consistent with the broad expression of the type I IFN receptor and its importance in promoting the antiviral state in most lineages (16). Interestingly, type I IFN signaling was not required for effective control of bacteria number in joint or other tissues, a contrast from findings with IFN-γ (Figs. 1, 3) (10, 11, 48). This observation raises the possibility that the type I signaling pathway could provide a novel therapeutic target for Lyme arthritis without disrupting the efficacy of ongoing antibacterial treatments.

It is generally accepted that *B. burgdorferi* can enter tissues following hematogenous spread, and that it is the response of the host to bacteria in the tissue that initiates an inflammatory response (5, 49). Therefore, a more precise ex vivo analysis of cells from the joint tissue was employed to assess the cellular dynamics of the response to *B. burgdorferi* invasion. Consistent with the radiation chimera experiment, both hematopoietic cells and fibroblasts and endothelial cells of the joint contributed to the robust IFN profile in infected joint tissue (Figs. 4, 6, Tables II, III). Evaluation of cells recovered from the naive joint revealed a much more limited ability to generate an IFN response to *B. burgdorferi*: only CD45$^+$ cells had this capability. However, both CD45$^+$ and CD45$^-$ cells responded to exogenous IFN-β by amplifying the production of IFN-inducible transcripts, indicating their potential contribution to the arthritis-associated response. Both CD45$^+$ and CD45$^-$ cells of the naive joint upregulated *Tnfα* in response to *B. burgdorferi* in vitro, simulating the potential contribution of IFN-independent signaling pathways during infection.

The ability of human and murine macrophages, monocytes, and dendritic cells to initiate a type I IFN response when stimulated with *B. burgdorferi* in vitro has been clearly documented; how-

Table II. Endothelial cells and fibroblasts are major contributors of IFN-inducible transcripts in joints of *B. burgdorferi*-infected C3H mice

		IFN-Inducible Genes			
Cell Type	Treatment	*Gbp2*	*Iigp*	*Oasl2*	*Stat1*
Leukocyte[a]	Media	2 ± 0.6[b]	ND	3 ± 0.8	10 ± 2.9
	Infected	**29 ± 3.3**[c]	**13 ± 3.7**	**19 ± 5.6**	21 ± 4.2
Endothelial	Media	36 ± 9.0	116 ± 30.1	3 ± 1.7	13 ± 5.7
	Infected	**447 ± 22.3**	**514 ± 62.9**	**44 ± 7.1**	**160 ± 12.7**
Fibroblast	Media	21 ± 2.9	11 ± 1.9	3 ± 1.5	6 ± 1.7
	Infected	**273 ± 39.9**	**188 ± 20.6**	**38 ± 11.1**	**71 ± 23.8**
Other	Media	7 ± 1.3	2 ± 0.9	2 ± 1.0	12 ± 2.4
	Infected	**112 ± 19.6**	**53 ± 15.9**	**14 ± 4.7**	**71 ± 15.5**
Unsorted	Media	28 ± 1.5	82 ± 6.2	4 ± 0.5	10 ± 0.4
	Infected	**134 ± 15.2**	**149 ± 20.7**	**30 ± 1.6**	**53 ± 7.8**

[a]RNA prepared from lineage-sorted joint cells at day 7 of infection.
[b]Mean ± SE for samples from four mice, normalized to *β-actin.*
[c]Bolded numbers indicate greater induction compared with mice treated with media alone, $p < 0.05$.

Table III. Endothelial cells and fibroblasts upregulate various chemokine transcripts in joints of *B. burgdorferi*-infected C3H mice

		Chemokines						
		T, NK Cells		Neutrophils		B Cells	Monocytes, Dendritic Cells	
Cell Type	Treatment	*Cxcl9*	*Cxcl10*	*Cxcl1*	*Cxcl2*	*Cxcl13*	*Ccl2*	*Ccl8*
Leukocyte[a]	Media	0.7 ± 0.4[b]	4 ± 2.4	3 ± 0.8	54 ± 13.2	0.3 ± 0.3	21 ± 3.4	ND
	Infected	5 ± 2.4	13 ± 4.9	9 ± 4.0	43 ± 10.8	**6 ± 0.9**	20 ± 8.2	0.2 ± 0.1
Endothelial	Media	7 ± 2.9	9 ± 8.6	6 ± 3.1	4 ± 2.4	ND	2 ± 1.3	ND
	Infected	**156 ± 11.2**[c]	**124 ± 21.4**	**25 ± 3.6**	4 ± 1.2	1.3 ± 1.3	3 ± 3.0	ND
Fibroblast	Media	0.5 ± 0.5	3 ± 1.6	61 ± 3.2	9 ± 3.0	0.9 ± 0.3	57 ± 8.5	0.3 ± 0.3
	Infected	**87 ± 33.0**	**119 ± 15.9**	**233 ± 30.6**	**49 ± 16.3**	7 ± 3.5	**226 ± 34.1**	**2.4 ± 0.6**
Other	Media	ND	2 ± 1.9	13 ± 3.3	3 ± 2.0	ND	6 ± 0.8	ND
	Infected	16 ± 8.5	**44 ± 7.7**	**36 ± 5.9**	7 ± 3.8	ND	22 ± 12.3	0.6 ± 0.6
Unsorted	Media	4 ± 0.5	7 ± 0.4	23 ± 1.1	16 ± 3.3	0.1 ± 0.06	23 ± 0.8	0.2 ± 0.05
	Infected	**42 ± 7.8**	**42 ± 4.2**	**31 ± 1.9**	24 ± 2.2	**6 ± 2.2**	**29 ± 2.4**	0.5 ± 0.1

[a]RNA prepared from lineage-sorted joint cells at day 7 of infection.
[b]Mean ± SE for samples from four mice, normalized to *β-actin.*
[c]Bolded numbers indicate greater induction compared with mice treated with media alone, $p < 0.05$.

ever, to our knowledge, this is the first study to directly assess the potential of cells of the joint tissue to mount this response. Our results are most consistent with a resident mononuclear cell initiating the IFN profile following phagocytosis of *B. burgdorferi* and processing *Borrelia* ligands capable of activating cellular sensors. Numerous laboratories studying the IFN response to *B. burgdorferi* have identified MyD88-dependent sensors, particularly TLR7/8, and MyD88-independent, IFN regulatory factor-3–dependent sensors capable of inducing type I IFN in cultures of mouse and human mononuclear cells (34–37, 50, 51). *B. burgdorferi* ligands implicated in this response include RNA, lipoproteins, and secreted bacterial components (25, 34, 36, 52). Interestingly, the $Ly6C^+$ inflammatory monocytes, whose recruitment has been implicated in the IFN response in other systems (41, 42, 53), were not increased in joint tissue until day 11 postinfection and, therefore, this expansion was not required for the day 7 IFN signal amplification (Fig. 5). The appearance of $Ly6C^+$ cells may have greater impact on later responses to *B. burgdorferi*, which shift to classic NF-κB–dependent production of cytokines and chemokines on days 11 and 14 postinfection (9).

Ex vivo analysis of cells recovered from joints of infected C3H mice revealed cell types contributing to the IFN transcriptional signature at day 7 postinfection. Whereas the contribution of myeloid cells to the profile was expected, the magnitude of the contribution made by endothelial cells and fibroblasts of the joint tissue was a surprise. Based on our finding that $CD45^-$ cells of joint of naive mice did not upregulate the IFN profile in response to *B. burgdorferi* alone but did respond well to exogenous IFN-β, we suspect that the robust responses of endothelial cells and joint fibroblasts from infected mice reflect the combined effects of *B. burgdorferi* and the autocrine/paracrine activity of type I IFN, together resulting in exuberant production of amplified type I IFN and downstream products (Figs. 4, 6, 8, Table II). The upregulation of *Stat1* transcripts at day 7 postinfection is consistent with the importance of the IFN receptor-dependent amplification stage of this response, even at this early time point.

Of particular importance to the development of Lyme arthritis was the finding that fibroblasts of the joint were the major producers of chemokines involved in recruitment of the hallmark cell of Lyme arthritis, the PMN (Table III). Consistent with these data is the documented role of fibroblast-like synoviocytes in promoting inflammation in RA (54). Brown and colleagues (55, 56) previously demonstrated the critical role of PMN-recruiting chemokines and their receptors in the development of Lyme arthritis, with monocyte chemokines playing an analogous role in carditis development. Our results point to the activated fibroblast (likely synovial) as the source of PMN and monocyte-recruiting chemokines in Lyme arthritis development and resolution. The relative contribution of fibroblasts occupying the joint space versus synoviocytes comprising the membranous synovial sheath could not be determined in this study. These findings indicate that activation of endothelial cells and fibroblasts in the joint sets the stage for subsequent recruitment of arthritis-defining inflammatory cells, as shown in phase 1 of Fig. 9. The importance of additional inflammatory pathways in the sustained recruitment resulting in arthritis development is suggested by the residual Lyme arthritis seen in C3H $IFNAR1^{-/-}$ mice as well as the ability of $CD45^-$ cells from the joint tissue to upregulate transcripts for TNF-α in response to *B. burgdorferi*. The development of severe Lyme arthritis is clearly influenced by multiple pathways activated simultaneously, with the full-blown lesion observed in C3H mice reflecting the combined effects. Fundamental to our model is the requisite involvement of joint-localized bacteria in every stage of lesion development.

Our findings suggest a model by which *B. burgdorferi* exits the vascular endothelium and enters the joint tissue, potentially encountering several types of cells (Fig. 9) (57, 58). Endothelial cells may be the first to encounter *B. burgdorferi* as it exits the blood, and human endothelial cells are known to engage TLR-MyD88–dependent signaling in response to *B. burgdorferi* (45). Fibroblasts are also abundant components of connective tissue of the joint, and the interaction of *B. burgdorferi* with synovial fibroblasts, fibrocytes, and extracellular matrix components of connective tissue has been well established (59, 60). Myeloid cells residing in the joint, possibly including macrophage-like synoviocytes and tissue macrophages, appear to trigger the type I IFN response (Fig. 9). This response most likely requires phagocytosis of *B. burgdorferi* and liberation of bacterial components that result in IFN regulatory factor-3 activation and type I IFN induction (25, 35, 36, 38, 50). Once type I IFN production is initiated, numerous cell types of the joint, particularly endothelial cells and synovial fibroblasts, engage the type I IFN receptor and join the IFN signature response, leading to a positive feedback that amplifies the signaling cascade and sets the stage for the development of severe Lyme arthritis, phase 2 (Fig. 9).

These observations are striking due to the association of excessive production of type I IFN with other inflammatory-based diseases, including patients with SLE and those receiving therapeutic doses of IFN-αβ for hepatitis and multiple sclerosis (14–16, 61). The recent recognition of an IFN signature response in a

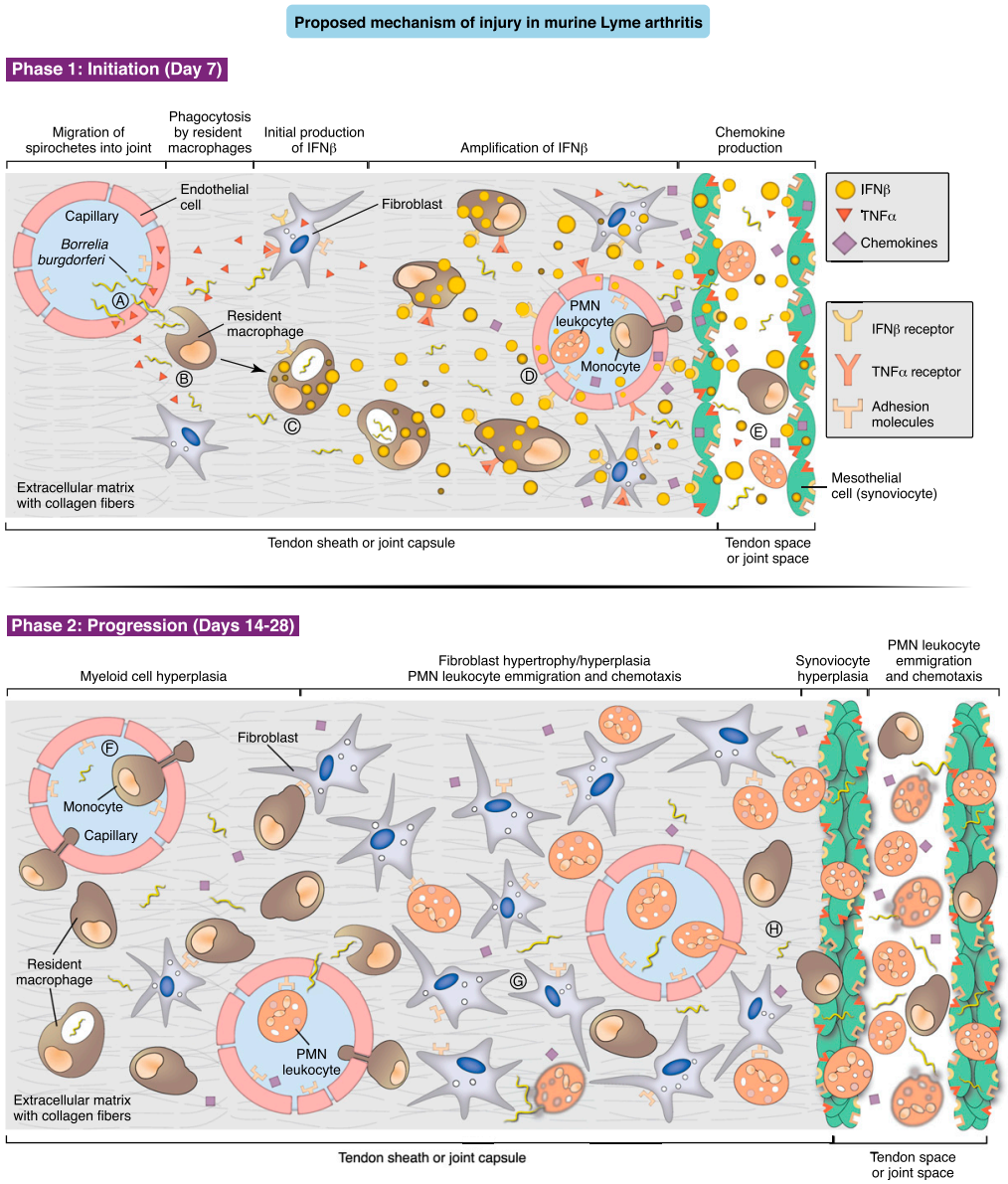

FIGURE 9. Proposed mechanism of injury in joint tissue of C3H mice infected with *B. burgdorferi.* Phase 1: Initiation of the localized inflammatory response. (**A**) Spirochetes migrate to joint tissue, triggering activation of endothelial cells and fibroblasts and upregulation of adhesion molecules. (**B**) Resident myeloid lineage cells, such as macrophages, phagocytose *B. burgdorferi*, triggering production of IFN-β (**C**). (**D**) IFN-β signal is amplified in an autocrine/paracrine fashion, involving a large number of cell types, including endothelial cells and fibroblasts. (**E**) Synoviocytes and endothelial cells produce a variety of chemokines, leading to a chemotactic gradient. Increased adhesion molecule expression potentiates leukocyte migration into tendon sheath and joint capsule. Phase 2: Progression to the joint lesion characteristic of Lyme arthritis (14–28 d). (**F**) Increased expression of cell adhesion molecules on vascular endothelial cells promotes attachment and extravasation of leukocytes into the extracellular matrix, and myeloid hyperplasia. (**G**) Fibroblast hyperplasia and increased vascularization develop within the tendon sheath, as well as (**H**) synoviocyte hyperplasia. IFN-β response is muted by this time point; thus, sustained inflammation most likely reflects effects of classic proinflammatory pathways activated by persisting *B. burgdorferi*. (Figure courtesy of James F. Zachary, University of Illinois-Urbana.)

subgroup of RA patients that fail to respond to targeted TNF-α blockade further suggests our findings may be broadly applicable to newly recognized patient groups (18, 19, 62). We propose the IFN-dependent Lyme arthritis in C3H mice to be a model to study the complex interactions that result in tissue-specific and systemic activation of pathological concentrations of type I IFN. We further propose that the similarities with RA, particularly the involvement of synovial fibroblasts in the amplification of the inflammatory response and recruitment of inflammatory cells, are highly relevant to disease development, and that understanding the dynamics of initiating and amplifying populations in pathological responses may have broad implications for inflammatory joint diseases.

Acknowledgments

We thank Kenneth C. Bramwell and members of the John Weis Laboratory for helpful discussion during the course of this study, the Flow Cytometry Core Facility for expert guidance, and Greg Stoddard in Biostatistics Core for assistance with statistical analysis.

Disclosures

The authors have no financial conflicts of interest.

References

1. Steere, A. C., and L. Glickstein. 2004. Elucidation of Lyme arthritis. *Nat. Rev. Immunol.* 4: 143–152.
2. Steere, A. C., R. T. Schoen, and E. Taylor. 1987. The clinical evolution of Lyme arthritis. *Ann. Intern. Med.* 107: 725–731.
3. Barthold, S. W., D. H. Persing, A. L. Armstrong, and R. A. Peeples. 1991. Kinetics of *Borrelia burgdorferi* dissemination and evolution of disease after intradermal inoculation of mice. *Am. J. Pathol.* 139: 263–273.
4. Barthold, S. W., D. S. Beck, G. M. Hansen, G. A. Terwilliger, and K. D. Moody. 1990. Lyme borreliosis in selected strains and ages of laboratory mice. *J. Infect. Dis.* 162: 133–138.
5. Radolf, J. D., M. J. Caimano, B. Stevenson, and L. T. Hu. 2012. Of ticks, mice and men: understanding the dual-host lifestyle of Lyme disease spirochaetes. *Nat. Rev. Microbiol.* 10: 87–99.
6. Weis, J. J., and L. K. Bockenstedt. 2010. Host response. In *Borrelia; Molecular Biology, Host Interaction and Pathogenesis.* D. S. Samuels and J. D. Radolf, eds. Caister Academinc Press, Norfolk, United Kingdom, p. 433–466.
7. Brown, C. R., A. Y. Lai, S. T. Callen, V. A. Blaho, J. M. Hughes, and W. J. Mitchell. 2008. Adenoviral delivery of interleukin-10 fails to attenuate experimental Lyme disease. *Infect. Immun.* 76: 5500–5507.
8. Brown, J. P., J. F. Zachary, C. Teuscher, J. J. Weis, and R. M. Wooten. 1999. Dual role of interleukin-10 in murine Lyme disease: regulation of arthritis severity and host defense. *Infect. Immun.* 67: 5142–5150.
9. Crandall, H., D. M. Dunn, Y. Ma, R. M. Wooten, J. F. Zachary, J. H. Weis, R. B. Weiss, and J. J. Weis. 2006. Gene expression profiling reveals unique pathways associated with differential severity of lyme arthritis. *J. Immunol.* 177: 7930–7942.
10. Brown, C. R., and S. L. Reiner. 1999. Experimental lyme arthritis in the absence of interleukin-4 or gamma interferon. *Infect. Immun.* 67: 3329–3333.
11. Sonderegger, F. L., Y. Ma, H. Maylor-Hagan, J. Brewster, X. Huang, G. J. Spangrude, J. F. Zachary, J. H. Weis, and J. J. Weis. 2012. Localized production of IL-10 suppresses early inflammatory cell infiltration and subsequent development of IFN-γ-mediated Lyme arthritis. *J. Immunol.* 188: 1381–1393.
12. Wang, X., Y. Ma, A. Yoder, H. Crandall, J. F. Zachary, R. S. Fujinami, J. H. Weis, and J. J. Weis. 2008. T cell infiltration is associated with increased Lyme arthritis in TLR2−/− mice. *FEMS Immunol. Med. Microbiol.* 52: 124–133.
13. Miller, J. C., Y. Ma, J. Bian, K. C. Sheehan, J. F. Zachary, J. H. Weis, R. D. Schreiber, and J. J. Weis. 2008. A critical role for type I IFN in arthritis development following *Borrelia burgdorferi* infection of mice. *J. Immunol.* 181: 8492–8503.
14. Santiago-Raber, M. L., R. Baccala, K. M. Haraldsson, D. Choubey, T. A. Stewart, D. H. Kono, and A. N. Theofilopoulos. 2003. Type-I interferon receptor deficiency reduces lupus-like disease in NZB mice. *J. Exp. Med.* 197: 777–788.
15. Wilson, L. E., D. Widman, S. H. Dikman, and P. D. Gorevic. 2002. Autoimmune disease complicating antiviral therapy for hepatitis C virus infection. *Semin. Arthritis Rheum.* 32: 163–173.
16. Pestka, S. 2007. The interferons: 50 years after their discovery, there is much more to learn. *J. Biol. Chem.* 282: 20047–20051.
17. van der Pouw Kraan, T. C., C. A. Wijbrandts, L. G. van Baarsen, A. E. Voskuyl, F. Rustenburg, J. M. Baggen, S. M. Ibrahim, M. Fero, B. A. Dijkmans, P. P. Tak, and C. L. Verweij. 2007. Rheumatoid arthritis subtypes identified by genomic profiling of peripheral blood cells: assignment of a type I interferon signature in a subpopulation of patients. *Ann. Rheum. Dis.* 66: 1008–1014.
18. van Baarsen, L. G., C. A. Wijbrandts, F. Rustenburg, T. Cantaert, T. C. van der Pouw Kraan, D. L. Baeten, B. A. Dijkmans, P. P. Tak, and C. L. Verweij. 2010. Regulation of IFN response gene activity during infliximab treatment in rheumatoid arthritis is associated with clinical response to treatment. *Arthritis Res. Ther.* 12: R11.
19. Mavragani, C. P., D. T. La, W. Stohl, and M. K. Crow. 2010. Association of the response to tumor necrosis factor antagonists with plasma type I interferon activity and interferon-beta/alpha ratios in rheumatoid arthritis patients: a post hoc analysis of a predominantly Hispanic cohort. *Arthritis Rheum.* 62: 392–401.
20. Müller, U., U. Steinhoff, L. F. Reis, S. Hemmi, J. Pavlovic, R. M. Zinkernagel, and M. Aguet. 1994. Functional role of type I and type II interferons in antiviral defense. *Science* 264: 1918–1921.
21. Yarilina, A., E. DiCarlo, and L. B. Ivashkiv. 2007. Suppression of the effector phase of inflammatory arthritis by double-stranded RNA is mediated by type I IFNs. *J. Immunol.* 178: 2204–2211.
22. Wooten, R. M., Y. Ma, R. A. Yoder, J. P. Brown, J. H. Weis, J. F. Zachary, C. J. Kirschning, and J. J. Weis. 2002. Toll-like receptor 2 is required for innate, but not acquired, host defense to *Borrelia burgdorferi*. *J. Immunol.* 168: 348–355.
23. Huang, X., L. J. Pierce, P. A. Cobine, D. R. Winge, and G. J. Spangrude. 2009. Copper modulates the differentiation of mouse hematopoietic progenitor cells in culture. *Cell Transplant.* 18: 887–897.
24. Ma, Y., J. C. Miller, H. Crandall, E. T. Larsen, D. M. Dunn, R. B. Weiss, M. Subramanian, J. H. Weis, J. F. Zachary, C. Teuscher, and J. J. Weis. 2009. Interval-specific congenic lines reveal quantitative trait loci with penetrant lyme arthritis phenotypes on chromosomes 5, 11, and 12. *Infect. Immun.* 77: 3302–3311.
25. Miller, J. C., H. Maylor-Hagen, Y. Ma, J. H. Weis, and J. J. Weis. 2010. The Lyme disease spirochete *Borrelia burgdorferi* utilizes multiple ligands, including RNA, for interferon regulatory factor 3-dependent induction of type I interferon-responsive genes. *Infect. Immun.* 78: 3144–3153.
26. Ma, Y., K. P. Seiler, K. F. Tai, L. Yang, M. Woods, and J. J. Weis. 1994. Outer surface lipoproteins of *Borrelia burgdorferi* stimulate nitric oxide production by the cytokine-inducible pathway. *Infect. Immun.* 62: 3663–3671.
27. Morrison, T. B., Y. Ma, J. H. Weis, and J. J. Weis. 1999. Rapid and sensitive quantification of *Borrelia burgdorferi*-infected mouse tissues by continuous fluorescent monitoring of PCR. *J. Clin. Microbiol.* 37: 987–992.
28. Sheehan, K. C., K. S. Lai, G. P. Dunn, A. T. Bruce, M. S. Diamond, J. D. Heutel, C. Dungo-Arthur, J. A. Carrero, J. M. White, P. J. Hertzog, and R. D. Schreiber. 2006. Blocking monoclonal antibodies specific for mouse IFN-alpha/beta receptor subunit 1 (IFNAR-1) from mice immunized by in vivo hydrodynamic transfection. *J. Interferon Cytokine Res.* 26: 804–819.
29. Meerpohl, H. G., M. L. Lohmann-Matthes, and H. Fischer. 1976. Studies on the activation of mouse bone marrow-derived macrophages by the macrophage cytotoxicity factor (MCF). *Eur. J. Immunol.* 6: 213–217.
30. Weis, J. J., B. A. McCracken, Y. Ma, D. Fairbairn, R. J. Roper, T. B. Morrison, J. H. Weis, J. F. Zachary, R. W. Doerge, and C. Teuscher. 1999. Identification of quantitative trait loci governing arthritis severity and humoral responses in the murine model of Lyme disease. *J. Immunol.* 162: 948–956.
31. Palucka, A. K., J. P. Blanck, L. Bennett, V. Pascual, and J. Banchereau. 2005. Cross-regulation of TNF and IFN-alpha in autoimmune diseases. *Proc. Natl. Acad. Sci. USA* 102: 3372–3377.
32. Meissner, N., S. Swain, K. McInnerney, S. Han, and A. G. Harmsen. 2010. Type-I IFN signaling suppresses an excessive IFN-gamma response and thus prevents lung damage and chronic inflammation during *Pneumocystis* (PC) clearance in CD4 T cell-competent mice. *Am. J. Pathol.* 176: 2806–2818.
33. Siednienko, J., T. Gajanayake, K. A. Fitzgerald, P. Moynagh, and S. M. Miggin. 2011. Absence of MyD88 results in enhanced TLR3-dependent phosphorylation of IRF3 and increased IFN-β and RANTES production. *J. Immunol.* 186: 2514–2522.
34. Petzke, M. M., A. Brooks, M. A. Krupna, D. Mordue, and I. Schwartz. 2009. Recognition of *Borrelia burgdorferi*, the Lyme disease spirochete, by TLR7 and TLR9 induces a type I IFN response by human immune cells. *J. Immunol.* 183: 5279–5292.
35. Salazar, J. C., S. Duhnam-Ems, C. La Vake, A. R. Cruz, M. W. Moore, M. J. Caimano, L. Velez-Climent, J. Shupe, W. Krueger, and J. D. Radolf. 2009. Activation of human monocytes by live *Borrelia burgdorferi* generates TLR2-dependent and -independent responses which include induction of IFN-beta. *PLoS Pathog.* 5: e1000444.
36. Cervantes, J. L., S. M. Dunham-Ems, C. J. La Vake, M. M. Petzke, B. Sahay, T. J. Sellati, J. D. Radolf, and J. C. Salazar. 2011. Phagosomal signaling by *Borrelia burgdorferi* in human monocytes involves Toll-like receptor (TLR) 2 and TLR8 cooperativity and TLR8-mediated induction of IFN-beta. *Proc. Natl. Acad. Sci. USA* 108: 3683–3688.
37. Cruz, A. R., M. W. Moore, C. J. La Vake, C. H. Eggers, J. C. Salazar, and J. D. Radolf. 2008. Phagocytosis of *Borrelia burgdorferi*, the Lyme disease spirochete, potentiates innate immune activation and induces apoptosis in human monocytes. *Infect. Immun.* 76: 56–70.
38. Shin, O. S., R. R. Isberg, S. Akira, S. Uematsu, A. K. Behera, and L. T. Hu. 2008. Distinct roles for MyD88 and Toll-like receptors 2, 5, and 9 in phagocytosis of *Borrelia burgdorferi* and cytokine induction. *Infect. Immun.* 76: 2341–2351.
39. Bolz, D. D., R. S. Sundsbak, Y. Ma, S. Akira, C. J. Kirschning, J. F. Zachary, J. H. Weis, and J. J. Weis. 2004. MyD88 plays a unique role in host defense but not arthritis development in Lyme disease. *J. Immunol.* 173: 2003–2010.
40. Auerbuch, V., D. G. Brockstedt, N. Meyer-Morse, M. O'Riordan, and D. A. Portnoy. 2004. Mice lacking the type I interferon receptor are resistant to *Listeria monocytogenes*. *J. Exp. Med.* 200: 527–533.
41. Lee, P. Y., J. S. Weinstein, D. C. Nacionales, P. O. Scumpia, Y. Li, E. Butfiloski, N. van Rooijen, L. Moldawer, M. Satoh, and W. H. Reeves. 2008. A novel type I IFN-producing cell subset in murine lupus. *J. Immunol.* 180: 5101–5108.
42. Seo, S. U., H. J. Kwon, H. J. Ko, Y. H. Byun, B. L. Seong, S. Uematsu, S. Akira, and M. N. Kweon. 2011. Type I interferon signaling regulates Ly6C(hi) monocytes and neutrophils during acute viral pneumonia in mice. *PLoS Pathog.* 7: e1001304.
43. Müller-Ladner, U., J. Kriegsmann, B. N. Franklin, S. Matsumoto, T. Geiler, R. E. Gay, and S. Gay. 1996. Synovial fibroblasts of patients with rheumatoid arthritis attach to and invade normal human cartilage when engrafted into SCID mice. *Am. J. Pathol.* 149: 1607–1615.
44. Pilling, D., T. Fan, D. Huang, B. Kaul, and R. H. Gomer. 2009. Identification of markers that distinguish monocyte-derived fibrocytes from monocytes, macrophages, and fibroblasts. *PLoS One* 4: e7475.
45. Wooten, R. M., T. B. Morrison, J. H. Weis, S. D. Wright, R. Thieringer, and J. J. Weis. 1998. The role of CD14 in signaling mediated by outer membrane lipoproteins of *Borrelia burgdorferi*. *J. Immunol.* 160: 5485–5492.
46. Narayan, K., D. Dail, L. Li, D. Cadavid, S. Amrute, P. Fitzgerald-Bocarsly, and A. R. Pachner. 2005. The nervous system as ectopic germinal center: CXCL13 and IgG in lyme neuroborreliosis. *Ann. Neurol.* 57: 813–823.

47. Müllegger, R. R., T. K. Means, J. J. Shin, M. Lee, K. L. Jones, L. J. Glickstein, A. D. Luster, and A. C. Steere. 2007. Chemokine signatures in the skin disorders of Lyme borreliosis in Europe: predominance of CXCL9 and CXCL10 in erythema migrans and acrodermatitis and CXCL13 in lymphocytoma. *Infect. Immun.* 75: 4621–4628.
48. Olson, C. M., Jr., T. C. Bates, H. Izadi, J. D. Radolf, S. A. Huber, J. E. Boyson, and J. Anguita. 2009. Local production of IFN-gamma by invariant NKT cells modulates acute Lyme carditis. *J. Immunol.* 182: 3728–3734.
49. Steere, A. C., J. Coburn, and L. Glickstein. 2004. The emergence of Lyme disease. *J. Clin. Invest.* 113: 1093–1101.
50. Moore, M. W., A. R. Cruz, C. J. LaVake, A. L. Marzo, C. H. Eggers, J. C. Salazar, and J. D. Radolf. 2007. Phagocytosis of *Borrelia burgdorferi* and *Treponema pallidum* potentiates innate immune activation and induces gamma interferon production. *Infect. Immun.* 75: 2046–2062.
51. Hawley, K. L., C. M. Olson, Jr., J. M. Iglesias-Pedraz, N. Navasa, J. L. Cervantes, M. J. Caimano, H. Izadi, R. R. Ingalls, U. Pal, J. C. Salazar, et al. 2012. CD14 cooperates with complement receptor 3 to mediate MyD88-independent phagocytosis of *Borrelia burgdorferi. Proc. Natl. Acad. Sci. USA* 109: 1228–1232.
52. Zhou, X., M. R. Miller, M. Motaleb, N. W. Charon, and P. He. 2008. Spent culture medium from virulent *Borrelia burgdorferi* increases permeability of individually perfused microvessels of rat mesentery. *PLoS One* 3: e4101.
53. Solodova, E., J. Jablonska, S. Weiss, and S. Lienenklaus. 2011. Production of IFN-β during *Listeria monocytogenes* infection is restricted to monocyte/macrophage lineage. *PLoS One* 6: e18543.
54. Laragione, T., M. Brenner, B. Sherry, and P. S. Gulko. 2011. CXCL10 and its receptor CXCR3 regulate synovial fibroblast invasion in rheumatoid arthritis. *Arthritis Rheum.* 63: 3274–3283.
55. Brown, C. R., V. A. Blaho, and C. M. Loiacono. 2003. Susceptibility to experimental Lyme arthritis correlates with KC and monocyte chemoattractant protein-1 production in joints and requires neutrophil recruitment via CXCR2. *J. Immunol.* 171: 893–901.
56. Montgomery, R. R., C. J. Booth, X. Wang, V. A. Blaho, S. E. Malawista, and C. R. Brown. 2007. Recruitment of macrophages and polymorphonuclear leukocytes in Lyme carditis. *Infect. Immun.* 75: 613–620.
57. Harman, M. W., S. M. Dunham-Ems, M. J. Caimano, A. A. Belperron, L. K. Bockenstedt, H. C. Fu, J. D. Radolf, and C. W. Wolgemuth. 2012. The heterogeneous motility of the Lyme disease spirochete in gelatin mimics dissemination through tissue. *Proc. Natl. Acad. Sci. USA* 109: 3059–3064.
58. Moriarty, T. J., M. U. Norman, P. Colarusso, T. Bankhead, P. Kubes, and G. Chaconas. 2008. Real-time high resolution 3D imaging of the lyme disease spirochete adhering to and escaping from the vasculature of a living host. *PLoS Pathog.* 4: e1000090.
59. Coburn, J., J. R. Fischer, and J. M. Leong. 2005. Solving a sticky problem: new genetic approaches to host cell adhesion by the Lyme disease spirochete. *Mol. Microbiol.* 57: 1182–1195.
60. Chmielewski, T., and S. Tylewska-Wierzbanowska. 2010. Interactions between *Borrelia burgdorferi* and mouse fibroblasts. *Pol. J. Microbiol.* 59: 157–160.
61. Tossberg, J. T., P. S. Crooke, M. A. Henderson, S. Sriram, D. Mrelashvili, S. Chitnis, C. Polman, S. Vosslamber, C. L. Verweij, N. J. Olsen, and T. M. Aune. 2012. Gene-expression signatures: biomarkers toward diagnosing multiple sclerosis. *Genes Immun.* 13: 146–154.
62. Vosslamber, S., H. G. Raterman, T. C. van der Pouw Kraan, M. W. Schreurs, B. M. von Blomberg, M. T. Nurmohamed, W. F. Lems, B. A. Dijkmans, A. E. Voskuyl, and C. L. Verweij. 2011. Pharmacological induction of interferon type I activity following treatment with rituximab determines clinical response in rheumatoid arthritis. *Ann. Rheum. Dis.* 70: 1153–1159.

CHAPTER 3

MICRORNA-146a PROVIDES FEEDBACK REGULATION OF LYME ARTHRITIS BUT NOT CARDITIS, DURING INFECTION WITH *BORRELIA BURGDORFERI*

Abstract

MicroRNAs have been shown to be important regulators of inflammatory and immune responses and are implicated in several immune disorders, including systemic lupus erythematosus and rheumatoid arthritis, but their role in Lyme borreliosis remains unknown. We performed a microarray screen for expression of miRNAs in joint tissue from three mouse strains infected with *Borrelia burgdorferi*. This screen identified upregulation of miR-146a, a key negative regulator of NF-κB signaling, in all three strains, suggesting it plays an important role in the *in vivo* response to *B. burgdorferi*. Infection of B6 miR-146a$^{-/-}$ mice with *B. burgdorferi* revealed a critical nonredundant role of miR-146a in modulating Lyme arthritis without compromising host immune response or heart inflammation. The impact of miR-146a was specifically localized to the joint, and did not impact lesion development or inflammation in the heart. Furthermore, B6 miR-146a$^{-/-}$ mice had elevated levels of NF-κB-regulated products in joint tissue and serum late in infection. Flow cytometry analysis of various lineages isolated from infected joint tissue of mice showed that myeloid cell infiltration was significantly greater in B6 miR-146a$^{-/-}$ mice, compared to B6, during *B. burgdorferi* infection. Using bone marrow-derived macrophages, we found that TRAF6, a known target of miR-146a involved in NF-κB activation, was dysregulated in resting and *B. burgdorferi*-stimulated B6 miR-146a$^{-/-}$ macrophages, and corresponded to elevated IL-1β, IL-6, and CXCL1 production. This dysregulated protein production was observed in macrophages treated with IL-10 prior to *B. burgdorferi* stimulation. Peritoneal macrophages from B6 miR-146a$^{-/-}$ mice also showed enhanced phagocytosis of *B. burgdorferi*. Together, these data

show that miR-146a-mediated regulation of TRAF6 and NF-κB, and downstream targets such as IL-1β, IL-6, and CXCL1, are critical for modulation of Lyme arthritis during chronic infection with *B. burgdorferi*.

Author Summary

Lyme Disease is caused by infection with the bacteria *Borrelia burgdorferi*, is transmitted through infected deer ticks (*Ixodes scapularis*), and often leads to arthritis that can persist, even after antibiotic treatment. Here, we have identified a microRNA that is critical in modulating Lyme arthritis, but not carditis. This microRNA, miR-146a, is a negative regulator of NF-κB signaling, known to be important in host defense against pathogens, and long suspected to play a role in Lyme arthritis development. Mice lacking miR-146a develop more severe arthritis and show signs of hyperactive NF-κB activation during the persistent phase of infection. Heart manifestations of disease were not altered. Furthermore, this severe arthritis is independent of host defense, since these mice are better able to clear invading bacteria in joints, and bacterial numbers are similar in heart and ear tissue. We identified TRAF6 as an important target of miR-146a-mediated NF-κB regulation of pro-inflammatory cytokines IL-6 and IL-1β, as well as chemokines CXCL1 and CXCL2. Our data demonstrate the importance of maintaining appropriate regulation of amplitude and resolution of NF-κB activation during *Borrelia burgdorferi* infection, and provide a novel model for elucidating the role of NF-κB in Lyme arthritis development, independent of effect on host defense.

Introduction

Lyme Disease is caused by infection with *Borrelia burgdorferi,* a tick-borne spirochete [1], and is the most common vector-borne disease in the United States with an estimated 300,000 cases per year [2]. Often, infection leads to acute arthritis in humans. Clinical manifestations of Lyme arthritis include inflammatory cell infiltration, edema, synovial hyperplasia, and remodeling of bone and connective tissue [3,4]. In some cases, infection can induce autoimmunity, despite treatment with antibiotics [5]. The reason why arthritis fails to resolve remains poorly understood, but is believed to be the result of dysregulation of host immune response to infection [6].

Several inbred mouse strains exhibit varying degrees of disease severity similar to human patients [7,8]. Whereas the C57BL/6 (B6) mouse strain develops mild arthritis, C3H and various knockout strains, such as B6 $IL10^{-/-}$ mice, develop moderate to severe arthritis [7,9]. Furthermore, the intensity of the inflammatory response for a given spirochete burden varies greatly among strains, implicating host immune response as driving arthritis development [9,10]. Our laboratory and others have used the mouse model system to elucidate key regulators of host immune response to infection.

Since its discovery, nuclear factor-kappa B (NF-κB) has been identified as a key regulator in many cellular functions, including inflammation and cancer [11]. *B. burgdorferi* lipoproteins are extremely potent activators of Toll-like receptor 2 (TLR2)-mediated NF-κB activation and cytokine production, and are important for host defense [12-16]. Mice lacking TLR2 or the adapter protein myeloid differentiation primary response gene (88) (MyD88) exhibit a failure to control infection [14,17-21]. Although

these knockout studies clearly demonstrate an important role of NF-κB in host defense, elucidating its role in inflammation and Lyme arthritis has remained elusive.

While NF-κB activation is critical in response to infection, downregulation is equally important to avoid excess inflammation, tissue damage, and autoimmunity [22]. MicroRNAs (miRNAs) have recently been identified as being important regulators of NF-κB [23] and autoimmunity [24]. These small regulatory RNAs are posttranscriptional regulators of gene expression [25], and one miRNA, miR-146a, has been shown to be a modulator of innate immune response to Toll-like receptor (TLR) ligands [26]. Targets of miR-146a include TNF receptor associated factor 6 (TRAF6) and IL-1 receptor associated kinase 1 (IRAK1), adaptor molecules downstream of the MyD88-dependent TLR and cytokine signaling pathways [27]. Importantly, miR-146a itself is upregulated by IL-1β and TLRs, including TLR2, and thus acts as a negative feedback regulator of NF-κB signaling, which is required for immune homeostasis *in vivo* [27-31].

Aberrant microRNA expression, particularly miR-146a, has been associated with a variety of inflammatory disorders [32]. In systemic lupus erythematosus, a functional variant in the miR-146a promoter is associated with disease risk [33], and abnormally low miR-146a expression has been associated with more severe symptoms [34]. In contrast, rheumatoid arthritis synovial fibroblasts express abnormally high levels of miR-146a [35,36], while osteoarthritis chondrocytes express variable levels miR-146a, correlating with disease severity [37,38].

Despite correlative evidence linking aberrant miRNA expression to diseases such as lupus, RA, and OA, determining whether miRNAs play an active role in pathogenesis has yet to be elucidated, and to our knowledge, no studies have examined the role of

miRNAs in Lyme arthritis. For these reasons, we sought to determine whether changes in miRNA expression contributed to host defense and Lyme arthritis development during *B. burgdorferi* infection.

Results

miR-146a is highly upregulated in B6, C3H, and B6 IL10$^{-/-}$ mice during infection

MicroRNA dysregulation has been associated with a number of inflammatory disorders, and we hypothesized that these may play an important role in response to *B. burgdorferi* infection and Lyme arthritis development. We therefore performed a genome-wide screen of changes in miRNA expression in joints of B6, C3H, and B6 IL-10$^{-/-}$ mice infected with *B. burgdorferi* at one and two weeks postinfection using an Agilent mouse microRNA microarray (Table 3.1, Table 3.S1). MicroRNAs differentially regulated included many that have been identified previously as important regulators of immune function. Interestingly, each infection model had a unique miRNA expression "signature," and we found that only a few dozen miRNAs showed changes in expression during infection. Most of these changes were in C3H mice, and may be due to both differences in inflammatory response and intrinsic differences in miRNA function between strains. At two weeks postinfection, two miRNAs, miR-21 and miR-146a, both induced by NF-κB and associated with TLR signaling, were the most highly upregulated in all three strains (Table 3.1), and were confirmed using qRT-PCR (Figure 3.1). Furthermore, these miRNAs maintained high expression, even at 4 weeks postinfection. Interestingly, miR-155 was significantly upregulated in B6 IL10$^{-/-}$ mice, but not in B6 or C3H mice. This microRNA is a proinflammatory NF-κB-induced miRNA associated

with T cell-dependent inflammation and autoimmunity [39-41], and expression is suppressed by IL-10 [42].

Of these, miR-146a was of particular interest, given recent reports showing a link between miR-146a and susceptibility to a variety of inflammatory disorders. Targets of miR-146a, IRAK1 and TRAF6 [27], are involved in TLR2/NF-κB activation, which is an important pathway in controlling *B. burgdorferi* infection [13,14,17-21]. Also, the observation that miR-146a was upregulated in all three strains suggested that this miRNA likely plays a general role in regulating the immune response to *B. burgdorferi*. For these reasons, our focus turned to studying miR-146a. A B6 miR-146a$^{-/-}$ knockout mouse was recently generated [28], which provided a powerful tool to evaluate the role of miR-146a in mildly arthritic B6 mice. While miR-146a was also upregulated in arthritis-susceptible C3H mice, we suspected that other genetic factors play a dominant role in arthritis development, including excessive Type I IFN production [43,44] and accumulation of undigested glycosaminoglycans in joint tissue [45]. These effects may limit the ability of miR-146a to modulate arthritis development in the C3H mouse model. It is tempting to speculate, however, that lack of miR-146a in the arthritis-susceptible C3H mouse would lead to even more severe arthritis, as has been reported in the C3H IL-10$^{-/-}$ mouse model [46].

Impact of miR-146a on Lyme arthritis, carditis, and host defense

Since miR-146a is an important negative regulator of NF-κB activation, we hypothesized that a B6 mouse deficient in miR-146a would develop more severe arthritis during infection with *B. burgdorferi* compared to WT controls. To avoid age-related pathologies associated with B6 miR-146a$^{-/-}$ mice [30], we used 6-8 week-old mice, which

is also the age of optimal arthritis in other mouse strains. Arthritis was assessed in *B. burgdorferi*-infected B6 and B6 miR-146a$^{-/-}$ mice. At 4 weeks postinfection, B6 miR-146a$^{-/-}$ mice developed significantly more severe arthritis. Several markers of arthritis were elevated in B6 miR-146a$^{-/-}$ mice, including ankle swelling (Figure 3.2A), number and severity of lesions observed, polymorphonuclear (PMN) cell infiltrate, reactive/reparative score (periosteal hyperplasia and new bone formation and remodeling), and tendon sheath thickness (Table 3.2). Cranial tibial tendon is enlarged in Figure 3.2B. Control (BSK-injected) mice showed no significant arthritis in either strain, and no significant difference between strains was seen in mononuclear cell infiltrate into inflammatory processes. Importantly, B6 miR-146a$^{-/-}$ mice did not display overwhelming numbers of bacteria; rather, they tended to have somewhat fewer bacteria in infected joints and similar burden in infected heart and ear tissue, as measured by *B. burgdorferi*-specific*16S rRNA* normalized to *β-actin* in joints and heart, and *recA* normalized to mouse *nidogen* in ear tissue (Figure 3.2C). This difference in bacterial load in joint tissue was likely not due to differences in antibody response since *B. burgdorferi*-specific IgM and IgG levels were similar between the two strains at 2 weeks and 4 weeks postinfection, respectively (Figure 3.2D). While this does not rule out the possibility that different borrelial proteins could be opsonic targets in the two strains, these data support the notion that increased arthritis observed in B6 miR-146a$^{-/-}$ mice was likely due to a defect in regulation of host immune function rather than compromised host defense. In fact, the decrease in *16S rRNA* in B6 miR-146a$^{-/-}$ mouse joints indicated that arthritis development was independent of bacterial density. This increased arthritis severity with accompanying decreases in bacterial burden is also observed in the B6 IL10$^{-/-}$ mouse

model of arthritis [9,47,48], and is believed to be due primarily to enhanced innate immune responses [49].

In addition to joints, the heart is another target of *B. burgdorferi* infection in mice. We therefore looked for evidence of miR-146a modulating inflammation in heart tissue. Mice are susceptible to Lyme carditis in an MHC-independent manner, and exhibit variation in disease severity, with C3H mice harboring a greater number of bacteria and developing more severe carditis and B6 mice being resistant and harboring fewer bacteria [7,50,51]. Lyme carditis is also observed in humans, and although rare, can be fatal [52]. To assess the role of miR-146a in modulating heart inflammation, B6, B6 miR-146a$^{-/-}$, and C3H mice were infected with *B. burgdorferi* for 3 weeks and hearts were removed and assessed for bacterial numbers and changes in transcripts of inflammatory genes. As was seen at 4 weeks postinfection (Figure 3.2C), bacterial burden, as measured by qRT-PCR analysis of *B. burgdorferi 16S rRNA*, was similar between B6 and B6 miR-146a$^{-/-}$ mice, and both trended lower than what was seen in heart tissue from C3H mice (Figure 3.3A). Lesions in the heart were also scored for carditis in B6, B6 miR-146a$^{-/-}$, and C3H mice at 3 weeks postinfection. Overall lesion scores were similar in B6 and B6 miR-146a$^{-/-}$ mice, and both trended lower than lesion severity in C3H mice (Figure 3.3B).

Lesions in hearts at 3 weeks postinfection were characterized by acute to subacute vasculitis/perivasculitis (see Figure 3.3C) of the 1) microvasculature (capillaries) at the base of the heart (in heart muscle) where the aorta and pulmonary arteries arise, 2) microvasculature (capillaries) within connective tissues supporting these arteries, and 3) microvasculature (capillaries) of the vasa vasorum of the aorta and pulmonary arteries. These lesions affected the vascular system, rather than being primary lesions of the heart

muscle (myocarditis). The character and pattern of distribution of these lesions suggested that inflammation of the microvasculature is the result of some type of localized target cell (i.e., endothelium) or target substance (i.e., bacteria) specificity for this location consistent with *Borrelial* adhesin-host ligand binding within the vascular endothelium [53,54]. Vascular turbulence or oxygen concentration could also be involved.

Lyme carditis is associated with macrophage infiltration [50], and invariant NKT cells have been shown to play a protective role in B6 mice [55]. We therefore used PCR analysis of macrophage (CD11b and F4/80) and NKT cell (CD4 and Vα14) markers to assess changes in cellularity in infected heart tissue (Figure 3.3D), as performed previously [56,57]. Significant upregulation of macrophage markers *CD11b* and *F4/80* was observed in all three strains, as expected based on previous research [50]. The magnitude of upregulation was not different between B6 and miR-146a deficient mice, indicating no role of miR-146a feedback on inflammation in this tissue. Interestingly, while *CD11b* and *F4/80* transcripts were also significantly upregulated in C3H mice, the degree of upregulation was somewhat less than upregulation observed in B6 and B6 miR-146a$^{-/-}$ mice at 3 weeks postinfection. Because these data are from whole heart tissue, they reflect cumulative changes in myeloid cell numbers from the entire heart, including changes in resident cardiac macrophages [58], which may dilute out lesion-specific changes identified by histopathology.

CD4 transcript levels were not significantly different between strains, but while both B6 and B6 miR-146a$^{-/-}$ mice contained similar levels of *Vα14* that trended higher at 3 weeks, C3H mice had very low levels of this transcript in both uninfected and infected heart tissue. This is consistent with significant variation of NKT cell numbers between

different mouse strains [57]. PCR analysis was also used to determine changes in expression of various inflammatory cytokines and chemokines in heart tissue (Figure 3.3D). As previously reported, C3H mice had elevated levels of *IFN*γ transcripts in infected heart tissue [59], which was significantly higher than *IFN*γ mRNA in B6 and B6 miR-146a$^{-/-}$ hearts. This trend was also observed for *IL6* transcripts, although there was significant variation in expression within C3H mice. No differences among B6, B6 miR-146a$^{-/-}$, and C3H mice were observed for transcripts of *IL1β, TNFα, Cxcl1, Cxcl2, Ccl2, IL10,* or *IL12* (data not shown). Together, these data suggest that the nature of host defense, macrophage and NKT cell proliferation and infiltration, as well as cytokine and chemokine expression, is very similar in infected B6 and B6 miR-146a$^{-/-}$ heart tissue, but is quite distinct from observations in carditis-susceptible C3H mice. Fundamental differences between strains have been reported previously in Lyme carditis studies comparing the effect of Stat1 [60] and Ccr2 [51] deficiencies on carditis-susceptible and carditis-resistant mouse strains. Together, these data show that while strain-specific variables influence differences in carditis susceptibility between B6 and C3H mice, miR-146a has no impact on carditis severity in B6 mice.

B6 miR-146a$^{-/-}$ mice exhibit hyperactive expression of NF-κB target cytokines and chemokines at 4 weeks postinfection

Because miR-146a is known to negatively regulate NF-κB activation, we compared transcripts of genes upregulated by NF-κB in infected joint tissue from B6 and B6 miR-146a$^{-/-}$ mice at 2 and 4 weeks postinfection. We observed that a number of NF-κB inducible genes were significantly elevated at 4 weeks postinfection (but not at 2 weeks), by qRT-PCR, in B6 miR-146a$^{-/-}$ joints, compared to WT, including cytokines *IL-*

1β and *IL-6,* as well as neutrophil chemokines *Cxcl1* and *Cxcl2* (Figure 3.4A). CXCL1 has been shown to be required for full arthritis development in C3H mice [61,62], and increased expression of this gene in B6 miR-146a$^{-/-}$ mice could be directly contributing to arthritis development through recruitment of neutrophils. This is supported by the increase in PMN infiltrate seen at 4 weeks by histopathology, shown in Table 3.2. Elevated *IL-1β* transcript level is also particularly interesting, since the IL-1 receptor (IL-1R) uses the same adaptors as TLR2/1 for signal transduction, is strongly upregulated by myeloid cells during phagocytosis of *B. burgdorferi* [63], and is dependent on IRAK1 and TRAF6, two miR-146a targets [27]. Furthermore, IL-1β stimulates miR-146a upregulation *in vitro* [27], suggesting that this miRNA negatively regulates IL-1β signaling. It is important to note that uninfected B6 miR-146a$^{-/-}$ mice did not exhibit any abnormalities in expression of these genes, indicating that this hyperactivity is due to a failure to downregulate the NF-κB response after infection, rather than general NF-κB hyperactivity, as is observed in aging B6 miR-146a$^{-/-}$ mice [30].

Only a distinct subset of inflammatory cytokines and chemokines (*IL-1β, IL-6, Cxcl1, Cxcl2*) appeared to be dysregulated in B6 miR-146a$^{-/-}$ joints. Transcript levels of other Lyme arthritis-associated genes (*IFNγ, Cxcl10, TNFα*) were very similar between the two strains (Figure 3.4A), and showed a peak in expression at 2 weeks postinfection, followed by resolution at 4 weeks. This is in contrast to arthritis-susceptible B6 IL10$^{-/-}$ mice, where previously published data show that in addition to upregulation in *IL-1β, IL-6, Cxcl1, Cxcl2, IFNγ*, and *Cxcl10* are upregulated 16-fold and 141-fold at 2 weeks, and 22-fold and 189-fold at 4 weeks, respectively [47]. These data together indicate that the

B6 miR-146a$^{-/-}$ mouse is distinct from the B6 IL10$^{-/-}$ model, which is associated with a dramatic IFNγ signature in joints and elevation of IFNγ in serum at 4 weeks p.i. [47,48].

In order to determine whether there was systemic dysregulation of NF-κB-inducible cytokines, serum was collected from *B. burgdorferi*-infected mice at 4 weeks postinfection and cytokine levels were measured by enzyme-linked immunosorbent assay (Figure 3.4B). B6 miR-146a$^{-/-}$ mice contained higher levels of IL-6 at 4 weeks postinfection, compared to wild-type, consistent with observations in joint tissue. TNFα and IL-12 serum levels were very similar between strains, and although levels of IFNγ varied widely in B6 miR-146a$^{-/-}$ mice, they were not significantly greater than B6 levels.

Effect of miR-146a in cell populations isolated from joints early in infection

To identify the effect of miR-146a in various joint cell populations during the early phage of infection *ex vivo,* we digested joints with purified collagenase to release cells into a single-cell solution in order to identify and isolate cell fractions based on lineage markers, including CD45 for leukocytes, CD11b for myeloid cells, CD31 for endothelial cells, and CD29 for fibroblast-enriched cells (Figure 3.5A). This method has been used in C3H mice to identify cellular sources of genes associated with the arthritogenic Type I IFN response early in infection, and is a sensitive assay to observe cell type-specific effects *ex vivo* that might be missed using whole joint tissue [43]. Using this method, we were able to determine the effect of miR-146a on specific cell types early in infection (Figure 3.5B). Levels of *IL-1β*, while trending higher in myeloid cells isolated from B6 miR-146a$^{-/-}$ mice, were not significantly different between the two strains. In B6 mice, three genes, *Cxcl2* and the IFN-inducible gene *Oasl2* (in myeloid

cells) and *Cxcl1* (in fibroblasts), tended to peak in expression at Day 7 postinfection. In contrast, transcripts were somewhat higher in uninfected B6 miR-146a$^{-/-}$ cell fractions vs. WT, and remained elevated throughout infection. This suggests that B6 miR-146a$^{-/-}$ mice may be poised to initiate a hyperactive immune response. There was no difference in lymphoid *IFNγ* expression between strains, which peaked at Day 14 postinfection, as was seen in whole joint tissue (Figure 3.4A). It is important to note that, unlike published observations in C3H mice [43], B6 miR-146a$^{-/-}$ mice did not exhibit a robust induction of IFN-responsive genes, such as *Oasl2,* in fibroblasts or endothelial cells at Day 7 postinfection (data not shown). Overall, these data, combined with data from Figure 3.4, suggest that a number of NF-κB-inducible genes in B6 miR-146a$^{-/-}$ mouse joints are poised for hyper-activation prior to infection, and peak at 4 weeks postinfection, indicating that miR-146a acts to resolve the inflammatory response late in infection, rather than limiting the amplitude of inflammation during early stages of infection.

Myeloid cell recruitment is increased in infected joints of B6 miR-146a$^{-/-}$ mice

During cell sorting, we observed differences in cellular infiltrate, particularly in the myeloid cell lineages, in joints during infection. Therefore, a more rigorous analysis of myeloid cells recruited to the joint by flow cytometry was performed at various times during infection. Using joint cell isolation methods described in Figure 3.5, myeloid cells were characterized from infected joints at 2 and 4 weeks postinfection using fluorescently labeled antibodies against CD11b, F4/80, Ly6C, Gr1, and CD206. CD11b+ myeloid cell populations clustered roughly into three populations, F4/80+ Ly6C^{lo} macrophages, Gr1^{hi} Ly6C^{int} PMNs, and Gr1^{int} Ly6C^{hi} monocytes (Figure 3.6A&B). Furthermore, F4/80+

Ly6C^{lo} macrophages expressed variable levels of CD206 (MRC1, Mannose Receptor C type 1), a marker of alternatively activated (M2-like) macrophages [64]. There was little difference between strains in mean fluorescence intensity (MFI) of MRC1 and Gr1 in each myeloid subpopulation, suggesting that they were phenotypically similar populations. However, while the number of these three myeloid populations in B6 mouse joints changed only modestly in B6 mice, myeloid cell numbers in B6 miR-146a$^{-/-}$ joints were significantly elevated at both 2 and 4 weeks postinfection (Figure 3.6C). An increased trend in PMN infiltration in B6 miR-146a$^{-/-}$ mice is also consistent with histopathology data shown in Table 3.2, despite the propensity of PMNs to lyse during enzymatic digestion of joint tissue, resulting in some sample to sample variation. Interestingly, there was little difference between strains in infiltrating lymphoid cells at 2 or 4 weeks postinfection (Figure 3.S1). These data, as well as the observation of similar *B. burgdorferi*-specific antibody levels (Figure 3.2D), suggest that arthritis and host defense phenotypes observed in B6 miR-146a$^{-/-}$ mice shown in Figure 3.2 and Table 3.2 are driven primarily by myeloid cells.

Bone marrow-derived macrophages from B6 miR-146a$^{-/-}$ mice are hyper-responsive to B. burgdorferi *and have elevated protein levels of TRAF6*

The data from Figure 3.6 implicated myeloid cells as contributors of arthritis development in B6 miR-146a$^{-/-}$ mice. We therefore turned to bone marrow-derived macrophages (BMDMs) to elucidate the molecular mechanism of miR-146a regulation of NF-κB during *B. burgdorferi* infection. BMDMs were cultured from bone marrow extracted from B6 or B6 miR-146a$^{-/-}$ mice and treated with *B. burgdorferi* for 6 and 24

hours. We then measured transcripts of *IL1β, IL6,* and *TNFα* (Table 3.3). Transcripts of *IL1β* were approximately 4-fold higher in B6 miR-146a$^{-/-}$ BMDMs, vs. WT, at both 6 and 24 hours, and *IL6* levels were 7.5-fold higher at 6 hours and 2.5-fold higher at 24 hours poststimulation. Interestingly, *TNFα* transcripts were only 20-30 percent higher in B6 miR-146a$^{-/-}$ BMDMs, compared to WT. Transcripts for all three cytokines were very low in uninfected cells, and were similar between the two strains (data not shown). This suggests that miR-146a effect on *IL1β* and *IL6* regulation is greater than its effect on *TNFα* expression.

We also measured levels of several NF-κB inducible cytokines by ELISA in cell supernatant from both B6 and B6 miR-146a$^{-/-}$ BMDMs at 24 hours poststimulation, including TNFα IL-1β, IL-6 and IL-12, CXCL1, and IL-10 (Figure 3.7A). After 24 hours of treatment with *B. burgdorferi*, three cytokines, IL-1β, IL-6, and IL-12, and the neutrophil chemokine CXCL1, were more abundant in B6 miR-146a$^{-/-}$ cell supernatant than in B6 cell supernatant, consistent with hyperactive NF-κB activation and transcript analysis (Table 3.3). Interestingly, TNFα, an early-response NF-κB cytokine, did not share this trend, which may be due to the relatively late time point used for this analysis [65]. Production of IL-10 was robust in both strains, although somewhat greater in miR-146a-deficient BMDMs.

Previous work from our laboratory showed that many macrophages are IL-10 producers in joints of B6 mice [48]. Also, macrophages produce high levels of IL-10 when treated with *B. burgdorferi in vitro*, which is important in regulating bacterial persistence [49] and immune response [46,66-68]. Data from Figure 3.6B also showed that many macrophages in joints of infected B6 and B6 miR-146a$^{-/-}$ mice express the

alternatively activated macrophage marker MRC1. While it is difficult to accurately determine the range of macrophage phenotypes present in joints, we used BMDMs pretreated with IL-10 as an *in vitro* model to study miR-146a effects on IL-10-stimulated macrophages. BMDMs were treated with 1ng/ml IL-10 for 4 hours prior to 24-hour *B. burgdorferi* stimulation. Surprisingly, while pretreatment with IL-10 led to an approximately 80 percent reduction in IL-6 production in B6 BMDMs, IL-10-mediated suppression of IL-6 in B6 miR-146a$^{-/-}$ BMDMs was drastically reduced, with only ~20 percent decrease in IL-6 production after IL-10 pretreatment, indicating that IL-10 was unable to effectively suppress IL-6 expression in the absence of miR-146a. These data are consistent with *in vivo* data showing consistently elevated IL-6 protein in serum from 4 week-infected B6 miR-146a$^{-/-}$ mice in Figure 3.4. However, IL-10 pretreatment did lead to significantly reduced IL-12 and TNFα production in both strains, as well as high production of IL-10, after *B. burgdorferi* treatment, consistent with an anti-inflammatory M2-like phenotype. Both IL-1β and CXCL1 remained higher in B6 miR-146a$^{-/-}$ BMDMs compared to B6 BMDMs, although IL-1β levels were unaffected, and CXCL1 levels were modestly reduced by IL-10 pretreatment. Importantly, levels of IL-12, TNFα, and IL-10 were very similar between the two strains, suggesting there was no miR-146a-mediated defect in M2 polarization in response to IL-10 pretreatment. This is consistent with *in vivo* observations, where TNFα, IL-12, and IFNγ serum protein levels were not significantly elevated in B6 miR-146a$^{-/-}$ mice at 4 weeks postinfection, relative to B6 mice (Figure 3.4B).

MicroRNAs, including miR-146a, have distinct mRNA targets, depending on cell type [69]. It was therefore important to determine the mRNA target most affected at the

protein level by the presence or absence of miR-146a in BMDMs. Immunoblot analysis was performed on protein extracts from B6 and B6 miR-146a$^{-/-}$ BMDMs treated for 24 hours with *B. burgdorferi* to measure protein levels of three targets of miR-146a, TRAF6, IRAK1, and STAT1 (Figure 3.7B). TRAF6 protein expression was elevated over 2-fold in both resting and stimulated B6 miR-146a$^{-/-}$ BMDMs compared to B6, while protein levels of IRAK1 were similar between strains. STAT1 protein was also higher in resting B6 miR-146a$^{-/-}$ BMDMs compared to B6, but this difference between strains was not observed after 24 hours stimulation. Transcript analysis of *Traf6*, *Irak1* and *Stat1* also show this trend (Figure 3.7C). It is interesting that in the case of TRAF6, the difference observed at the protein level was greater than that seen at the transcript level, where transcripts were typically only 30-50 percent greater in B6 miR-146a$^{-/-}$ BMDMs vs. B6 BMDMs, suggesting that miR-146a effect on translational inhibition is more pronounced than its effect on mRNA stability. This is consistent with a growing body of evidence suggesting that microRNA-mediated translational repression is dependent on inhibition of translation initiation, rather than mRNA degradation [70,71]. The difference between protein and transcript levels of these three genes (Figure 3.7B, C) strongly suggests that posttranscriptional regulatory mechanisms including, but not limited to, microRNA-mediated repression, play an important role in determining cellular protein levels. STAT1 is known to be regulated by a large number of posttranslational modifications that affect function [72]. Both STAT1 and IRAK1 protein levels have been shown to be tightly regulated through ubiquitin E3 ligase-directed degradation [73,74]. In the case of IRAK1 and STAT1, these data suggest that miR-146a-independent regulatory mechanisms seem to be dominant compared to miR-146a-mediated regulation. Taken together, TRAF6

protein levels appear to be the most sensitive to the presence or absence of miR-146a in myeloid cells, and imply miR-146a-mediated translational repression of TRAF6 is required to properly regulate production of NF-κB-induced cytokines in response to *B. burgdorferi.* The lack of difference in STAT1 protein level is also consistent with a failure to observe significant differences between B6 and B6 miR-146a$^{-/-}$ mice in the IFN response (Figures 3.4&3.5).

Macrophages lacking miR-146a have increased phagocytic activity

One possible explanation for reduced numbers of *B. burgdorferi* in joints of infected B6 miR-146a$^{-/-}$ mice is that macrophages lacking miR-146a are more highly phagocytic. In order to measure phagocytic activity, peritoneal macrophages were collected from B6 and B6 mir-146a$^{-/-}$ mice and stimulated with GFP-labeled *B. burgdorferi* for 1 or 2 hours at 10:1 MOI. Phagocytosis of GFP-*B. burgdorferi* was measured by flow cytometry (Figure 3.8A&B). At both 1 and 2 hours poststimulation, peritoneal macrophages lacking miR-146a had significantly higher numbers of GFP+ cells, as well as a higher MFI for GFP in GFP+ macrophages. These data suggest that there are more B6 miR-146a$^{-/-}$ peritoneal macrophages associated with higher numbers of bacteria than WT cells.

Flow cytometry was unable to distinguish localization of the cell-associated bacteria. To determine whether GFP-*B. burgdorferi* were intracellular or adhering to the cell surface, confocal microscopy was used to visualize the bacteria associated with peritoneal macrophages. Peritoneal macrophages were stimulated with GFP-*B. burgdorferi* at 100:1 MOI for 1 hour and stained for the lysosomal protein LAMP1 (red), the macrophage-specific surface protein F4/80 (blue), and nuclei were stained with DAPI

(gray, Figure 3.8C). Bacteria were visible adhering to cell surface (white triangle), inside macrophage pseudopodia (white arrow) and inside cells associated with LAMP1 (white chevron). While bacteria adhering to the cell surface and inside pseudopodia had a spirochetal shape, bacteria associated with lysosomes were amorphous, and formed bright GFP puncta, indicative of bacterial degradation. These bright GFP puncta were predominant throughout the entire sample, as represented in the image in Figure 3.8C for B6 mice, and in Figure 3.S2 for B6 miR-146a$^{-/-}$ mice. This indicates that phagocytosis occurs very rapidly as previously reported [65], and the flow cytometry analysis infers that miR-146a modulates the level of phagocytic activity. Although the mechanism is unknown, similar transcript levels were seen for TLR2, CD14, as well as the scavenger receptor MARCO (data not shown), which have been recently implicated in *B. burgdorferi* uptake [75-78]. Previous reports showing phagocytosis influencing cytokine production in human mononuclear cells [78], and B6 MyD88$^{-/-}$ BMDMs being defective in bacterial internalization [79], are consistent with B6 miR-146a$^{-/-}$ BMDMs having elevated cytokine production and enhanced phagocytic activity (Figure 3.7, Table 3.3, Figure 3.8). While more research is necessary to elucidate this mechanism, these data suggest that B6 miR-146a$^{-/-}$ macrophages have enhanced phagocytosis, and may help explain why joint tissue from B6 miR-146a$^{-/-}$ mice contains fewer numbers of spirochetes (Figure 3.2C).

Discussion

These data have allowed us to generate a model (Figure 3.9) where miR-146a is upregulated during *B. burgdorferi* infection, and acts as a nonredundant suppressor of inflammation and arthritis (Figures 3.1&3.2). Interestingly, lack of miR-146a had no

effect on heart inflammation and carditis (Figure 3.3), indicating fundamental differences between arthritis and carditis development. Differences in carditis severity between B6 and C3H mice are believed to be closely associated with differences in bacterial dissemination and clearance between the two strains [80]. This is consistent with the positive correlation between bacterial numbers and heart lesion severity in B6, B6 miR-146a$^{-/-}$, and C3H mice (Figure 3.3A-B), and with previous reports showing no correlation between quantitative trait loci associated with arthritis severity and bacterial numbers in heart tissue [81,82]. Importantly, differential contribution of NF-κB regulation was not predicted from studies with mice deficient in TLR2 and MyD88, as both hearts and joint tissues displayed increased presence of *B. burgdorferi* [18,19,83].

Numerous studies have revealed different mechanisms of pathogenesis in carditis development and differing contributions of innate and adaptive responses in bacterial clearance and resolution of carditis and arthritis. For example, although antibody response plays an essential role in resolution of arthritis, a greater role for CD4+ T cells and iNKT cells as sources of IFNγ are reported in protection and resolution of Lyme carditis [55,60,84-86]. Other gene knockout and cytokine blocking studies have shown tissue-specific effects of IL-10 [46] and chemokines [51,62] on arthritis and carditis severity. These results suggest future microRNA studies on carditis should focus on those miRs known to influence the balance of CD4+ T cells [87] and iNKT cell function, such as miR-150 and miR-181a/b [88-90].

Myeloid cells respond to a variety of *Borrelia* stimuli through TLRs that lead to activation of NF-κB and upregulation of hundreds of genes involved in controlling infection and initiating the adaptive response. miR-146a is also upregulated, and is an

important check on the amplitude and duration of the NF-κB response. In the absence of this microRNA, this response is dysregulated, leading to increased transcription of certain NF-κB-inducible cytokines and chemokines in infected joint tissue, primarily late in infection (Figures 3.4&3.5). Myeloid cells exhibit excessive proliferation and infiltration into joint tissue of B6 miR-146a$^{-/-}$ mice, have increased phagocytic activity, and produce excess cytokines such as IL-1β, IL-6, and CXCL1, leading to inflammation of synovial tissue and arthritis development (Figures 3.6-3.8). Regulation of the inflammatory response via a miR-146a-mediated negative feedback loop is critical for resolution of the NF-κB response during the persistent phase of infection, and mice lacking this miRNA are poised to develop arthritis upon infection with *B. burgdorferi*.

NF-κB activation in response to *B. burgdorferi* infection is a double-edged sword. On one hand, NF-κB activation is critical in mounting an effective immune response to control infection; on the other hand, dysregulated activation leads to inflammation and arthritis. Because of the dual nature of NF-κB in inflammation and host defense, decoupling these two roles has been difficult. Knockout models using B6 TLR2$^{-/-}$ or MyD88$^{-/-}$ mice have shown the important role of NF-κB in host defense, but because these mice have such a severe innate defect in bacterial defense, elucidating the role of NF-κB in arthritis using these models has remained difficult. The B6 miR-146a$^{-/-}$ mouse model of Lyme arthritis is unique in that it effectively decouples these two roles, leaving the bactericidal function intact while increasing the amplitude of proinflammatory NF-κB activation. This has allowed us to identify its role in arthritis development, independent of its role in host defense, and suggests that miR-146a could be a valuable therapeutic target for control of inflammation without compromising ability to clear an infection.

MicroRNAs are a unique class of regulatory molecules. Unlike transcription factors, they do not act as on/off switches; rather they function as "fine tuners" of gene expression [26]. We have taken advantage of this property to decouple the roles of NF-κB in host defense and inflammation. Young B6 miR-146a$^{-/-}$ mice are phenotypically similar to wild-type B6 mice, and it is only upon chronic exposure to inflammatory stimuli that immunological defects are seen [29]. Consistent with this, endotoxin tolerance is highly dependent upon miR-146a expression in THP-1 cells [91]. Using Lyme arthritis as a model, we have shown that mice lacking this key miRNA fail to adequately maintain immune homeostasis, and develop inflammatory arthritis during a chronic bacterial infection (Figure 3.2, Table 3.2).

This model is also distinct from other mouse models of Lyme arthritis. For example, C3H mice exhibit a robust Type I IFN expression profile early in infection, which contributes to arthritis, and is absent in the mildly arthritic B6 mouse [43,44,47]. This IFN response was also absent miR-146a$^{-/-}$ mice, similar to B6. Furthermore, B6 IL10$^{-/-}$ mice, a model for Th1-mediated arthritis, have a very pronounced IFNγ signature beginning at 14 days postinfection that persists for several weeks [48]. This pattern was also not observed in the arthritic B6 miR-146a$^{-/-}$ mice (Figures 3.4&3.5, Figure 3.S1). Additionally, while B6 miR-146a$^{-/-}$ and B6 IL10$^{-/-}$ mice both exhibit increased bacterial clearance, likely due to an enhanced myeloid response to phagocytosis of bacteria [63], only B6 IL10$^{-/-}$ mice show enhanced antibody response [49]. It was somewhat surprising that B6 miR-146a$^{-/-}$ mice did not exhibit a strong T-cell-mediated phenotype, based on parameters tested, since other studies have shown an important role of miR-146a in regulating Th1 responses [31,92]. It is possible that the elevated myeloid response could

eventually lead to a dysregulated T-cell response in some cases. Indeed, several B6 miR-146a$^{-/-}$ mice did have elevated serum IFNγ at 4 weeks postinfection, although this was the exception rather than the rule, and average levels did not achieve statistical significance compared to wild-type mice (Figure 3.4C). It may also be possible that robust production of IL-10 seen in B6 miR-146a$^{-/-}$ mice is sufficient to suppress any T-cell dysregulation due to lack of miR-146a. Nevertheless, the results of this study show that arthritis is influenced principally by hyperactive myeloid cell activation.

The role of miR-146a in regulating NF-κB activation was consistent with the observed defect in downregulation of NF-κB-dependent cytokines and chemokines *IL-1β, IL-6*, *Cxcl1,* and *Cxcl2,* in B6 miR-146a$^{-/-}$ mice at 4 weeks postinfection (Figure 3.4). Dysregulation of *Cxcl1* in these mice was particularly interesting because previous studies have shown that C3H mice lacking CXCL1 have reduced neutrophil infiltration and arthritis [61,62]. This neutrophil chemokine is tightly regulated both at the transcriptional and posttranscriptional level by both TLR-dependent and cytokine-dependent mechanisms [93]. Data from Figure 3.7 suggest that excess cytokine production by B6 miR-146a$^{-/-}$ macrophages may lead to enhanced CXCL1 production by resident cells *in vivo*. Therefore, miR-146a, expressed primarily in leukocytes [29], likely has cell-extrinsic effects on nonhematopoietic cell function and arthritis development. Recently, IL-6 has been shown to be an important downstream target of miR-146a in regulating hematopoiesis and myeloproliferation [29]. This is consistent with increased IL-6 production shown in Figure 3.4 and Figure 3.7, and corresponding increase in myeloid cell infiltration into joint tissue (Figure 3.6). Thus, miR-146a-mediated

regulation of several cytokines and chemokines likely has a combined effect on inflammatory responses.

Increased phagocytic activity, as well as elevated IL-1β production (Figures 3.7&3.8), point to a previously unrecognized role of miR-146a in phagocytosis and caspase-1 activation. While this role remains to be elucidated, previous research has shown that *B. burgdorferi* induces caspase-1-dependent IL-1β production, and caspase-1 is important for inflammatory cell influx into joint tissue [94]. Additionally, phagocytosis of live *B. burgdorferi* is a potent activator of IL-1 β in human PBMCs [95].

Targets of miR-146a have been studied in many cell types, and it is becoming increasingly evident that the modulatory effect of miR-146a is dependent on cell type and physiological condition. For example, STAT1 appears to be an important miR-146a target in regulatory T-cells [92], and IRAK1 and TRAF6 both appear to be important miR-146a targets in splenocytes [31] and in human monocytes [30]. This study highlights the particular role of miR-146a targeting TRAF6 in myeloid cells (Figure 3.7), indicating that miR-146a function is, to a certain degree, cell type-specific. Importantly, several observations in the B6 miR-146a$^{-/-}$ mouse model are recapitulated in Lyme disease patients. Joint fluid and synovial tissue from antibiotic-refractory Lyme arthritis patients contain higher levels of IL-6 and IL-1β, as well as Th1 cytokines and chemokines, compared with patients whose arthritis is resolved after antibiotic treatment, and IL-1β remains elevated in these treatment-refractory patients long after antibiotic therapy [96,97]. Thus, the B6 miR-146a$^{-/-}$ model of Lyme arthritis could be a useful tool in further understanding how regulation of NF-κB is related to Lyme disease pathogenesis.

Materials and Methods

Ethics statement

Mice were housed in the University of Utah Comparative Medicine Center (Salt Lake City, UT), following strict adherence to the guidelines according to the National Institutes of Health for the care and use of laboratory animals, as described in the Guide for the Care and Use of Laboratory Animals, 8th Edition. Protocols conducted in this study were approved and carried out in accordance to the University of Utah Institutional Animal Care and Use Committee (Protocol Number 12-01005). Mouse experiments were performed under isofluorane anesthesia, and every effort was made to minimize suffering.

Mice, bacterial cultures and infections, and assessment of arthritis severity

C3H, C57BL/6, and B6.129P2-*IL-10tm1Cgn*/J (B6 IL-$10^{-/-}$) mice were obtained from Jackson Laboratories. B6 miR-$146a^{-/-}$ KO mice on a pure C57BL/6 background were generated as described [28]. Mice were infected with $2x10^4$ bacteria of *B. burgdorferi* strain N40 (provided by S. Barthold, University of California, Davis, CA) by intradermal injection into the skin of the back. Infection was confirmed in mice sacrificed before 14 d of infection by culturing bladder tissue in BSK II media containing 6 percent rabbit serum (Sigma-Aldrich), phosphamycin, and rifampicin. ELISA quantification of *B. burgdorferi*-specific IgM and IgG concentrations was used to confirm infection in mice sacrificed at and after 14 d of infection as described [17]. Ankle measurements were obtained using a metric caliper. Rear ankle joints were prepared for assessment of histopathology by removal of the skin and fixation of tissue in 10 percent neutral buffered

formalin. Decalcified joints were embedded in paraffin, sectioned at 3 μm, and stained with H&E. Each slide was scored from 0 to 5 for various aspects of disease, including polymorphonuclear leukocyte (PMN) and mononuclear cell (lymphocytes, monocytes, macrophages) infiltration into inflammatory processes, tendon sheath thickening (hypertrophy and hyperplasia of surface cells and/or underlying dense sheets of cells resembling immature fibroblasts, synoviocytes, and/or granulation tissue), reactive/reparative responses (periosteal hyperplasia and new bone formation and remodeling), and overall lesion (composite score based on all lesions observed in 6-8 sections per joint), with 5 representing the most severe lesion, and 0 representing no lesion. Ankle measurements and arthritic lesions were assessed in coded samples.

Hearts of B6, B6 miR-146a$^{-/-}$, and C3H mice were assessed for carditis by histopathologic evaluation at 3 weeks postinfection. Hearts were fixed in 10 percent neutral buffered formalin, embedded in paraffin, sectioned at 3 μm, and stained with H&E. Lesion scoring was performed in a blinded fashion based on a composite of 11 sections per sample, with a score of 5 representing the maximum lesion and 0 representing no lesion.

miRNA microarray

Microarray analysis was performed with the assistance of the University of Utah Microarray and Bioinformatics core facilities. Whole joint RNA was purified from mouse joints (3-4 mice per sample group) using miRNeasy kit (Qiagen). RNA quality was determined using a Bioanalyzer 2100 and RNA 6000 Nano Chip (Agilent Technologies). Agilent Mouse miRNA microarray v2 (8x15k) was hybridized with Cyanine-3 labeled miRNA (using 100 ng total RNA) using the Agilent one-color GE hybridization and

wash kit. Slides were scanned in a G2505C Microarray Scanner at 2 um resolution (Agilent Technologies). TIF files generated from the scanned microarray image were analyzed in the Agilent Feature Extraction Software (v.10.5), which was used to calculate feature intensities, background measurements, and statistical analyses. Data sets for each biological sample were then filtered and log(2) transformed using an in-house java script, and were uploaded into Geospiza GeneSifter Analysis Edition (Perkin Elmer). Pair-wise analysis between groups was performed using a quality cutoff for both groups of 1, normalizing to median values, with a cutoff value of 2-fold change compared to uninfected controls.

Isolation of DNA from ear tissue and quantification of B. burgdorferi

DNA was prepared from ear tissues frozen at the time of sacrifice. Tissue was incubated in 50 mM NaOH for 1 hour at 93°C and neutralized with 1M Tris (pH 8). Quantification of *B. burgdorferi recA* normalized to the mouse *nidogen* was performed using a Roche LC-480 using previously published primers [18].

Preparation of single-cell suspensions from mouse tissue

Single-cell suspensions were prepared as previously described [43]. Skin was removed from rear ankle joints and digested for 1 hour at 37°C in RPMI 1640 containing 0.2 mg/ml purified enzyme blend for tissue dissociation (Roche) and 100 μg/ml DNase I (Sigma-Aldrich), following partial removal of tissue from bone using 20-gauge syringe needles. Single cell suspension was filtered through a 100 μm cell strainer and red blood cells were lysed using ammonium-chloride-potassium (ACK) lysing buffer.

Isolation of RNA and quantitative RT-PCR

For all experiments examining expression in heart and joint tissue, RNA was purified from the heart or tibiotarsal joints with the skin removed. Tissue was immediately immersed in RNA stabilization solution (Qiagen) and stored at -80°C. Total RNA was recovered from homogenized tissue using the miRNeasy kit (Qiagen). For FACS-sorted cell populations, sorted cells were collected directly in flow tubes containing 0.5 ml RNA stabilization solution (Qiagen) and RNA was recovered using the miRNeasy kit (Qiagen). RNA from BMDMs was recovered using guanidium thiocyanate-phenol-chloroform extraction reagent (Invitrogen). RNA recovered from tissue and cells was reverse transcribed, and transcripts were quantified using a Roche LC-480 according to our previously described protocols [47]. For mature miRNA quantification, cDNA was synthesized using the mercury Locked Nucleic Acid Universal RT microRNA PCR, Polyadenylation and cDNA synthesis kit (Exiqon), and miR-146a, 5S rRNA Locked Nucleic Acid primer sets were used (Exiqon) to quantify miRNA using a Roche LC-480. Other primer sequences used in this study were as follows: *Itgam* (CD11b) FWD (5'-CCTTCATCAACACAACCAGAGTGG-3') REV (5'-CGAGGTGCTCCTAAAACCAAGC-3'), *Irak1* FWD (5'-TGTGCCGCTTCTACAAAGTG-3') REV (5'-TGTGAACGAGGTCAGCTACG-3') *Traf6* FWD (5'-AAGCCTGCATCATCAAATCC-3') REV (5'-CTGGCACTTCTGGAAAGGAC-3'). Primer sequences for *B. burgdorferi 16S rRNA*, *β-actin*, *Il1β*, *Stat1, Tnfa, Oasl2* [47], *Vα14, F4/80* [48] *Il10, Ifng*, *Cxcl10, Il6* [44] *Cxcl1*, *Cxcl2*, *Pecam1* (CD29), and *Ptprc* (CD45) [43] can be found in indicated citations.

Flow cytometry

All flow cytometry data were analyzed using FlowJo (v.5) software. Sorting experiments were performed using a BD FACSAria II. All other FACS data were collected on a BD LSRII flow cytometer. 7-aminoactinomycin D (eBioscience) or DAPI (Invitrogen) was used in all experiments, and dead cells and cell doublets were excluded from analyses. All Abs used for flow cytometry were purchased from either BioLegend or eBioscience. Unconjugated F_c blocking Ab (clone 93; BioLegend) was included in all Ab-labeling experiments. Position of gates for sorting and analysis was based on analysis of appropriate isotype controls. Fluorochrome-conjugated Abs and isotype controls used in this study were as follows: APC/Cy7-conjugated anti-CD11b (M1/70) and anti-CD45.2 (104); FITC-conjugated anti-CD8a (53-6.7), anti-CD11b (M1/70), and anti-Gr-1 (RB6-8C5); PerCP/Cy5.5-conjugated anti-Ly6C (HK1.4), anti-CD4 (RM4-4), and anti-CD31 (390); PE-conjugated anti-F4/80 (BM8), anti-LAMP-1 (1D4B), and anti-NK1.1 (PK136); PE/Cy-7–conjugated anti-CD4 (GK1.5) and anti-TCR β (H57-597); APC-conjugated anti-CD206 (MMR) and anti-F4/80 (BM8); and Brilliant Violet 605-conjugated anti-B220 (RA3-6B2). Confirmation of cell sorting efficiency was performed using qRT-PCR of surface markers used.

Bone marrow-derived macrophage stimulation

Bone marrow-derived macrophages (BMDMs) were isolated from the femurs and tibias of mice, as previously described [98]. Macrophage cultures were plated in 12-well plates at a density of 6×10^5/ml in media containing the serum replacement Nutridoma (Roche) and stimulated with live *B. burgdorferi* cN40 (7.5×10^6/ml). Priming of macrophages was performed by preincubating cells with 1 ng/ml mouse recombinant IL-

10 for 4 hours prior to addition of *B. burgdorferi.* After 24 hours, cell supernatants were collected and analyzed by enzyme-linked immunosorbent assay (ELISA). For expression analysis, RNA was collected from cells at 6 hours and 24 hours poststimulation, and mRNA quantification was performed by qRT-PCR using methods described above.

ELISA analysis of mouse serum and cell supernatant

Blood from mice was obtained by submandibular puncture at the time of euthanasia. Blood was allowed to clot, centrifuged, and serum was collected and stored at -20°C prior to analysis. Cell supernatant was used immediately or stored at -20°C prior to analysis. Cytokine concentration in serum samples and cell supernatant was detected by sandwich ELISA using capture and biotinylated antibodies against mouse IL-1β (clones B122 and Poly5158, Biolegend), IL-6 (clones MP5-20F3 and MP5-32C11, BD Biosciences), IL-10 (clones JESS-2A5 and SXC-1, BD Biosciences), IL-12 (clones C15.6 and C17.8, BD Biosciences), IFNγ (clones R46A2 and XMG1.2, BD Biosciences), TNFα (clones G281-2626 and MP6-XT3, BD Biosciences), and CXCL1 (clone 48415 and Cat BAF453, R&D Systems).

Immunoblot analysis

Cells were washed and lysed at 4° C. with NP-40 lysis buffer (0.5 percent NP-40) for 1 hour followed by boiling for 5 minutes in SDS sample buffer. Protein concentration was measured using a BCA protein assay (Thermo Scientific). Proteins were separated by polyacrylamide gel electrophoresis (PAGE) and transferred overnight at 4°C. onto an Immobilon-P membrane (Millipore). Membrane was blocked with 5% milk in TBST and stained with the following antibodies: rabbit anti-TRAF6 (clone H-274, Santa Cruz),

rabbit anti-IRAK1 (clone D51G7, Cell Signaling), rabbit anti-STAT1 (Cell Signaling #H9172S), and rabbit anti-β-actin (clone 13E5, Cell Signaling) as a loading control. Horseradish peroxidase-conjugated goat anti-rabbit IgG (BioRad) was used as a secondary antibody prior to incubation with enhanced chemoluminescent substrate (Thermo Scientific). Membrane was exposed to autoradiography film (GeneMate) and developed using a medical film processor (SRX-701, Konica Minolta).

Phagocytosis Assay

Mice received an intraperitoneal (IP) injection of 3 ml of 3 percent thioglycollate 4 days prior to harvesting of peritoneal macrophages. Macrophages were removed from sacrificed mice by IP injection of 5 ml ice-cold PBS. Red blood cells were lysed using ACK lysis buffer. $5x10^5$ cells were adhered to a 12-well plate in RPMI+10 percent FBS for 4 hours, after which cells were washed and unadhered cells removed. $5x10^6$ *B. burgdorferi* strain N40 constitutively expressing GFP under the flaB promoter [99] (a gift from Dr. Jay Carroll) were added to cells in RPMI.B (75 percent RPMI+10 percent FBS+25 percent BSKII), as described [100], plates were centrifuged at 500g for 5 minutes and incubated for 1 or 2 hours, after which cells were washed gently 3x in warm PBS and gently removed from the plate using a cell scraper. Cells were washed 2x with ice-cold PBS and supernatant discarded following centrifugation. Washed cells were then resuspended in flow buffer and analyzed by flow cytometry using a BD LSRII flow cytometer. As a negative control, untreated cells and cells incubated with unlabeled *B. burgdorferi* N40 were used.

Confocal microscopy

Peritoneal macrophages were harvested as described above and allowed to adhere to the surface of etched microscope cover slides for 4 hours. Cells were incubated with GFP-*B. burgdorferi* for 1 hour at a 100:1 MOI as described above, followed by 4x washes with warm PBS, fixed in 4 percent paraformaldehyde, and incubated with antibody blocking solution (3 percent BSA 0.05 percent milk 0.2 percent Tween20 in PBS) for 1 hour at RT. Cells were then stained with PE-conjugated LAMP-1, APC-conjugated F4/80, and DAPI for 1 hour in antibody solution (1 percent BSA 0.02 percent Tween20 in PBS), washed and mounted onto a glass slide using fluorescent mounting reagent (Calbiochem EMD Millipore). Confocal imaging was performed on a FV1000 inverted confocal microscope (Olympus) using FV10-ASW software (Olympus). Images were taken using a 60x oil lens with a 1024x1024 2x zoom, and captured at a plane dissecting the middle of cell nuclei. All imaging was performed at the University of Utah Cell Imaging Core Facility, with the assistance of Dr. Christopher Rodesh.

Data and statistical analysis

Microarray data statistical analysis was performed using the Agilent Feature Extraction Software (v.10.5) and Geospiza GeneSifter Analysis Edition (Perkin Elmer), as described. Raw and adjusted p values were derived by Welch's *t* test with Benjamini and Hochberg correction, using a raw p value cutoff of $p < 0.05$ signifying statistical significance. All other graphical data represent the mean ± SEM. Statistical analysis was performed using Prism 5.0c software. Multiple-sample data sets were analyzed by one-way ANOVA with Dunnet's or Tukey's post hoc test for pair-wise comparisons, as

appropriate and indicated in figure legends. Two-sample data sets were analyzed by Student *t* test. Categorical data for histopathology were assessed by Mann-Whitney *U* test. Statistical significance indicated in figure legends.

References

1. Burgdorfer W, Barbour AG, Hayes SF, Benach JL, Grunwaldt E, et al. (1982) Lyme disease-a tick-borne spirochetosis? Science 216: 1317-1319.

2. Kuehn BM (2013) CDC estimates 300,000 US cases of Lyme disease annually. JAMA 310: 1110.

3. Steere AC, Glickstein L (2004) Elucidation of Lyme arthritis. Nat Rev Immunol 4: 143-152.

4. Steere AC, Schoen RT, Taylor E (1987) The clinical evolution of Lyme arthritis. Ann Intern Med 107: 725-731.

5. Drouin EE, Seward RJ, Strle K, McHugh G, Katchar K, et al. (2013) A novel human autoantigen, endothelial cell growth factor, is a target of T and B cell responses in patients with Lyme disease. Arthritis Rheum 65: 186-196.

6. Duray PH, Steere AC (1988) Clinical pathologic correlations of Lyme disease by stage. Ann N Y Acad Sci 539: 65-79.

7. Barthold SW, Beck DS, Hansen GM, Terwilliger GA, Moody KD (1990) Lyme borreliosis in selected strains and ages of laboratory mice. J Infect Dis 162: 133-138.

8. Barthold SW, Persing DH, Armstrong AL, Peeples RA (1991) Kinetics of Borrelia burgdorferi dissemination and evolution of disease after intradermal inoculation of mice. Am J Pathol 139: 263-273.

9. Brown JP, Zachary JF, Teuscher C, Weis JJ, Wooten RM (1999) Dual role of interleukin-10 in murine Lyme disease: regulation of arthritis severity and host defense. Infect Immun 67: 5142-5150.

10. Ma Y, Seiler KP, Eichwald EJ, Weis JH, Teuscher C, et al. (1998) Distinct characteristics of resistance to Borrelia burgdorferi-induced arthritis in C57BL/6N mice. Infect Immun 66: 161-168.

11. DiDonato JA, Mercurio F, Karin M (2012) NF-kappaB and the link between inflammation and cancer. Immunol Rev 246: 379-400.

12. Weis JJ, Ma Y, Erdile LF (1994) Biological activities of native and recombinant Borrelia burgdorferi outer surface protein A: dependence on lipid modification. Infect Immun 62: 4632-4636.

13. Hirschfeld M, Kirschning CJ, Schwandner R, Wesche H, Weis JH, et al. (1999) Cutting edge: inflammatory signaling by Borrelia burgdorferi lipoproteins is mediated by toll-like receptor 2. J Immunol 163: 2382-2386.

14. Alexopoulou L, Thomas V, Schnare M, Lobet Y, Anguita J, et al. (2002) Hyporesponsiveness to vaccination with Borrelia burgdorferi OspA in humans and in TLR1- and TLR2-deficient mice. Nat Med 8: 878-884.

15. Aliprantis AO, Yang RB, Mark MR, Suggett S, Devaux B, et al. (1999) Cell activation and apoptosis by bacterial lipoproteins through toll-like receptor-2. Science 285: 736-739.

16. Brightbill HD, Libraty DH, Krutzik SR, Yang RB, Belisle JT, et al. (1999) Host defense mechanisms triggered by microbial lipoproteins through toll-like receptors. Science 285: 732-736.

17. Wooten RM, Ma Y, Yoder RA, Brown JP, Weis JH, et al. (2002) Toll-like receptor 2 is required for innate, but not acquired, host defense to Borrelia burgdorferi. J Immunol 168: 348-355.

18. Bolz DD, Sundsbak RS, Ma Y, Akira S, Kirschning CJ, et al. (2004) MyD88 plays a unique role in host defense but not arthritis development in Lyme disease. J Immunol 173: 2003-2010.

19. Liu N, Montgomery RR, Barthold SW, Bockenstedt LK (2004) Myeloid differentiation antigen 88 deficiency impairs pathogen clearance but does not alter inflammation in Borrelia burgdorferi-infected mice. Infect Immun 72: 3195-3203.

20. Behera AK, Hildebrand E, Bronson RT, Perides G, Uematsu S, et al. (2006) MyD88 deficiency results in tissue-specific changes in cytokine induction and inflammation in interleukin-18-independent mice infected with Borrelia burgdorferi. Infect Immun 74: 1462-1470.

21. Bockenstedt LK, Liu N, Schwartz I, Fish D (2006) MyD88 deficiency enhances acquisition and transmission of Borrelia burgdorferi by Ixodes scapularis ticks. Infect Immun 74: 2154-2160.

22. Ruland J (2011) Return to homeostasis: downregulation of NF-kappaB responses. Nat Immunol 12: 709-714.

23. Boldin MP, Baltimore D (2012) MicroRNAs, new effectors and regulators of NF-kappaB. Immunol Rev 246: 205-220.

24. Hu R, O'Connell RM (2013) MicroRNA control in the development of systemic autoimmunity. Arthritis Res Ther 15: 202.

25. Yates LA, Norbury CJ, Gilbert RJ (2013) The long and short of microRNA. Cell 153: 516-519.

26. O'Neill LA, Sheedy FJ, McCoy CE (2011) MicroRNAs: the fine-tuners of Toll-like receptor signalling. Nat Rev Immunol 11: 163-175.

27. Taganov KD, Boldin MP, Chang KJ, Baltimore D (2006) NF-kappaB-dependent induction of microRNA miR-146, an inhibitor targeted to signaling proteins of innate immune responses. Proc Natl Acad Sci U S A 103: 12481-12486.

28. Zhao JL, Rao DS, Boldin MP, Taganov KD, O'Connell RM, et al. (2011) NF-kappaB dysregulation in microRNA-146a-deficient mice drives the development of myeloid malignancies. Proc Natl Acad Sci U S A 108: 9184-9189.

29. Zhao JL, Rao DS, O'Connell RM, Garcia-Flores Y, Baltimore D (2013) MicroRNA-146a acts as a guardian of the quality and longevity of hematopoietic stem cells in mice. Elife 2: e00537.

30. Boldin MP, Taganov KD, Rao DS, Yang L, Zhao JL, et al. (2011) miR-146a is a significant brake on autoimmunity, myeloproliferation, and cancer in mice. J Exp Med 208: 1189-1201.

31. Yang L, Boldin MP, Yu Y, Liu CS, Ea CK, et al. (2012) miR-146a controls the resolution of T cell responses in mice. J Exp Med 209: 1655-1670.

32. Chan EK, Ceribelli A, Satoh M (2013) MicroRNA-146a in autoimmunity and innate immune responses. Ann Rheum Dis 72 Suppl 2: ii90-95.

33. Luo X, Yang W, Ye DQ, Cui H, Zhang Y, et al. (2011) A functional variant in microRNA-146a promoter modulates its expression and confers disease risk for systemic lupus erythematosus. PLoS Genet 7: e1002128.

34. Tang Y, Luo X, Cui H, Ni X, Yuan M, et al. (2009) MicroRNA-146A contributes to abnormal activation of the type I interferon pathway in human lupus by targeting the key signaling proteins. Arthritis Rheum 60: 1065-1075.

35. Nakasa T, Miyaki S, Okubo A, Hashimoto M, Nishida K, et al. (2008) Expression of microRNA-146 in rheumatoid arthritis synovial tissue. Arthritis Rheum 58: 1284-1292.

36. Stanczyk J, Pedrioli DM, Brentano F, Sanchez-Pernaute O, Kolling C, et al. (2008) Altered expression of MicroRNA in synovial fibroblasts and synovial tissue in rheumatoid arthritis. Arthritis Rheum 58: 1001-1009.

37. Miyaki S, Asahara H (2012) Macro view of microRNA function in osteoarthritis. Nat Rev Rheumatol 8: 543-552.

38. Yamasaki K, Nakasa T, Miyaki S, Ishikawa M, Deie M, et al. (2009) Expression of MicroRNA-146a in osteoarthritis cartilage. Arthritis Rheum 60: 1035-1041.

39. Hu R, Huffaker TB, Kagele DA, Runtsch MC, Bake E, et al. (2013) MicroRNA-155 confers encephalogenic potential to Th17 cells by promoting effector gene expression. J Immunol 190: 5972-5980.

40. O'Connell RM, Kahn D, Gibson WS, Round JL, Scholz RL, et al. (2010) MicroRNA-155 promotes autoimmune inflammation by enhancing inflammatory T cell development. Immunity 33: 607-619.

41. O'Connell RM, Rao DS, Chaudhuri AA, Boldin MP, Taganov KD, et al. (2008) Sustained expression of microRNA-155 in hematopoietic stem cells causes a myeloproliferative disorder. J Exp Med 205: 585-594.

42. McCoy CE, Sheedy FJ, Qualls JE, Doyle SL, Quinn SR, et al. (2010) IL-10 inhibits miR-155 induction by toll-like receptors. J Biol Chem 285: 20492-20498.

43. Lochhead RB, Sonderegger FL, Ma Y, Brewster JE, Cornwall D, et al. (2012) Endothelial cells and fibroblasts amplify the arthritogenic type I IFN response in murine Lyme disease and are major sources of chemokines in Borrelia burgdorferi-infected joint tissue. J Immunol 189: 2488-2501.

44. Miller JC, Ma Y, Bian J, Sheehan KC, Zachary JF, et al. (2008) A critical role for type I IFN in arthritis development following Borrelia burgdorferi infection of mice. J Immunol 181: 8492-8503.

45. Bramwell KK, Ma Y, Weis JH, Chen X, Zachary JF, et al. (2014) Lysosomal beta-glucuronidase regulates Lyme and rheumatoid arthritis severity. J Clin Invest 124: 311-320.

46. Brown CR, Lai AY, Callen ST, Blaho VA, Hughes JM, et al. (2008) Adenoviral delivery of interleukin-10 fails to attenuate experimental Lyme disease. Infect Immun 76: 5500-5507.

47. Crandall H, Dunn DM, Ma Y, Wooten RM, Zachary JF, et al. (2006) Gene expression profiling reveals unique pathways associated with differential severity of lyme arthritis. J Immunol 177: 7930-7942.

48. Sonderegger FL, Ma Y, Maylor-Hagan H, Brewster J, Huang X, et al. (2012) Localized production of IL-10 suppresses early inflammatory cell infiltration and subsequent development of IFN-gamma-mediated Lyme arthritis. J Immunol 188: 1381-1393.

49. Lazarus JJ, Meadows MJ, Lintner RE, Wooten RM (2006) IL-10 deficiency promotes increased Borrelia burgdorferi clearance predominantly through enhanced innate immune responses. J Immunol 177: 7076-7085.

50. Ruderman EM, Kerr JS, Telford SR, 3rd, Spielman A, Glimcher LH, et al. (1995) Early murine Lyme carditis has a macrophage predominance and is independent of major histocompatibility complex class II-CD4+ T cell interactions. J Infect Dis 171: 362-370.

51. Montgomery RR, Booth CJ, Wang X, Blaho VA, Malawista SE, et al. (2007) Recruitment of macrophages and polymorphonuclear leukocytes in Lyme carditis. Infect Immun 75: 613-620.

52. Centers for Disease C, Prevention (2013) Three sudden cardiac deaths associated with Lyme carditis - United States, November 2012-July 2013. MMWR Morb Mortal Wkly Rep 62: 993-996.

53. Antonara S, Chafel RM, LaFrance M, Coburn J (2007) Borrelia burgdorferi adhesins identified using in vivo phage display. Mol Microbiol 66: 262-276.

54. Coburn J, Leong J, Chaconas G (2013) Illuminating the roles of the Borrelia burgdorferi adhesins. Trends Microbiol 21: 372-379.

55. Olson CM, Jr., Bates TC, Izadi H, Radolf JD, Huber SA, et al. (2009) Local production of IFN-gamma by invariant NKT cells modulates acute Lyme carditis. J Immunol 182: 3728-3734.

56. Schilling JD, Machkovech HM, Kim AH, Schwendener R, Schaffer JE (2012) Macrophages modulate cardiac function in lipotoxic cardiomyopathy. Am J Physiol Heart Circ Physiol 303: H1366-1373.

57. Rymarchyk SL, Lowenstein H, Mayette J, Foster SR, Damby DE, et al. (2008) Widespread natural variation in murine natural killer T-cell number and function. Immunology 125: 331-343.

58. Epelman S, Lavine KJ, Beaudin AE, Sojka DK, Carrero JA, et al. (2014) Embryonic and adult-derived resident cardiac macrophages are maintained through distinct mechanisms at steady state and during inflammation. Immunity 40: 91-104.

59. Kelleher Doyle M, Telford SR, 3rd, Criscione L, Lin SR, Spielman A, et al. (1998) Cytokines in murine lyme carditis: Th1 cytokine expression follows expression of proinflammatory cytokines in a susceptible mouse strain. J Infect Dis 177: 242-246.

60. Brown CR, Blaho VA, Fritsche KL, Loiacono CM (2006) Stat1 deficiency exacerbates carditis but not arthritis during experimental lyme borreliosis. J Interferon Cytokine Res 26: 390-399.

61. Brown CR, Blaho VA, Loiacono CM (2003) Susceptibility to experimental Lyme arthritis correlates with KC and monocyte chemoattractant protein-1 production in joints and requires neutrophil recruitment via CXCR2. J Immunol 171: 893-901.

62. Ritzman AM, Hughes-Hanks JM, Blaho VA, Wax LE, Mitchell WJ, et al. (2010) The chemokine receptor CXCR2 ligand KC (CXCL1) mediates neutrophil recruitment and is critical for development of experimental Lyme arthritis and carditis. Infect Immun 78: 4593-4600.

63. Salazar JC, Duhnam-Ems S, La Vake C, Cruz AR, Moore MW, et al. (2009) Activation of human monocytes by live Borrelia burgdorferi generates TLR2-dependent and -independent responses which include induction of IFN-beta. PLoS Pathog 5: e1000444.

64. Gordon S (2003) Alternative activation of macrophages. Nat Rev Immunol 3: 23-35.

65. Chung Y, Zhang N, Wooten RM (2013) Borrelia burgdorferi elicited-IL-10 suppresses the production of inflammatory mediators, phagocytosis, and expression of co-stimulatory receptors by murine macrophages and/or dendritic cells. PLoS One 8: e84980.

66. Dennis VA, Jefferson A, Singh SR, Ganapamo F, Philipp MT (2006) Interleukin-10 anti-inflammatory response to Borrelia burgdorferi, the agent of Lyme disease: a possible role for suppressors of cytokine signaling 1 and 3. Infect Immun 74: 5780-5789.

67. Gautam A, Dixit S, Philipp MT, Singh SR, Morici LA, et al. (2011) Interleukin-10 alters effector functions of multiple genes induced by Borrelia burgdorferi in macrophages to regulate Lyme disease inflammation. Infect Immun 79: 4876-4892.

68. Gautam A, Dixit S, Embers M, Gautam R, Philipp MT, et al. (2012) Different patterns of expression and of IL-10 modulation of inflammatory mediators from macrophages of Lyme disease-resistant and -susceptible mice. PLoS One 7: e43860.

69. O'Connell RM, Rao DS, Baltimore D (2012) microRNA regulation of inflammatory responses. Annu Rev Immunol 30: 295-312.

70. Meijer HA, Kong YW, Lu WT, Wilczynska A, Spriggs RV, et al. (2013) Translational repression and eIF4A2 activity are critical for microRNA-mediated gene regulation. Science 340: 82-85.

71. Jackson RJ, Hellen CU, Pestova TV (2010) The mechanism of eukaryotic translation initiation and principles of its regulation. Nat Rev Mol Cell Biol 11: 113-127.

72. Stark GR, Darnell JE, Jr. (2012) The JAK-STAT pathway at twenty. Immunity 36: 503-514.

73. Tanaka T, Soriano MA, Grusby MJ (2005) SLIM is a nuclear ubiquitin E3 ligase that negatively regulates STAT signaling. Immunity 22: 729-736.

74. Butler MP, Hanly JA, Moynagh PN (2007) Kinase-active interleukin-1 receptor-associated kinases promote polyubiquitination and degradation of the Pellino family: direct evidence for PELLINO proteins being ubiquitin-protein isopeptide ligases. J Biol Chem 282: 29729-29737.

75. Petnicki-Ocwieja T, Chung E, Acosta DI, Ramos LT, Shin OS, et al. (2013) TRIF mediates Toll-like receptor 2-dependent inflammatory responses to Borrelia burgdorferi. Infect Immun 81: 402-410.

76. Hawley KL, Martin-Ruiz I, Iglesias-Pedraz JM, Berwin B, Anguita J (2013) CD14 targets complement receptor 3 to lipid rafts during phagocytosis of Borrelia burgdorferi. Int J Biol Sci 9: 803-810.

77. Hawley KL, Olson CM, Jr., Iglesias-Pedraz JM, Navasa N, Cervantes JL, et al. (2012) CD14 cooperates with complement receptor 3 to mediate MyD88-independent phagocytosis of Borrelia burgdorferi. Proc Natl Acad Sci U S A 109: 1228-1232.

78. Cervantes JL, Dunham-Ems SM, La Vake CJ, Petzke MM, Sahay B, et al. (2011) Phagosomal signaling by Borrelia burgdorferi in human monocytes involves Toll-like receptor (TLR) 2 and TLR8 cooperativity and TLR8-mediated induction of IFN-beta. Proc Natl Acad Sci U S A 108: 3683-3688.

79. Shin OS, Isberg RR, Akira S, Uematsu S, Behera AK, et al. (2008) Distinct roles for MyD88 and Toll-like receptors 2, 5, and 9 in phagocytosis of Borrelia burgdorferi and cytokine induction. Infect Immun 76: 2341-2351.

80. Armstrong AL, Barthold SW, Persing DH, Beck DS (1992) Carditis in Lyme disease susceptible and resistant strains of laboratory mice infected with Borrelia burgdorferi. Am J Trop Med Hyg 47: 249-258.

81. Weis JJ, McCracken BA, Ma Y, Fairbairn D, Roper RJ, et al. (1999) Identification of quantitative trait loci governing arthritis severity and humoral responses in the murine model of Lyme disease. J Immunol 162: 948-956.

82. Roper RJ, Weis JJ, McCracken BA, Green CB, Ma Y, et al. (2001) Genetic control of susceptibility to experimental Lyme arthritis is polygenic and exhibits consistent

linkage to multiple loci on chromosome 5 in four independent mouse crosses. Genes Immun 2: 388-397.

83. Wang G, Ma Y, Buyuk A, McClain S, Weis JJ, et al. (2004) Impaired host defense to infection and Toll-like receptor 2-independent killing of Borrelia burgdorferi clinical isolates in TLR2-deficient C3H/HeJ mice. FEMS Microbiol Lett 231: 219-225.

84. Barthold SW, Feng S, Bockenstedt LK, Fikrig E, Feen K (1997) Protective and arthritis-resolving activity in sera of mice infected with Borrelia burgdorferi. Clin Infect Dis 25 Suppl 1: S9-17.

85. Bockenstedt LK, Kang I, Chang C, Persing D, Hayday A, et al. (2001) CD4+ T helper 1 cells facilitate regression of murine Lyme carditis. Infect Immun 69: 5264-5269.

86. Anguita J, Samanta S, Revilla B, Suk K, Das S, et al. (2000) Borrelia burgdorferi gene expression in vivo and spirochete pathogenicity. Infect Immun 68: 1222-1230.

87. Baumjohann D, Ansel KM (2013) MicroRNA-mediated regulation of T helper cell differentiation and plasticity. Nat Rev Immunol 13: 666-678.

88. Bezman NA, Chakraborty T, Bender T, Lanier LL (2011) miR-150 regulates the development of NK and iNKT cells. J Exp Med 208: 2717-2731.

89. Zheng Q, Zhou L, Mi QS (2012) MicroRNA miR-150 is involved in Valpha14 invariant NKT cell development and function. J Immunol 188: 2118-2126.

90. Zietara N, Lyszkiewicz M, Witzlau K, Naumann R, Hurwitz R, et al. (2013) Critical role for miR-181a/b-1 in agonist selection of invariant natural killer T cells. Proc Natl Acad Sci U S A 110: 7407-7412.

91. Nahid MA, Pauley KM, Satoh M, Chan EK (2009) miR-146a is critical for endotoxin-induced tolerance: IMPLICATION IN INNATE IMMUNITY. J Biol Chem 284: 34590-34599.

92. Lu LF, Boldin MP, Chaudhry A, Lin LL, Taganov KD, et al. (2010) Function of miR-146a in controlling Treg cell-mediated regulation of Th1 responses. Cell 142: 914-929.

93. Hamilton T, Li X, Novotny M, Pavicic PG, Jr., Datta S, et al. (2012) Cell type- and stimulus-specific mechanisms for post-transcriptional control of neutrophil chemokine gene expression. J Leukoc Biol 91: 377-383.

94. Oosting M, van de Veerdonk FL, Kanneganti TD, Sturm P, Verschueren I, et al. (2011) Borrelia species induce inflammasome activation and IL-17 production through a caspase-1-dependent mechanism. Eur J Immunol 41: 172-181.

95. Moore MW, Cruz AR, LaVake CJ, Marzo AL, Eggers CH, et al. (2007) Phagocytosis of Borrelia burgdorferi and Treponema pallidum potentiates innate immune activation and induces gamma interferon production. Infect Immun 75: 2046-2062.

96. Strle K, Shin JJ, Glickstein LJ, Steere AC (2012) Association of a Toll-like receptor 1 polymorphism with heightened Th1 inflammatory responses and antibiotic-refractory Lyme arthritis. Arthritis Rheum 64: 1497-1507.

97. Shin JJ, Glickstein LJ, Steere AC (2007) High levels of inflammatory chemokines and cytokines in joint fluid and synovial tissue throughout the course of antibiotic-refractory lyme arthritis. Arthritis Rheum 56: 1325-1335.

98. Meerpohl HG, Lohmann-Matthes ML, Fischer H (1976) Studies on the activation of mouse bone marrow-derived macrophages by the macrophage cytotoxicity factor (MCF). Eur J Immunol 6: 213-217.

99. Carroll JA, Stewart PE, Rosa P, Elias AF, Garon CF (2003) An enhanced GFP reporter system to monitor gene expression in Borrelia burgdorferi. Microbiology 149: 1819-1828.

100. Lazarus JJ, Kay MA, McCarter AL, Wooten RM (2008) Viable Borrelia burgdorferi enhances interleukin-10 production and suppresses activation of murine macrophages. Infect Immun 76: 1153-1162.

Figure 3.1. PCR validation of miRNA microarray results. qRT-PCR analysis of miR-146a, miR-21, and miR-155 expression normalized to 5S rRNA from *B. burgdorferi*-infected joints of B6, C3H, and IL-$10^{-/-}$ mice at 1, 2, or 4 weeks postinfection (n=3-4). Shown is fold change in expression compared to uninfected controls ± SEM. * indicates statistically significant increase in expression vs. uninfected controls by ANOVA followed by Dunnett's post-hoc test, α=0.05.

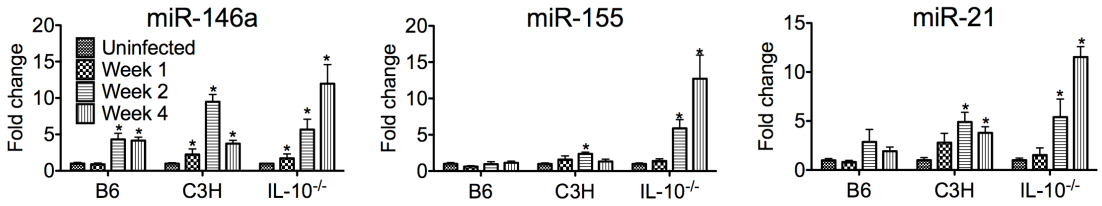
miR-146a
miR-155
miR-21
Fold change
Uninfected
Week 1
Week 2
Week 4
B6
C3H
IL-10-/-

Figure 3.2. B6 miR-146a$^{-/-}$ mice develop more severe arthritis at 4 weeks postinfection independent of bacterial burden. Arthritis severity was determined for *B. burgdorferi*-infected B6 or B6 miR-146a$^{-/-}$ mice at 4 weeks postinfection. (A) Blinded measurements of rear ankles of mice were taken before infection and at 4 weeks postinfection, and change in ankle measurement is shown. (B) Representative images of H&E-stained tibiotarsal joints from BSK-injected (control) and 4 week-infected B6 and B6 miR-146a$^{-/-}$ mice used for histopathology scoring (see Table 3.2). Cranial tibial tendons of infected joints are enlarged to show detail of tendon sheath thickening and PMN infiltrate. (C) Bacterial burden was determined by quantifying *B. burgdorferi*-specific *16S rRNA* normalized to 1000 *β-actin* for joint and heart tissue, and *recA*, normalized to 1000 *nidogen for ear tissue*. Pooled from two independent infection experiments (n≥9 mice per experiment) for joints, and from one experiment for heart and ear tissue (n=5 mice). Statistical significance was determined by Student *t* test (*$p<0.01$). (D) Antibody concentrations were estimated in serum collected from *B. burgdorferi*-infected B6 and B6 miR-146a$^{-/-}$ mice as described in materials and methods. IgM was measured at 2 weeks postinfection (n=4) and IgG was measured at 4 weeks postinfection (n=9-10). Data are representative of 2 independent experiments (n.s.: no significant difference between strains).

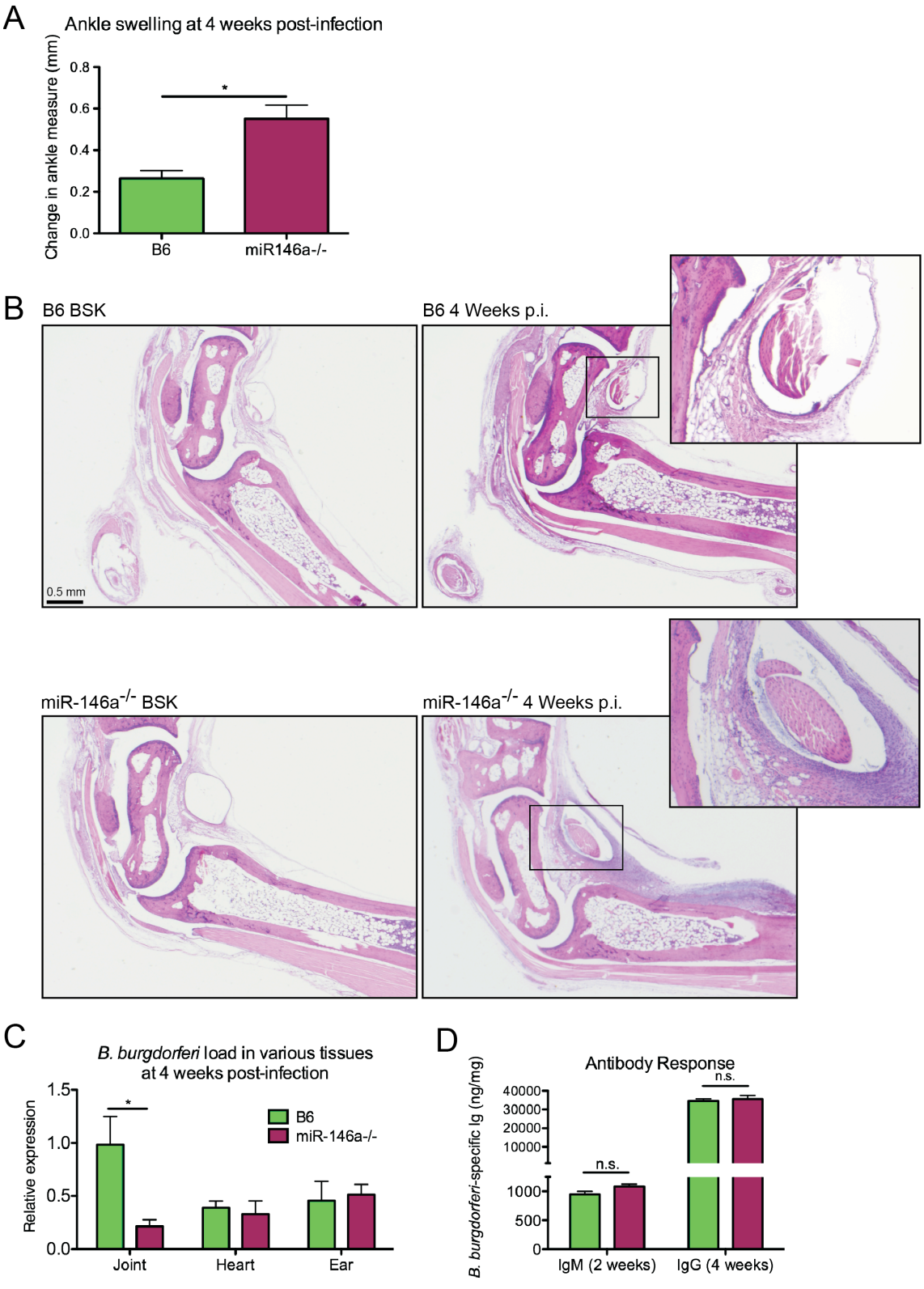
A
Ankle swelling at 4 weeks post-infection
Change in ankle measure (mm)
0.8
0.6
0.4
0.2
0.0
*
B6
miR146a-/-
B
B6 BSK
B6 4 Weeks p.i.
0.5 mm
miR-146a-/- BSK
miR-146a-/- 4 Weeks p.i.
C
B. burgdorferi load in various tissues
at 4 weeks post-infection
Relative expression
1.5
1.0
0.5
0.0
*
B6
miR-146a-/-
Joint
Heart
Ear
D
Antibody Response
B. burgdorferi-specific Ig (ng/mg)
40000
30000
20000
10000
1000
500
0
n.s.
n.s.
IgM (2 weeks)
IgG (4 weeks)

Figure 3.3. B6 and B6 miR-146a$^{-/-}$ mice have similar *B. burgdorferi* burden and similar levels of inflammation in heart tissue, distinct from C3H mice. Mice were infected with *B. burgdorferi* for 3 weeks, after which hearts were collected for analysis of bacterial burden and inflammation. (A) Bacterial presence was quantified with *B. burgdorferi*-specific *16S rRNA,* normalized to 1000 *β-actin* by qRT-PCR. (B) Carditis was blindly assessed using histopathologic evaluation to score lesion severity in heart tissue from B6, B6 miR-146a$^{-/-}$, and C3H mice infected with *B. burgdorferi* for 3 weeks. (C) H&E-stained sections of infected B6, B6 miR-146a$^{-/-}$, and C3H hearts (10x magnification top row, 40x magnification bottom row), with the intraventricular septum (ivs), coronary artery (ca), pulmonary artery (pa), and aorta (a) labeled as indicated. The inflammatory response in these lesions was a mixture of neutrophils and mononuclear inflammatory cells such as lymphocytes and macrophages. (D) Transcripts for *CD11b, F4/80, CD4* and *Vα14*, *IFNγ* and *IL6* were measured by qRT-PCR, normalized to *β-actin.* 4 mice were used for each strain, and statistically significant difference between groups by ANOVA followed by Tukey's post-hoc test are indicated (*$p<0.05$). For lesion scoring, Mann-Whitney *U* test was used to determine whether there were statistical significant differences between groups, with p value indicated (n=4 mice per strain).

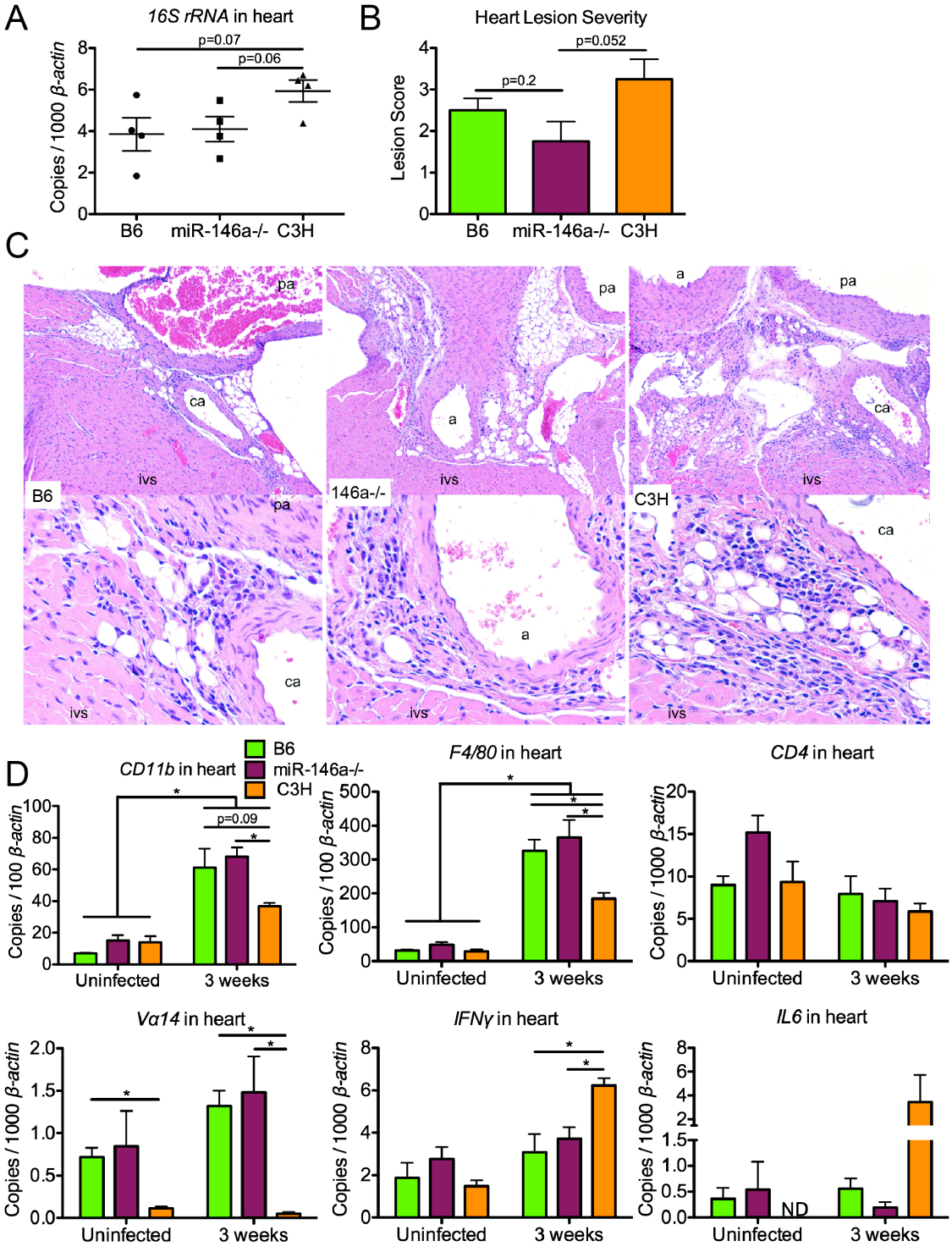
A
16S rRNA in heart
p=0.07
p=0.06
Copies / 1000 β-actin
B6
miR-146a-/-
C3H
B
Heart Lesion Severity
p=0.2
p=0.052
Lesion Score
C
B6
146a-/-
C3H
pa
ca
ivs
a
D
B6
miR-146a-/-
C3H
CD11b in heart
F4/80 in heart
CD4 in heart
Vα14 in heart
IFNγ in heart
IL6 in heart
Copies / 100 β-actin
Copies / 1000 β-actin
p=0.09
Uninfected
3 weeks
ND

Figure 3.4. B6 miR-146a$^{-/-}$ mice exhibit hyperactive expression of a subset of NF-κB target cytokines and chemokines at 4 weeks postinfection. (A) RNA was isolated from *B. burgdorferi*-infected rear ankle joints at 2 and 4 weeks postinfection and transcript levels of *IL6, IL1β, Cxcl1, Cxcl2, IFNγ, Cxcl10,* and *TNFα* were measured by qRT-PCR, normalized to *β-actin*. (B) Serum from *B. burgdorferi*-infected mice was collected by cheek bleed at 4 weeks postinfection, and IL-6, TNFα, IL-12, and IFN-γ protein concentration was measured by ELISA. Statistically significant differences between groups by ANOVA followed by Tukey's post-hoc test are indicated (*$p<0.05$, $n\geq9$ mice per group).

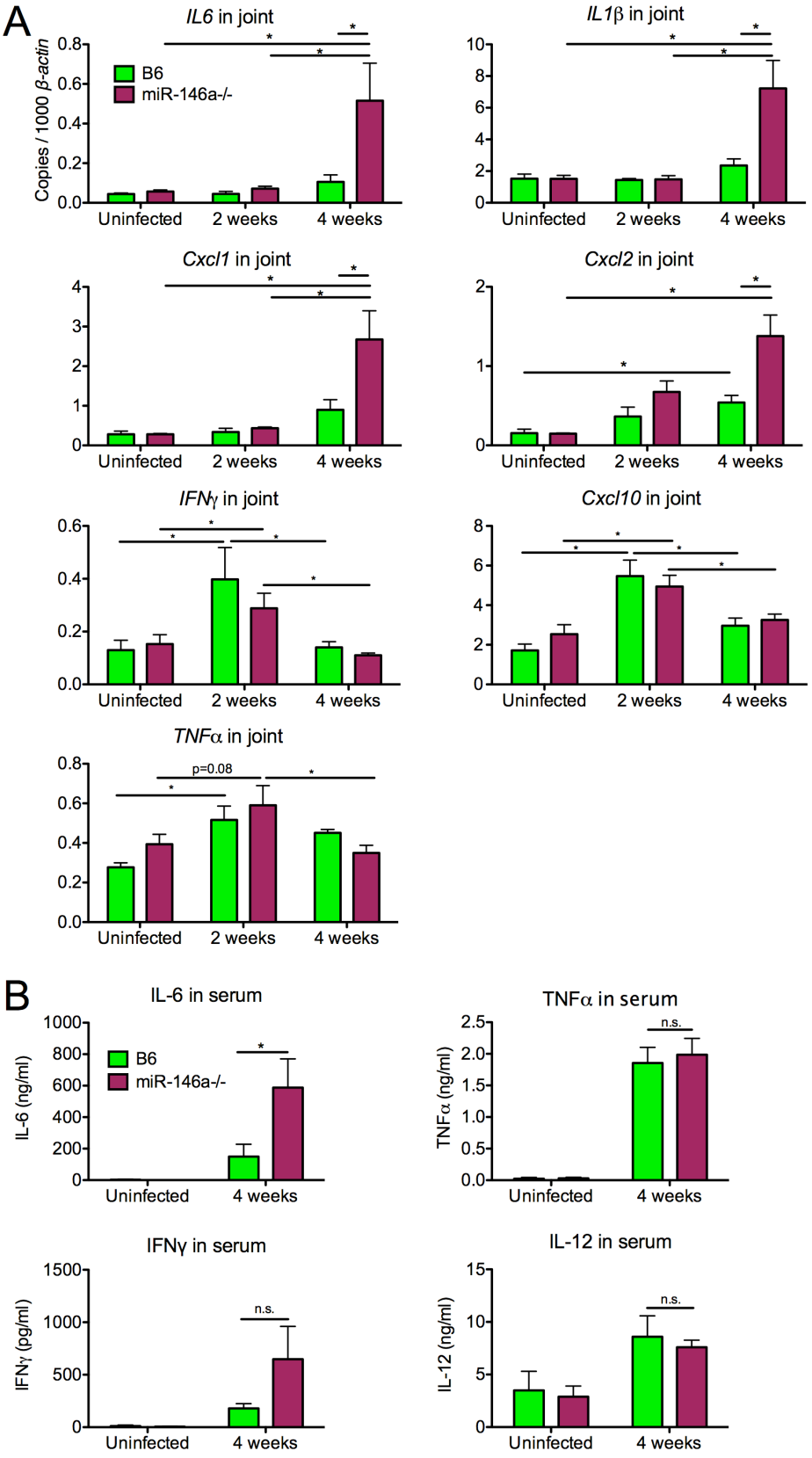
A
IL6 in joint
IL1β in joint
Cxcl1 in joint
Cxcl2 in joint
IFNγ in joint
Cxcl10 in joint
TNFα in joint
Copies / 1000 β-actin
B6
miR-146a-/-
Uninfected
2 weeks
4 weeks
p=0.08
B
IL-6 in serum
TNFα in serum
IFNγ in serum
IL-12 in serum
IL-6 (ng/ml)
TNFα (ng/ml)
IFNγ (pg/ml)
IL-12 (ng/ml)
n.s.

Figure 3.5. Effect of miR-146a in isolated joint cell populations early in infection. (A) FACS analysis of cells released from joint tissue of B6 mice uninfected or infected with *B. burgdorferi* for 7 or 14 days. Single-cell suspensions of tissue were prepared as described in materials and methods, and cells were stained according to myeloid (CD45+ CD11b+), lymphoid (CD45+ CD11b-), endothelial (CD45- CD31+), or fibroblast-enriched (CD45- CD31- CD29+) lineages, following gating to exclude debris, dead cells, and cell doublets. (B) Cells sorted into various lineages depicted in (A) were analyzed for transcript levels of *Cxcl2*, *IL1β,* and *Oasl2* in myeloid cells, *Cxcl1* in fibroblast-enriched cells, and *IFNγ* in lymphoid cells, normalized to *β-actin*. Data are representative of two independent experiments (n=4 mice for each group).

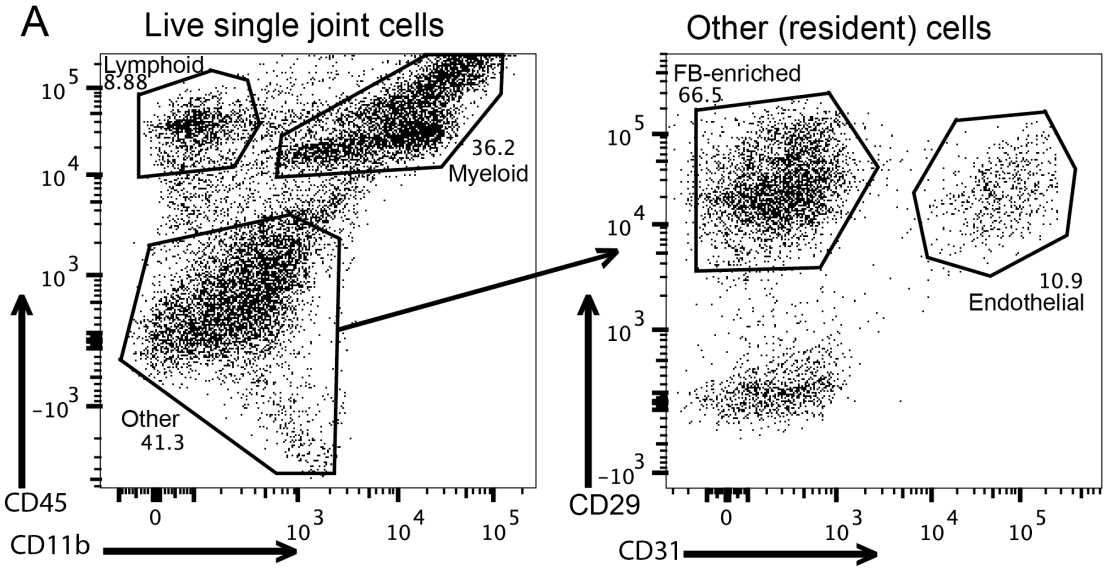
A
Live single joint cells
Other (resident) cells
Lymphoid
8.88
36.2
Myeloid
Other
41.3
CD45
CD11b
FB-enriched
66.5
10.9
Endothelial
CD29
CD31

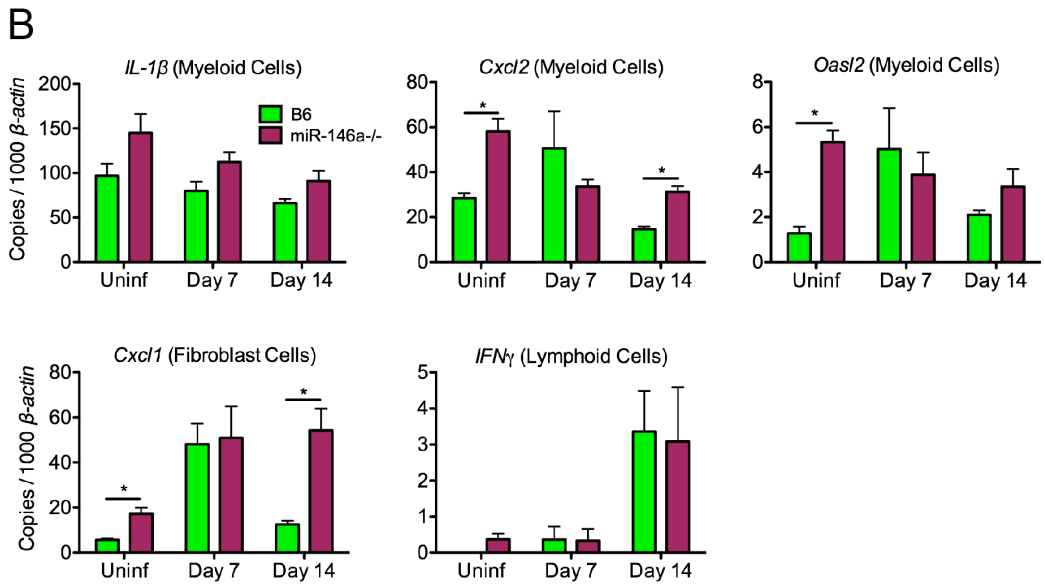
B
IL-1β (Myeloid Cells)
Cxcl2 (Myeloid Cells)
Oasl2 (Myeloid Cells)
Cxcl1 (Fibroblast Cells)
IFNγ (Lymphoid Cells)
Copies / 1000 β-actin
B6
miR-146a-/-
Uninf
Day 7
Day 14

Figure 3.6. Myeloid cell recruitment is increased in infected joints of B6 miR-146a$^{-/-}$ mice. (A) Representative flow cytometry analysis of CD11b+ cells released from joint tissue of B6 or B6 miR-146a$^{-/-}$ mice infected with *B. burgdorferi* for 2 or 4 weeks, following gating to exclude debris, dead cells, and cell doublets. Numbers indicate gate percentages. (B) Representative histogram showing MRC1 (Mannose Receptor, C type 1, CD206) and Gr1 fluorescent intensity in macrophages (Mϕ), polymorphonuclear cells (PMNs), and monocyte gates, as shown in (A). Gray shaded area indicates B6 mice and the black line indicates B6 miR-146a$^{-/-}$ mice. Bar graph on right shows average mean fluorescence intensity of macrophages, PMNs, and monocytes isolated from 14 day-infected B6 or miR-146a$^{-/-}$ mouse joints (n=4). (C) Total numbers of myeloid cell populations in joints of uninfected or *B. burgdorferi*-infected mice at 2 and 4 weeks postinfection from B6 or B6 miR-146a$^{-/-}$ mice. Cell populations were identified by flow cytometric analysis with macrophages defined as CD11b+ F4/80+ Ly6C^{lo}, polymorphonuclear cells (PMNs) as CD11b+ Gr1^{hi} Ly6C^{int}, and monocytes as CD11b+ Gr1^{int} Ly6C^{hi}. Statistically significant differences between groups by ANOVA followed by Tukey's post-hoc test are indicated (*$p<0.05$). For selected values not reaching statistical significance cutoff, p values are listed. Representative of 2 independent experiments (n=4 for each group).

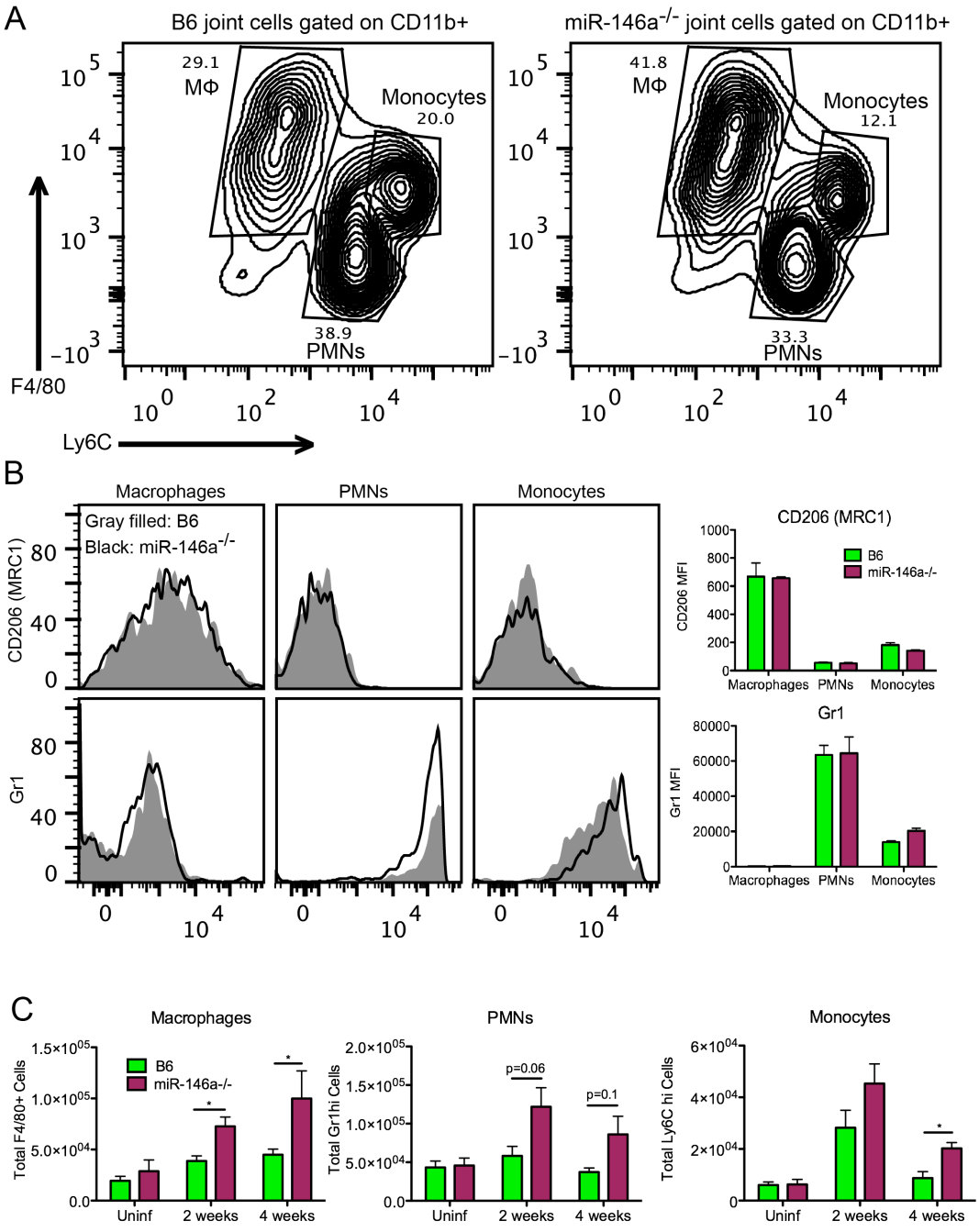
A
B6 joint cells gated on CD11b+
miR-146a-/- joint cells gated on CD11b+
29.1
MΦ
Monocytes
20.0
38.9
PMNs
41.8
MΦ
Monocytes
12.1
33.3
PMNs
F4/80
Ly6C
B
Macrophages
PMNs
Monocytes
Gray filled: B6
Black: miR-146a-/-
CD206 (MRC1)
Gr1
CD206 MFI
Gr1 MFI
B6
miR-146a-/-
C
Macrophages
PMNs
Monocytes
Total F4/80+ Cells
Total Gr1hi Cells
Total Ly6C hi Cells
p=0.06
p=0.1
Uninf
2 weeks
4 weeks

Figure 3.7. Bone marrow-derived Macrophages from B6 miR-146a$^{-/-}$ mice are hyper-responsive to *B. burgdorferi* and have elevated levels of TRAF6. (A) Analysis of cytokine secretion of *B. burgdorferi*-treated BMDMs. Bone marrow-derived macrophages (BMDMs) from B6 (black) or B6 miR-146a$^{-/-}$ (white) mice were pretreated for 4 hours in the presence or absence of recombinant mouse IL-10. Following pretreatment, cells were stimulated with *B. burgdorferi* for 24 hours. Cell supernatant was collected and secretion of IL-6, IL-1β, CXCL1, IL-12, TNFα, and IL-10 was measured by ELISA. (B) Immunoblot analysis of TRAF6, IRAK1, and STAT1 in *B. burgdorferi*-treated BMDMs from B6 (WT) or B6 miR-146a$^{-/-}$ (KO) mice. BMDMs were stimulated with media alone or *B. burgdorferi* for 24 hours and cells were lysed using NP-40. Quantification was determined based on band intensity, normalized to β-actin, with B6 (WT) value set to 1. (C) *Traf6, Irak1,* and *Stat1* mRNA levels were quantified using qRT-PCR, normalized to *β-actin.* Significant differences between groups by ANOVA followed by Tukey's post-hoc test are indicated (*$p<0.05$). Representative of at least 2 independent experiments (n=3-4 for each group).

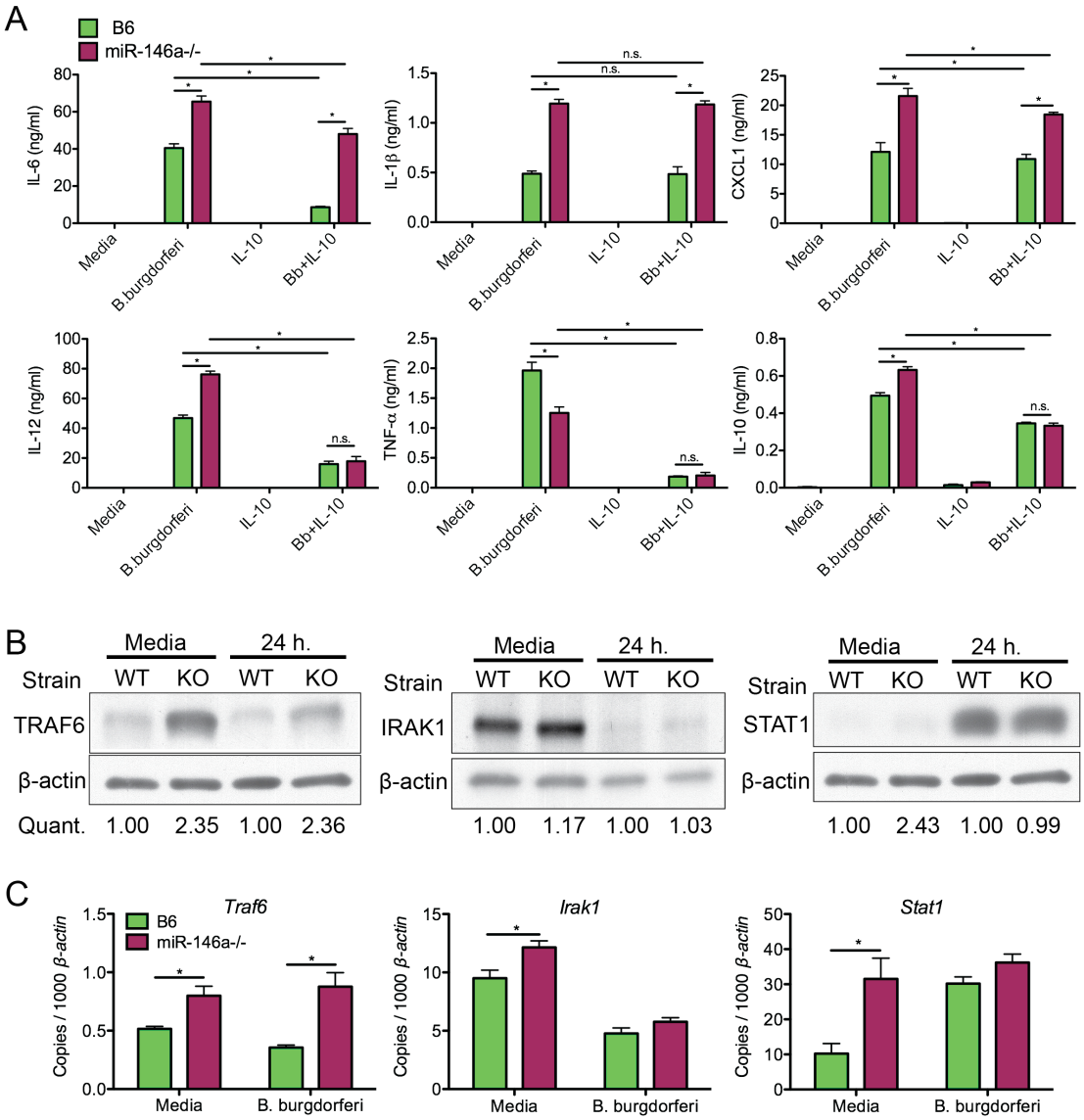
A
B6
miR-146a-/-
IL-6 (ng/ml)
IL-1β (ng/ml)
CXCL1 (ng/ml)
IL-12 (ng/ml)
TNF-α (ng/ml)
IL-10 (ng/ml)
Media
B.burgdorferi
IL-10
Bb+IL-10
n.s.
B
Media
24 h.
Strain
WT
KO
TRAF6
IRAK1
STAT1
β-actin
Quant.
1.00 2.35 1.00 2.36
1.00 1.17 1.00 1.03
1.00 2.43 1.00 0.99
C
Traf6
Irak1
Stat1
Copies / 1000 β-actin
B6
miR-146a-/-
Media
B. burgdorferi

Figure 3.8. B6 miR-146a$^{-/-}$ peritoneal macrophages exhibit increased phagocytic activity. (A) Representative plots of peritoneal macrophages isolated from B6 or B6 miR-146a$^{-/-}$ mice and incubated with GFP-*B. burgdorferi* for 1 or 2 hours at 10:1 MOI. Box indicates GFP+ fraction, and number in top-right corner is percent GFP+. Control is using cells only. (B) Mean percent GFP+ and GFP mean fluorescence intensity for flow analysis shown in (A). Representative of two independent experiments (n=3 for each experiment). Significant differences between groups by ANOVA followed by Tukey's post-hoc test are indicated (*$p<0.05$). (C) Confocal images of B6 peritoneal macrophages incubated with GFP-*B. burgdorferi* for 1 hour at 100:1 MOI. Panels are (from top-left) cell nuclei (gray, DAPI), GFP-*B. burgdorferi* (green), lysosomes (red, LAMP-1), cell membrane (blue, F4/80), bright-field, and overlaid images. White bar indicates scale. White arrow shows a bacterium associated with a macrophage pseudopod, chevron indicates bright GFP puncta associated with intracellular lysosomes, and triangle indicates a cell surface-associated bacterium. Representative of two biological replicates. Similar images of B6 miR-146a$^{-/-}$ macrophages can be found in supplemental data.

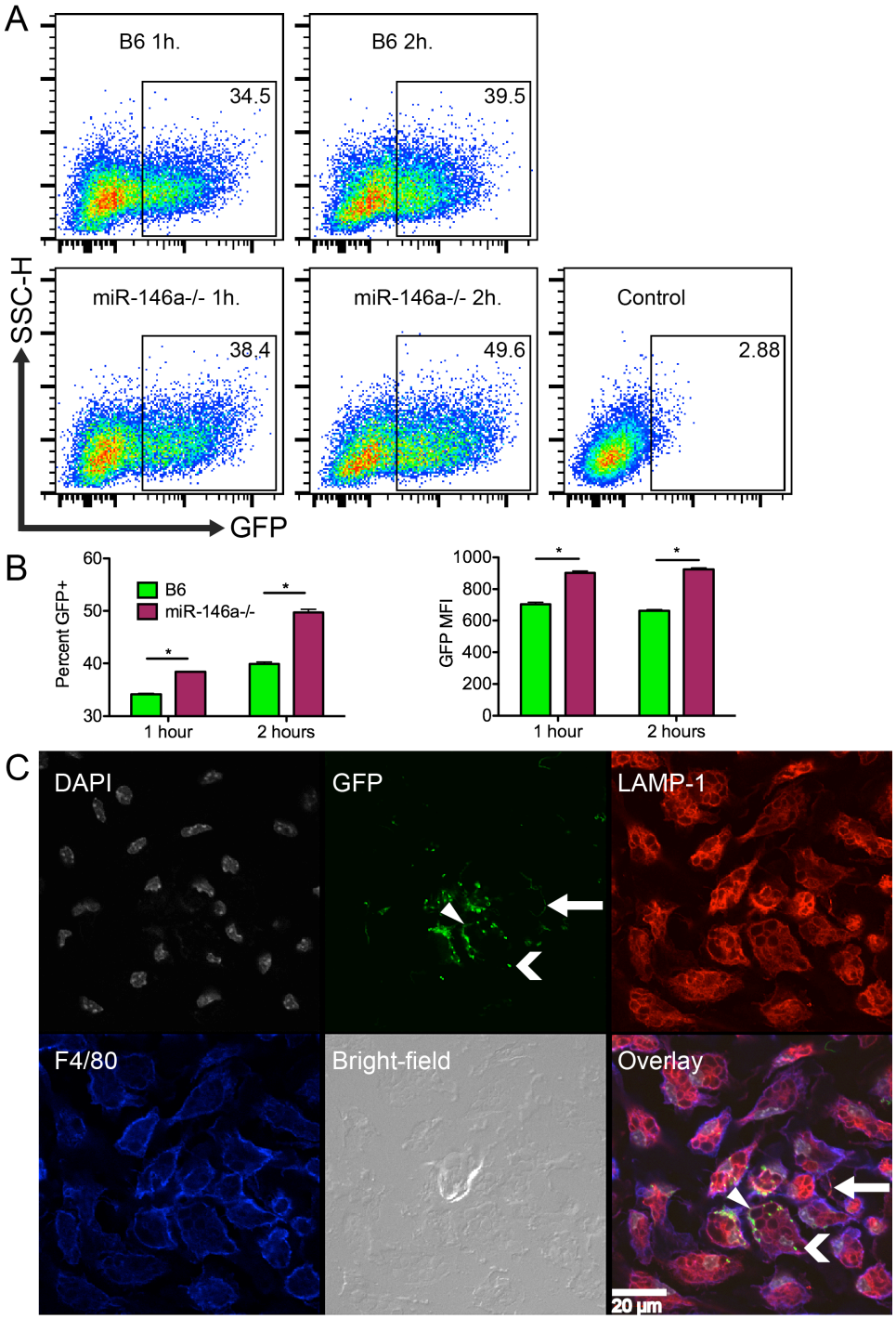
A
B6 1h.
34.5
B6 2h.
39.5
miR-146a-/- 1h.
38.4
miR-146a-/- 2h.
49.6
Control
2.88
SSC-H
GFP
B
Percent GFP+
B6
miR-146a-/-
1 hour
2 hours
GFP MFI
C
DAPI
GFP
LAMP-1
F4/80
Bright-field
Overlay
20 µm

Figure 3.9. Model of miR-146a function as a suppressor of arthritis during persistent *B. burgdorferi* infection. Regulatory role of miR-146a in myeloid cells present in joint tissue as a negative regulator of Toll-like receptor (TLR) signaling through suppression of adaptor proteins, particularly TRAF6.

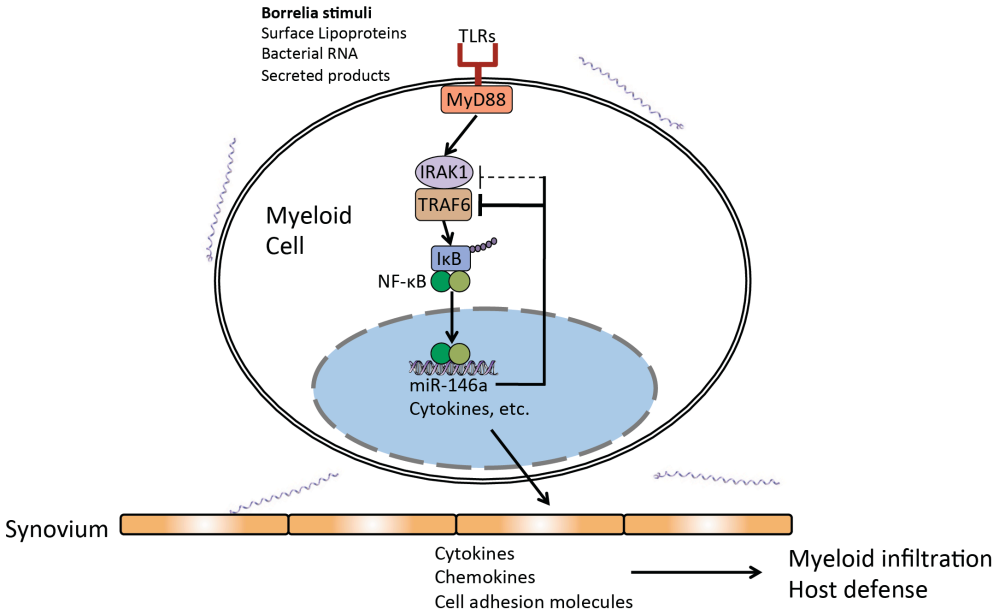
Borrelia stimuli
Surface Lipoproteins
Bacterial RNA
Secreted products
TLRs
MyD88
IRAK1
TRAF6
Myeloid
Cell
IκB
NF-κB
miR-146a
Cytokines, etc.
Synovium
Cytokines
Chemokines
Cell adhesion molecules
Myeloid infiltration
Host defense

Figure 3.S1. Lymphocyte infiltration into joints of *B. burgdorferi*-infected mice is similar between WT and miR-146a$^{-/-}$ mice. Flow cytometry analysis of lymphoid cells released from joint tissue of B6 or B6 miR-146a$^{-/-}$ mice infected with *B. burgdorferi* for 2 or 4 weeks, following gating to exclude debris, dead cells, and cell doublets. Cell lineages defined as follows: T cells (CD45+ TCRβ+), B cells (CD45+ B220+), and NK cells (CD45+ NK1.1+). No significance was observed between any groups by ANOVA followed by Tukey's post-hoc test (*$p<0.05$).

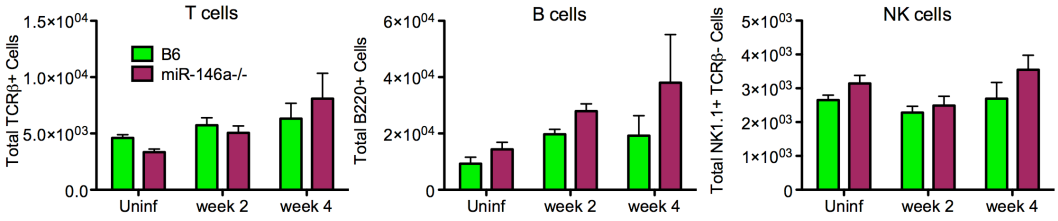
T cells
B6
miR-146a-/-
Total TCRβ+ Cells
1.5×10^04
1.0×10^04
5.0×10^03
0.0
Uninf
week 2
week 4
B cells
Total B220+ Cells
6×10^04
4×10^04
2×10^04
0
Uninf
week 2
week 4
NK cells
Total NK1.1+ TCRβ- Cells
5×10^03
4×10^03
3×10^03
2×10^03
1×10^03
0
Uninf
week 2
week 4

Figure 3.S2. Confocal images of B6 miR-146a$^{-/-}$ peritoneal macrophages incubated with GFP-*B. burgdorferi*. Panels are (from top-left) cell nuclei (gray, DAPI), GFP-*B. burgdorferi* (green), lysosomes (red, LAMP-1), cell membrane (blue, F4/80), bright-field, and overlay fields. White bar indicates scale.

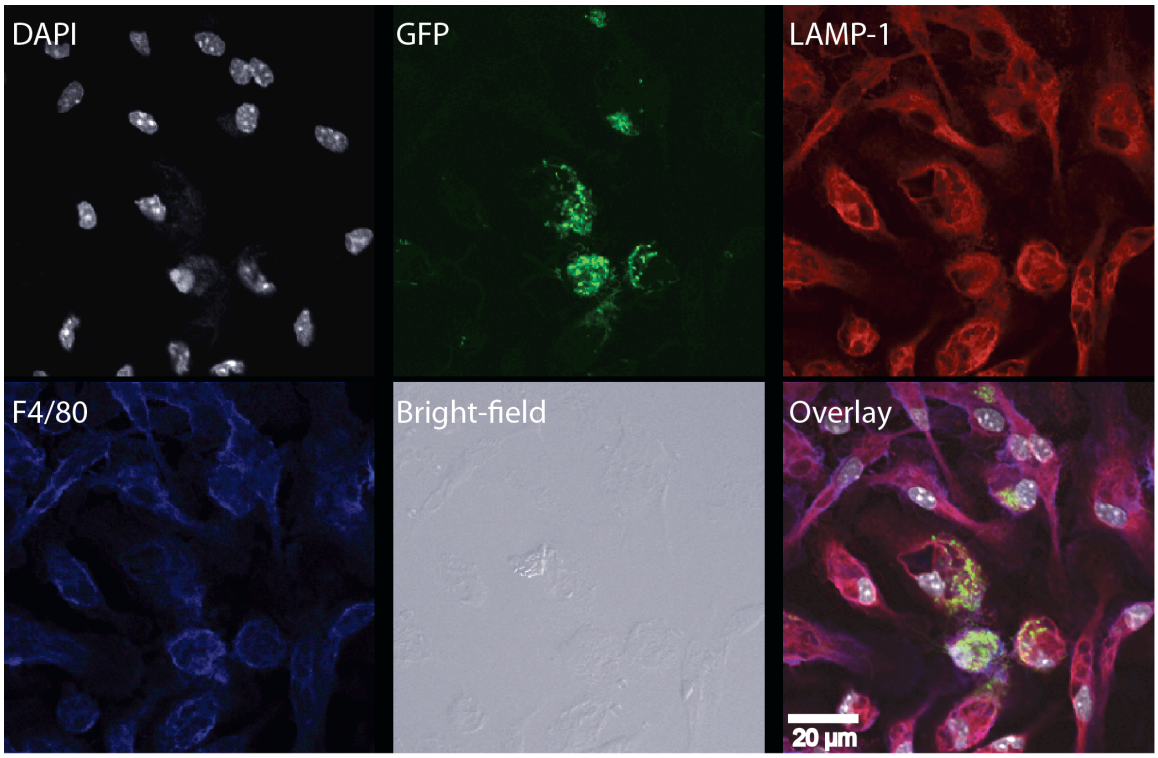
DAPI
GFP
LAMP-1
F4/80
Bright-field
Overlay
20 µm

Table 3.1. MicroRNAs most highly changed in expression, based on microarray, in joints of different mouse strains.

B6		C3H		IL-10$^{-/-}$	
miRNA	**Fold Δ**	**miRNA**	**Fold Δ**	**miRNA**	**Fold Δ**
miR-146a	5.67	miR-146a	10.8	miR-21	6.08
miR-21	3.92	miR-21	8.12	miR-146a	5.34
miR-706	3.47	miR-142-3p	6.54	miR-155	5.12
miR-29b	2.31	miR-142-5p	4.99	miR-193b	-3.04
miR-715	2.24	miR-34a	4.4	miR-150	-2.56
miR-340-5p	2.21	miR-18a	3.35	miR-145	-2.43
miR-34a	2.16	miR-19b	3.08	miR-181a	-2.37
miR-689	2.12	miR-145	-3.07	miR-181b	-2.29

List of 8 most highly differentially expressed miRNAs in *B. burgdorferi*-infected joints of B6, C3H, and B6 IL-10$^{-/-}$ mice at 2 weeks postinfection, based on Agilent mouse miRNA microarray. Shown is fold-change in expression compared to uninfected controls. Significance was determined using Welch's *t*-test with Benjamini and Hochberg correction ($p<0.05$, n=3-4 mice per group).

Table 3.2. Histopathology scores of arthritis severity for B6 and B6 miR-146a$^{-/-}$ mice.

Strain	Overall Lesion	PMN Infiltrate	Mono-nuclear Infiltrate	Sheath Thickness	Reactive-Reparative	Total Score
B6	1.53 (.21)	1.05 (.25)	0.58 (.14)	1.42 (.22)	0.26 (.15)	4.84 (.79)
miR-146a$^{-/-}$	**2.84 (.26)**	**2.21 (.26)**	0.37 (.11)	**2.74 (.26)**	**1.58 (.25)**	**9.74 (.97)**

Histopathology scores of rear ankle joints of B6 and B6 miR-146a$^{-/-}$ mice infected with B. burgdorferi for 4 weeks. Scores of 0-5, with 5 being most severe, were assigned to each sample. Total score is the sum of scores from each category. Values shown are the mean (±SE), and bold numbers indicate statistically significant difference between strains using Mann-Whitney U test ($p<0.01$), pooled from two independent infection experiments (n=9-10 each).

Table 3.3. mRNA expression of induced cytokines in BMDMs from B6 and B6 miR-146a$^{-/-}$ mice after 6 and 24 hours stimulation with *B. burgdorferi*.

Strain	6 hours			24 hours		
	IL1β	*IL6*	*TNFα*	*IL1β*	*IL6*	*TNFα*
B6	56.2±2.5	0.008±0.002	127.3±6.6	109.7±12.7	1.07±0.46	6.42±0.58
miR-146a$^{-/-}$	236±8.7	0.06±0.007	168.2±14.7	446.8±14.0	2.67±0.35	7.91±0.37
Fold Δ	**4.2**	**7.5**	**1.3**	**4.1**	**2.5**	**1.2**

Induced transcript levels of *IL1β, IL6,* and *TNFα* (normalized to 1000 *β-actin*) in B6 and B6 miR-146a$^{-/-}$ BMDMs stimulated with *B. burgdorferi* for 6 or 24 hours. Data shown are mean±SE, as well as fold-difference (Fold Δ) of expression in miR-146a$^{-/-}$ vs. B6. Transcript levels of uninfected cells were very low and similar between strains (not shown). Representative of 3 independent experiments (n≥3 for each experiment).

Table 3.S1. MicroRNAs with greater than 2-fold change in expression in joints of mouse strains, based on Agilent miRNA microarray analysis.

Group 1:	B6 control			
Group 2:	B6 week 1			
Statistics:	Welchs t-test			
Correction:	Benjamini and Hochberg			
Gene Identifier	Ratio	Direction	p-value	adj. p-value
mmu-miR-139-3p	2.74	Down	0.0136889	0.0211556
mmu-miR-466g	2.58	Down	0.0036082	0.0068155
mmu-miR-466f-3p	2.49	Down	0.0011125	0.0063042
mmu-miR-202-3p	2.29	Down	0.0031243	0.0066392
mmu-miR-466i	2.28	Down	0.0018722	0.0064726
mmu-miR-689	2.27	Up	5.069E-04	0.0043087
mmu-miR-21	2.14	Up	6.63E-05	0.0011274
mmu-miR-18a	2.04	Up	0.0026652	0.0064726
mmu-miR-467f	2.04	Down	0.0020589	0.0064726
mmu-miR-494	2.03	Up	0.0026516	0.0064726
mmu-miR-29b	2.01	Up	0.0075675	0.0128647
Group 1:	B6 control			
Group 2:	B6 week 2			
Statistics:	Welchs t-test			
Correction:	Benjamini and Hochberg			
Gene Identifier	Ratio	Direction	p-value	adj. p-value
mmu-miR-146a	5.67	Up	1.765E-04	0.0065313
mmu-miR-21	3.92	Up	0.0054998	0.0422948
mmu-miR-706	3.47	Up	0.0068586	0.0422948
mmu-miR-29b	2.31	Up	0.0314381	0.1292457
mmu-miR-715	2.24	Up	0.0027000	0.0369090
mmu-miR-340-5p	2.21	Up	0.0247291	0.1143724
mmu-miR-34a	2.16	Up	0.0065130	0.0422948
mmu-miR-689	2.12	Up	0.0239135	0.1143724
mghv-miR-M1-2	2.01	Up	0.0029926	0.0369090
Group 1:	C3H control			
Group 2:	C3H week 1			
Statistics:	Welchs t-test			
Correction:	Benjamini and Hochberg			
Gene Identifier	Ratio	Direction	p-value	adj. p-value
mmu-miR-144	10.72	Up	0.0059985	0.0118504

Table 3.S1. Continued

mmu-miR-466f-3p	7.74	Down	0.0208671	0.0225365
mmu-miR-136	6.63	Up	0.0015580	0.0071312
mmu-miR-720	6.13	Up	0.0036499	0.0109498
mmu-miR-466i	6.1	Down	0.0074614	0.0118504
mmu-miR-142-3p	5.92	Up	0.0072559	0.0118504
mmu-miR-142-5p	5.01	Up	0.0030635	0.0103393
mmu-miR-301a	4.96	Up	0.0116770	0.0153280
mmu-miR-467f	4.71	Down	0.0090167	0.0135251
mmu-miR-1187	3.57	Down	0.0013349	0.0071312
mmu-miR-574-5p	3.31	Down	0.0015847	0.0071312
mmu-miR-669n	3.28	Down	3.785E-04	0.0051109
mmu-miR-19b	2.96	Up	0.0129689	0.0153280
mmu-miR-376a	2.88	Up	2.651E-04	0.0051109
mmu-miR-101a	2.88	Up	0.0121775	0.0153280
mmu-miR-574-3p	2.61	Down	0.0388088	0.0388083
mmu-miR-29a*	2.6	Up	0.0068457	0.0118504
mmu-miR-18a	2.55	Up	0.0050183	0.0112913
mmu-miR-338-3p	2.43	Up	6.400E-04	0.0057607
mmu-miR-21	2.33	Up	0.0040851	0.0110298
mmu-miR-145	2.26	Down	0.0074154	0.0118504
mmu-miR-669f	2.21	Down	0.0044967	0.0110375
mmu-miR-340-5p	2.21	Up	0.0095250	0.0135355
mmu-miR-434-5p	2.19	Up	0.0361220	0.0375114
mmu-miR-101b	2.09	Up	0.0130571	0.0153280
mmu-miR-30e	2.06	Up	0.0188380	0.0211928
mmu-miR-7a	2.04	Up	0.0028723	0.0103393

Group 1:	C3H control			
Group 2:	C3H week 2			
Statistics:	Welchs t-test			
Correction:	Benjamini and Hochberg			
Gene Identifier	Ratio	Direction	p-value	adj. p-value
mmu-miR-146a	10.8	Up	8.35443E-04	5.64E-03
mmu-miR-21	8.12	Up	5.09E-07	1.37E-05
mmu-miR-142-3p	6.54	Up	0.004686706	1.27E-02
mmu-miR-142-5p	4.99	Up	0.011309152	1.70E-02
mmu-miR-34a	4.4	Up	2.43294E-04	3.28E-03
mmu-miR-18a	3.35	Up	0.001501822	6.76E-03
mmu-miR-19b	3.08	Up	0.00711288	1.36E-02

Table 3.S1. Continued

mmu-miR-145	3.07	Down	0.006830074	1.36E-02
mmu-miR-342-3p	3.01	Up	0.018902847	2.55E-02
mmu-miR-7a	2.92	Up	0.004152087	1.25E-02
mmu-miR-466g	2.84	Down	0.013821859	1.96E-02
mmu-miR-466f-3p	2.78	Down	0.003301523	1.11E-02
mmu-miR-340-5p	2.73	Up	0.010107969	1.61E-02
mmu-miR-130b	2.65	Up	0.001815616	7.00E-03
mmu-miR-362-5p	2.51	Up	6.84423E-04	5.64E-03
mmu-miR-466i	2.36	Down	0.007286134	1.36E-02
mmu-miR-17*	2.28	Up	0.00761823	1.36E-02
mmu-miR-29b	2.27	Up	0.027154031	3.49E-02
mmu-miR-146b	2.18	Up	0.001483454	6.76E-03
mmu-miR-574-3p	2.11	Down	0.008046157	1.36E-02
mmu-miR-467f	2.07	Down	0.007130363	1.36E-02

Group 1:	IL10 ko control			
Group 2:	IL10 ko week 1			
Statistics:	Welchs t-test			
Correction:	Benjamini and Hochberg			
Gene Identifier	Ratio	Direction	p-value	adj. p-value
mmu-miR-133a	2.19	Up	0.011191776	0.01939199
mmu-miR-133b	2.14	Up	0.012927996	0.01939199
mmu-miR-146a	2.05	Up	0.041399321	0.04139932

Group 1:	IL10 ko control			
Group 2:	IL10 ko week 2			
Statistics:	Welchs t-test			
Correction:	Benjamini and Hochberg			
Gene Identifier	Ratio	Direction	p-value	adj. p-value
mmu-miR-21	6.08	Up	5.98E-06	1.19505E-04
mmu-miR-146a	5.34	Up	3.85517E-04	0.003344354
mmu-miR-155	5.12	Up	5.01653E-04	0.003344354
mmu-miR-193b	3.04	Down	0.006862146	0.015113973
mmu-miR-150	2.56	Down	0.001735425	0.008677123
mmu-miR-145	2.43	Down	0.007556986	0.015113973
mmu-miR-181a	2.37	Down	0.005549417	0.015113973
mmu-miR-181b	2.29	Down	0.011713074	0.018020113
mmu-let-7b	2.17	Down	0.016701305	0.020876632
mmu-miR-151-5p	2.16	Down	0.011158357	0.018020113

Table 3.S1. Continued

mmu-let-7c	2.15	Down	0.018191511	0.021401778
mmu-miR-195	2.14	Down	0.015536991	0.020876632
mmu-miR-196b	2.14	Down	0.01946987	0.021633189
mmu-miR-199b*	2.09	Down	0.026609241	0.026609241
mmu-miR-497	2.08	Down	0.016139593	0.020876632
mmu-miR-365	2.07	Down	0.022465838	0.023648251
mmu-miR-23b	2.07	Down	0.006067439	0.015113973
mmu-miR-142-3p	2.07	Up	0.008642346	0.015713356
mmu-miR-7a	2.07	Up	0.006185229	0.015113973
mmu-miR-342-3p	2.01	Up	0.002969385	0.011877542

All microRNAs with greater than 2-fold change in expression in *B. burgdorferi*-infected joints of B6, C3H, and B6 IL-$10^{-/-}$ mice at 1 and 2 weeks postinfection, compared to uninfected controls, based on Agilent mouse miRNA microarray. Shown is gene name, fold-change, direction of fold-change, p-value and adjusted p-value. Significance was determined using Welch's *t*-test with Benjamini and Hochberg correction ($p<0.05$, n=3-4 mice per group).

CHAPTER 4

DISCUSSION

Overview

The immune system is a network of various cell types, tissues, and organs, working in concert to detect and eliminate pathogens. Upon infection, rapid and robust innate immune activation is required to limit pathogen spread. While this is important in host defense, pathogen-mediated inflammation also leads to tissue damage. It is therefore also essential for the immune response to be tightly regulated in terms of both amplitude and duration, and to fully resolve following pathogen clearance. Failure to properly regulate an immune response to infection can lead to inflammatory disease and autoimmunity. Lyme arthritis is an excellent example of an inflammatory disease caused by infection of an arthritogenic pathogen, *Borrelia burgdorferi* [1]. Infection can trigger a wide range of disease severity, from mild joint pain and acute arthritis, to severe prolonged treatment-refractory arthritis [2]. This chronic inflammation in some cases primes the immune system to develop autoimmune arthritis [3,4]. Thus, this disease can be used as a model for elucidating the link between pathogen-induced inflammation and development of autoimmune diseases such as rheumatoid arthritis, systemic lupus erythematosus, multiple sclerosis, and type 1 diabetes [5-8].

The mouse model of Lyme arthritis is a powerful tool in elucidating the molecular and genetic mechanisms of pathological inflammation. Mice are natural hosts for the pathogen [9], disease pathology in mice is similar in many ways to human disease [10], and many immunological tools are available in the mouse model system, allowing for very sophisticated study of this disease [11]. Lyme disease research has yielded many important discoveries about inflammation, immune function, and host-pathogen interactions [12]. Building upon these previous discoveries, this thesis identifies novel

aspects of regulatory mechanisms involved in host immune response and arthritis development.

Cellular Sources of Type I Interferon in Lyme Arthritis

A robust type I IFN response early in infection with *B. burgdorferi* was initially identified in joints of arthritis-susceptible C3H mice by microarray analysis [13]. This led to the hypothesis that dysregulation of type I IFN early in infection contributes to increased Lyme arthritis later in infection. This hypothesis was tested by Miller et al. [14] using a neutralizing antibody targeting the type I interferon receptor (IFNAR), and confirmed using a knockout C3H IFNAR$^{-/-}$ mouse, shown in Chapter 2. These two experiments supported this hypothesis, directly linking preclinical dysregulation of type I interferon to severe arthritis later in infection.

Arthritic joint tissue is a complex array of many cell types, including immune cells such as macrophages, neutrophils, B cells, and T cells; as well as resident cells, including endothelial cells, fibroblasts, and chondrocytes. Many cell types are capable of producing and responding to type I IFN [15]. It was therefore important to identify the relevant cell types contributing to the pathological upregulation of the interferon expression profile. Because of the complex nature of joint tissue, identifying the relevant cell types *ex vivo* required development of novel methods of analysis. A system of isolating joint cells followed by cell sorting allowed for *ex vivo* analysis of various cell lineages. This method was utilized to show that (1) while both resident and hematopoietic cells from naïve mouse joints were capable of responding to *B. burgdorferi* stimulation, only hematopoietic cells were able to initiate a type I IFN response; and (2) endothelial cells and fibroblasts were primary contributors of the type I IFN response in infected mouse

joints. This highlights the importance of studying complex biological systems within the context of their cellular environment, and emphasizes the critical role of resident cells in immune function and disease pathogenesis. The clinical relevance of this finding is supported by a recent patient study suggesting that excessive endothelial cell activation and proliferation through production of ECGF can contribute to autoimmunity in many Lyme arthritis patients [4].

It has been known for over 35 years that lupus patients produce very high levels of type I IFN [16], which is produced by plasmacytoid dendritic cells responding to self nucleic acids through TLRs and other pathogen recognition receptors [17]. Furthermore, there are cases where individuals undergoing interferon treatment for hepatitis C have developed clinical systemic lupus erythematosus [18,19]. The strong connection between lupus and type I IFN has resulted in testing of potential anti-interferon pharmaceuticals as a therapeutic [20].

It has also recently been reported that children predisposed to type 1 diabetes exhibit a preclinical type I IFN signature prior to disease onset, but this signature is absent in patients with active disease [21]. Furthermore, this signature is likely the result of a heritable hyperactive type I IFN response to viral infection [22,23]. This is strikingly similar to our observations in C3H mice, which have a robust and transient preclinical type I IFN signature early in infection with *B. burgdorferi* [13], and contributes to disease severity, as shown in Chapter 2 and by Miller et al. [14]. Thus, elucidating the molecular mechanisms of the arthritogenic type I IFN response in the C3H mouse model of Lyme arthritis may provide critical insight into not only Lyme arthritis development, but lupus and type 1 diabetes as well.

MicroRNA-146a Is an Immune Modulator in Lyme Arthritis

Since their discovery, microRNAs have been shown to be important regulators of many cellular processes, including immune response to infection, inflammation, and autoimmunity [24]. Several microRNAs, including miR-146a and miR-155, have been shown to be upregulated through TLR-mediated NF-κB activation, and act as negative and positive regulators of inflammation, respectively [25,26]. These and other microRNAs are also associated with inflammatory and autoimmune diseases [27], suggesting that microRNAs play a role in disease pathogenesis. Because of this, it was reasonable to predict that microRNAs also played a role in regulating the immune response to *B. burgdorferi*.

As discussed in Chapter 3, expression analysis of microRNAs differentially expressed in joints of infected C3H, B6, and B6 IL10$^{-/-}$ mice revealed that a number of microRNAs were upregulated and downregulated in joints at 1 and 2 weeks postinfection. Of the over 600 microRNAs examined, only several dozen showed significant changes in expression during infection. Each mouse strain contained a unique set of microRNAs differentially expressed, as well as a small number of microRNAs whose expression profile was similar between two or more strains. Among those shared by all three strains was miR-146a, previously identified as an important negative regulator of NF-κB activation [28]. This microRNA was highly upregulated in all three strains, suggesting that it plays an important immune-modulatory role in response to *B. burgdorferi* infection.

MicroRNA-146a functions as an negative feedback regulator of NF-κB activation by suppressing translation of IRAK1 and TRAF6, proteins involved in TLR signaling

[25]. TLR-mediated activation of the innate immune response is critical in controlling *B. burgdorferi* infection [29], so it was not surprising to find that this important regulator was upregulated. It was unknown, however, whether this observation had functional relevance in the context of Lyme arthritis. Fortunately, a B6 miR-146a$^{-/-}$ mouse was available [30], so it was possible to ask whether arthritis-resistant mice lacking this negative NF-κB regulator would develop more severe arthritis, and if there would be an effect on host defense.

Upon infection, B6 mice lacking miR-146a develop more severe arthritis than wild-type B6 mice, and exhibit a hyperactive NF-κB response. Furthermore, these mice had modestly fewer numbers of bacteria in their joints, had similar *B. burgdorferi* numbers in heart and skin tissue, and had similar carditis compared to wild-type mice. This finding was significant for two reasons: first, it demonstrated that microRNA-mediated regulation was required for suppression of joint inflammation; second, this finding showed for the first time that hyperactive TLR/NF-κB activation led to increased arthritis severity. While this had long been suspected, it was difficult to show definitively, since mice lacking TLR2 or the adapter protein MyD88 have a severe host defense defect, contain extremely high numbers of bacteria in joints and other tissue, and still develop severe arthritis, despite having a defective pro-inflammatory TLR/MyD88/NF-κB signaling pathway [29,31]. In contrast, the B6 miR-146a$^{-/-}$ mouse had only a modest effect on host defense and increased the amplitude of this signaling pathway, thereby acting as a "fine tuner" of NF-κB activation [32]. The observation that these mice still develop severe arthritis shows that the amplitude of this signaling pathway is directly linked to pathological inflammation.

Another important finding in these studies was that B6 miR-146a$^{-/-}$ macrophages responded to *B. burgdorferi* stimulation in distinct ways. For example, peritoneal macrophages from B6 miR-146a$^{-/-}$ mice were more highly phagocytic than wild-type B6 peritoneal macrophages. This finding shows that miR-146a is involved in regulation of phagocytic activity, although the precise molecular mechanism remains unknown. Additionally, bone marrow-derived macrophages were refractory to treatment with the anti-inflammatory cytokine IL-10, and still produced high levels, compared to wild-type macrophages, of pro-inflammatory cytokines and chemokines after *B. burgdorferi* stimulation. This was likely due to significantly elevated protein levels of TRAF6, a protein important in TLR/NF-κB activation.

Roles of miR-155 and IL-10 in Host Response to *B. burgdorferi*

In addition to miR-146a, miR-155 was also identified in the microRNA microarray. Unlike miR-146a, however, this pro-inflammatory microRNA was exclusively upregulated in arthritic B6 IL10$^{-/-}$ mouse joints (Chapter 3). This finding suggests that IL-10 suppresses miR-155 expression in mouse joints, which was shown to occur in macrophages by McCoy et al. [33]. IL-10 is a key anti-inflammatory cytokine and is critical in limiting a wide range of inflammatory responses through downregulation of Th1 cytokines, inhibition of NF-κB activity, and suppression of M1 macrophage activity [34]. IL-10 is also an important regulator of Lyme arthritis severity in mice and humans [35,36]. In contrast to IL-10, miR-155 is a pro-inflammatory microRNA that targets several immune genes, including the transcription factor PU.1 and two negative regulators, SHIP1 and SOCS1, suppressors of AKT and IFN signaling, respectively [37]. Furthermore, miR-155 regulates myeloid cell, T-cell, and B-cell function [26,38-40], and

is critical in regulating hematopoiesis and autoimmunity [41,42]. Importantly, elevated miR-155 expression is associated with inflammatory diseases such as lupus [43] and rheumatoid arthritis [44].

There was reason to think that IL-10-mediated regulation of miR-155 was functionally relevant, since others have shown several opposing immune phenotypes in mice lacking either IL-10 or miR-155. For example, compared to wild-type B6 mice, B6 $IL10^{-/-}$ mice exhibit increased Lyme arthritis [45], have an arthritogenic IFNγ signature [35], develop severe lymphadenopathy and produce high levels of *B. burgdorferi*-specific antibodies [46], and have a dysregulated innate immune response, which contributes to increased arthritis severity and elevated bacterial clearance [46,47]. Also, administration of exogenous IL-10 limited collagen-induced arthritis progression in mice [48] (but not Lyme arthritis [49]). Conversely, B6 miR-$155^{-/-}$ mice have impaired B cell response and IgG class switching [39,40,50], reduced IFNγ production by T cells [42], and are protected from autoimmune arthritis [51]. However, no studies had been done to determine to what degree the immunosuppressive activity of IL-10 was due to its downregulation of the proinflammatory microRNA miR-155.

To test whether this IL-10-mediated miR-155 suppression affects host response to *B. burgdorferi* and Lyme arthritis development, a B6 $IL10^{-/-}$ miR-$155^{-/-}$ double knockout (DKO) mouse was generated (Appendix A). Using this mouse in the context of Lyme borreliosis, it was found that many, but not all, immune modulatory effects of IL-10 are dependent upon IL-10-mediated suppression of miR-155.

Upon infection, B6 $IL10^{-/-}$ miR-$155^{-/-}$ DKO mice had lower levels of *B. burgdorferi*-specific IgG than either B6 $IL10^{-/-}$ or wild-type B6 mice, and nearly

undetectable levels of the IgG1 isotype, consistent with previous observations in the B6 miR-155$^{-/-}$ mouse [39], suggesting that miR-155 is absolutely required for IgG1 production. Interestingly, while IL-10 deficiency resulted in elevated IgG2C isotype levels over wild-type, lack of miR-155 resulted in levels of IgG2C similar to wild-type, and DKO mice had IgG2C levels similar to both B6 and B6 miR-155$^{-/-}$ mice. These data show that miR-155 is not required for IgG2C class switching (in contrast to IgG1), and that IL-10-mediated regulation of miR-155 regulates IgG2C production.

This difference in IgG production and class switching, however, had no influence on arthritis severity or host defense. This is consistent with previous data showing IgG1 isotype production does not influence Lyme arthritis [52]. Whereas B6 and B6 miR-155$^{-/-}$ mice developed mild Lyme arthritis and had moderate numbers of spirochetes in joint tissue, B6 IL-10$^{-/-}$ and DKO mice developed severe arthritis while harboring very low numbers of bacteria. These data show that immune suppressor functions of IL-10 independent of miR-155 regulation were overwhelmingly responsible for increased arthritis severity and enhanced host defense. This was also seen for serum levels of IL-12, a cytokine involved in macrophage activation of T cells, which was significantly elevated in both strains lacking IL-10, but was not elevated in the two IL-10-sufficient strains. Similarly, the IFNγ profile was upregulated in both B6 IL10$^{-/-}$ and DKO mouse joint tissue, but not in B6 or B6 miR-155$^{-/-}$ mice. This was due in part to the complex cellular environment of the joint, since the IFN profile of macrophages stimulated with *B. burgdorferi* was largely dependent upon the presence of miR-155, and the enhanced upregulation of interferon-inducible genes such as *Cxcl9* and *Cxcl10* seen in IL10$^{-/-}$ macrophages returned to near wild-type levels in DKO macrophages. Also consistent

with a cell environment-dependent miR-155 effect on IFNγ, serum levels of IFNγ were somewhat reduced in the DKO mouse, compared to the B6 IL10$^{-/-}$ mouse, suggesting a role of miR-155 in systemic, but not localized IFN production. This also points to joint-localized IFNγ production, rather than systemic IFN levels, as being the arthritogenic IFN source. Overall, these data show that there are distinct and opposing roles of miR-155 and IL-10 in regulation of the innate and adaptive immune response to *B. burgdorferi* infection.

MicroRNAs in the Clinical Setting

These and other studies have clearly shown that microRNAs play a critical role in modulating numerous signaling pathways, and that defects in microRNA function often leads to disease [37]. Naturally, one may speculate that microRNA-based therapeutics may be an attractive new class of drugs. While there is some promise for use of miRNA-targeted therapy for HCV patients [53], large barriers exist for miRNA-based treatment, particularly in regards to microRNA delivery. Some progress has been made in the use of exosomes and macromolecules for cell- and tissue-specific microRNA delivery, and efforts are underway to develop novel methods of using both miRNA antagonists and miRNA mimics in a clinical setting [54-60].

Of more immediate clinical interest is the potential of microRNAs as a diagnostic tool [61]. Many microRNAs are secreted into the bloodstream, allowing for microRNA screening to be performed during routine blood testing, and abnormally high or low levels of certain microRNAs may be a molecular biomarker of dysregulated pathways [61]. In the case of Lyme arthritis, the microarray screen discussed in Chapter 3 showed that arthritis-susceptible C3H and B6 IL10$^{-/-}$ mice have very distinct microRNA

expression profiles, likely reflecting the different mechanisms of arthritis development between these two models. Many inflammatory diseases, including Lyme arthritis, are complex multifactorial disorders, and microRNA expression as a diagnostic tool could be used to quickly identify dysregulated pathways, leading to more personalized treatment.

Murine Lyme Arthritis as a Model for Inflammatory and Autoimmune Diseases

Chronic inflammation and dysregulation of TLR signaling can lead to severe inflammatory diseases such as systemic lupus erythematosus [62], rheumatoid arthritis [63-65], type 1 diabetes [66], and multiple sclerosis [67]. Autoimmune arthritis can also be driven by pathogenic gut microbiota [68]. There is increasing consensus in the field of autoimmunity that priming the immune response is a necessary stage in autoimmune development [5]. Also, as mentioned earlier, type I IFN is associated with several autoimmune diseases, such as lupus [16] and more recently, type 1 diabetes [21]. These autoimmune diseases all share similarities, in that there appears to be an innate immune trigger that sets the stage for clinical disease. Lyme arthritis is unique in that the trigger is a known pathogen [1] that is the causative agent of disease pathogenesis, thus fulfilling Koch's postulates [69]. Furthermore, mice are natural hosts of *B. burgdorferi,* which allows for study of host-pathogen interaction and disease progression within a natural environment.

Functional studies on the role of microRNAs in inflammatory diseases provide unique opportunities to examine the role of essential pathways in disease progression or resistance, where the "fine tuning" effect rendered by microRNAs can be used to model many complex diseases. Elucidating the role of TLR signaling in Lyme arthritis is a

perfect example. TLR2 and MyD88 knockout mice had severe defects in signaling which led to severely impaired host defense due to their essential role in immune response to pathogens [29,31]. While these findings shed valuable light on the necessity of TLR2 in host defense, the inability to decouple host defense and inflammation using these knockout systems made identifying the role of TLR signaling in arthritis development difficult. This difficulty was overcome using the B6 miR-146a$^{-/-}$ mouse model, which maintained a functional (albeit hyperactive) TLR signaling pathway, and therefore had no defect in host defense.

Many individuals contain polymorphisms in genes that render proteins (or microRNAs) slightly more or slightly less active, without ablating the protein's (or miR's) function completely, which is often lethal. These individuals may be at risk for developing certain diseases, if they are exposed to environmental triggers, such as a viral or bacterial infection. Individuals containing hypermorphic alleles of genes involved in NF-κB activation (or hypomorphic alleles of genes involved in NF-κB repression) would be expected to be phenotypically similar to the B6 miR-146a$^{-/-}$ mouse. Indeed, one study discussed previously has shown that individuals containing a certain polymorphism in TLR1 are susceptible to treatment-refractory Lyme arthritis [70]. These individuals have a cytokine expression profile that is in many ways similar to the profile seen in B6 miR-146a$^{-/-}$ mice. Another study showed that individuals who had low antibody titers after vaccination with OspA (a *B. burgdorferi* lipoprotein) also had low expression of TLR1 on the surface of macrophages [71]. Additionally, several studies have shown that polymorphisms in miR-146a targets IRAK1 [72,73], TRAF6 [74,75], miR-146a [76], and the miR-146a target sequence within the 3' UTR of IRAK1 [77] are associated with

susceptibility to rheumatic diseases. Since susceptibility to these diseases appears to share this common pathway, it is reasonable to suppose that B6 miR-146a$^{-/-}$ mice would also be more susceptible to models of these diseases as well. This is, in fact, the case. For example, in addition to developing more severe Lyme arthritis, B6 miR-146a$^{-/-}$ mice also develop more severe ankle swelling in the K/BxN serum transfer model of rheumatoid arthritis (Appendix C), and exogenous addition of miR-146a partially ameliorated arthritis symptoms in the collagen-induced arthritis mouse model [78]. Thus we see that microRNA knockout mice may be used as powerful tools for studying the mechanism of disease progression for many clinically relevant inflammatory and autoimmune diseases.

References

1. Burgdorfer W, Barbour AG, Hayes SF, Benach JL, Grunwaldt E, et al. (1982) Lyme disease-a tick-borne spirochetosis? Science 216: 1317-1319.

2. Steere AC, Schoen RT, Taylor E (1987) The clinical evolution of Lyme arthritis. Ann Intern Med 107: 725-731.

3. Drouin EE, Seward RJ, Strle K, McHugh G, Katchar K, et al. (2013) A novel human autoantigen, endothelial cell growth factor, is a target of T and B cell responses in patients with Lyme disease. Arthritis Rheum 65: 186-196.

4. Londono D, Cadavid D, Drouin EE, Strle K, McHugh G, et al. (2014) Antibodies to endothelial cell growth factor and obliterative microvascular lesions in synovia of patients with antibiotic-refractory Lyme arthritis. Arthritis Rheumatol.

5. Holmdahl R, Malmstrom V, Burkhardt H (2014) Autoimmune priming tissue attack and chronic inflammation - The three stages of rheumatoid arthritis. Eur J Immunol.

6. Cusick MF, Libbey JE, Fujinami RS (2013) Multiple sclerosis: autoimmunity and viruses. Curr Opin Rheumatol 25: 496-501.

7. Afonso G, Mallone R (2013) Infectious triggers in type 1 diabetes: is there a case for epitope mimicry? Diabetes Obes Metab 15 Suppl 3: 82-88.

8. Harley JB, Harley IT, Guthridge JM, James JA (2006) The curiously suspicious: a role for Epstein-Barr virus in lupus. Lupus 15: 768-777.

9. Tilly K, Rosa PA, Stewart PE (2008) Biology of infection with Borrelia burgdorferi. Infect Dis Clin North Am 22: 217-234, v.

10. Barthold SW, Persing DH, Armstrong AL, Peeples RA (1991) Kinetics of Borrelia burgdorferi dissemination and evolution of disease after intradermal inoculation of mice. Am J Pathol 139: 263-273.

11. Radolf JD, Caimano MJ, Stevenson B, Hu LT (2012) Of ticks, mice and men: understanding the dual-host lifestyle of Lyme disease spirochaetes. Nat Rev Microbiol 10: 87-99.

12. Weis JJ (2002) Host-pathogen interactions and the pathogenesis of murine Lyme disease. Curr Opin Rheumatol 14: 399-403.

13. Crandall H, Dunn DM, Ma Y, Wooten RM, Zachary JF, et al. (2006) Gene expression profiling reveals unique pathways associated with differential severity of lyme arthritis. J Immunol 177: 7930-7942.

14. Miller JC, Ma Y, Bian J, Sheehan KC, Zachary JF, et al. (2008) A critical role for type I IFN in arthritis development following Borrelia burgdorferi infection of mice. J Immunol 181: 8492-8503.

15. Trinchieri G (2010) Type I interferon: friend or foe? J Exp Med 207: 2053-2063.

16. Hooks JJ, Moutsopoulos HM, Geis SA, Stahl NI, Decker JL, et al. (1979) Immune interferon in the circulation of patients with autoimmune disease. N Engl J Med 301: 5-8.

17. Shrivastav M, Niewold TB (2013) Nucleic Acid Sensors and Type I Interferon Production in Systemic Lupus Erythematosus. Front Immunol 4: 319.

18. Niewold TB, Swedler WI (2005) Systemic lupus erythematosus arising during interferon-alpha therapy for cryoglobulinemic vasculitis associated with hepatitis C. Clin Rheumatol 24: 178-181.

19. Bockle BC, Baltaci M, Ratzinger G, Graziadei I, Vogel W, et al. (2012) Hepatitis C and autoimmunity: a therapeutic challenge. J Intern Med 271: 104-106.

20. Kirou KA, Gkrouzman E (2013) Anti-interferon alpha treatment in SLE. Clin Immunol 148: 303-312.

21. Ferreira RC, Guo H, Coulson RM, Smyth DJ, Pekalski ML, et al. (2014) A type I interferon transcriptional signature precedes autoimmunity in children genetically at-risk of type 1 diabetes. Diabetes.

22. Kayserova J, Vcelakova J, Stechova K, Dudkova E, Hromadkova H, et al. (2014) Decreased dendritic cell numbers but increased TLR9-mediated interferon-alpha production in first degree relatives of type 1 diabetes patients. Clin Immunol.

23. Boucas AP, de Oliveira Fdos S, Canani LH, Crispim D (2013) The role of interferon induced with helicase C domain 1 (IFIH1) in the development of type 1 diabetes mellitus. Arq Bras Endocrinol Metabol 57: 667-676.

24. O'Connell RM, Rao DS, Chaudhuri AA, Baltimore D (2010) Physiological and pathological roles for microRNAs in the immune system. Nat Rev Immunol 10: 111-122.

25. Taganov KD, Boldin MP, Chang KJ, Baltimore D (2006) NF-kappaB-dependent induction of microRNA miR-146, an inhibitor targeted to signaling proteins of innate immune responses. Proc Natl Acad Sci U S A 103: 12481-12486.

26. O'Connell RM, Taganov KD, Boldin MP, Cheng G, Baltimore D (2007) MicroRNA-155 is induced during the macrophage inflammatory response. Proc Natl Acad Sci U S A 104: 1604-1609.

27. Hu R, O'Connell RM (2013) MicroRNA control in the development of systemic autoimmunity. Arthritis Res Ther 15: 202.

28. Zhao JL, Rao DS, Boldin MP, Taganov KD, O'Connell RM, et al. (2011) NF-kappaB dysregulation in microRNA-146a-deficient mice drives the development of myeloid malignancies. Proc Natl Acad Sci U S A 108: 9184-9189.

29. Wooten RM, Ma Y, Yoder RA, Brown JP, Weis JH, et al. (2002) Toll-like receptor 2 is required for innate, but not acquired, host defense to Borrelia burgdorferi. J Immunol 168: 348-355.

30. Boldin MP, Taganov KD, Rao DS, Yang L, Zhao JL, et al. (2011) miR-146a is a significant brake on autoimmunity, myeloproliferation, and cancer in mice. J Exp Med 208: 1189-1201.

31. Bolz DD, Sundsbak RS, Ma Y, Akira S, Kirschning CJ, et al. (2004) MyD88 plays a unique role in host defense but not arthritis development in Lyme disease. J Immunol 173: 2003-2010.

32. O'Neill LA, Sheedy FJ, McCoy CE (2011) MicroRNAs: the fine-tuners of Toll-like receptor signalling. Nat Rev Immunol 11: 163-175.

33. McCoy CE, Sheedy FJ, Qualls JE, Doyle SL, Quinn SR, et al. (2010) IL-10 inhibits miR-155 induction by toll-like receptors. J Biol Chem 285: 20492-20498.

34. Hofmann SR, Rosen-Wolff A, Tsokos GC, Hedrich CM (2012) Biological properties and regulation of IL-10 related cytokines and their contribution to autoimmune disease and tissue injury. Clin Immunol 143: 116-127.

35. Sonderegger FL, Ma Y, Maylor-Hagan H, Brewster J, Huang X, et al. (2012) Localized production of IL-10 suppresses early inflammatory cell infiltration and subsequent development of IFN-gamma-mediated Lyme arthritis. J Immunol 188: 1381-1393.

36. Vudattu NK, Strle K, Steere AC, Drouin EE (2013) Dysregulation of CD4+CD25(high) T cells in the synovial fluid of patients with antibiotic-refractory Lyme arthritis. Arthritis Rheum 65: 1643-1653.

37. O'Connell RM, Rao DS, Baltimore D (2012) microRNA regulation of inflammatory responses. Annu Rev Immunol 30: 295-312.

38. Hu R, Huffaker TB, Kagele DA, Runtsch MC, Bake E, et al. (2013) MicroRNA-155 confers encephalogenic potential to Th17 cells by promoting effector gene expression. J Immunol 190: 5972-5980.

39. Vigorito E, Perks KL, Abreu-Goodger C, Bunting S, Xiang Z, et al. (2007) microRNA-155 regulates the generation of immunoglobulin class-switched plasma cells. Immunity 27: 847-859.

40. Rodriguez A, Vigorito E, Clare S, Warren MV, Couttet P, et al. (2007) Requirement of bic/microRNA-155 for normal immune function. Science 316: 608-611.

41. O'Connell RM, Rao DS, Chaudhuri AA, Boldin MP, Taganov KD, et al. (2008) Sustained expression of microRNA-155 in hematopoietic stem cells causes a myeloproliferative disorder. J Exp Med 205: 585-594.

42. O'Connell RM, Kahn D, Gibson WS, Round JL, Scholz RL, et al. (2010) MicroRNA-155 promotes autoimmune inflammation by enhancing inflammatory T cell development. Immunity 33: 607-619.

43. Wang H, Peng W, Ouyang X, Li W, Dai Y (2012) Circulating microRNAs as candidate biomarkers in patients with systemic lupus erythematosus. Transl Res 160: 198-206.

44. Stanczyk J, Pedrioli DM, Brentano F, Sanchez-Pernaute O, Kolling C, et al. (2008) Altered expression of MicroRNA in synovial fibroblasts and synovial tissue in rheumatoid arthritis. Arthritis Rheum 58: 1001-1009.

45. Brown JP, Zachary JF, Teuscher C, Weis JJ, Wooten RM (1999) Dual role of interleukin-10 in murine Lyme disease: regulation of arthritis severity and host defense. Infect Immun 67: 5142-5150.

46. Lazarus JJ, Meadows MJ, Lintner RE, Wooten RM (2006) IL-10 deficiency promotes increased Borrelia burgdorferi clearance predominantly through enhanced innate immune responses. J Immunol 177: 7076-7085.

47. Murthy PK, Dennis VA, Lasater BL, Philipp MT (2000) Interleukin-10 modulates proinflammatory cytokines in the human monocytic cell line THP-1 stimulated with Borrelia burgdorferi lipoproteins. Infect Immun 68: 6663-6669.

48. Walmsley M, Katsikis PD, Abney E, Parry S, Williams RO, et al. (1996) Interleukin-10 inhibition of the progression of established collagen-induced arthritis. Arthritis Rheum 39: 495-503.

49. Brown CR, Lai AY, Callen ST, Blaho VA, Hughes JM, et al. (2008) Adenoviral delivery of interleukin-10 fails to attenuate experimental Lyme disease. Infect Immun 76: 5500-5507.

50. Thai TH, Calado DP, Casola S, Ansel KM, Xiao C, et al. (2007) Regulation of the germinal center response by microRNA-155. Science 316: 604-608.

51. Bluml S, Bonelli M, Niederreiter B, Puchner A, Mayr G, et al. (2011) Essential role of microRNA-155 in the pathogenesis of autoimmune arthritis in mice. Arthritis Rheum 63: 1281-1288.

52. Potter MR, Noben-Trauth N, Weis JH, Teuscher C, Weis JJ (2000) Interleukin-4 (IL-4) and IL-13 signaling pathways do not regulate Borrelia burgdorferi-induced arthritis in mice: IgG1 is not required for host control of tissue spirochetes. Infect Immun 68: 5603-5609.

53. Janssen HL, Reesink HW, Lawitz EJ, Zeuzem S, Rodriguez-Torres M, et al. (2013) Treatment of HCV infection by targeting microRNA. N Engl J Med 368: 1685-1694.

54. Hatakeyama H, Murata M, Sato Y, Takahashi M, Minakawa N, et al. (2014) The systemic administration of an anti-miRNA oligonucleotide encapsulated pH-sensitive liposome results in reduced level of hepatic microRNA-122 in mice. J Control Release 173: 43-50.

55. Monaghan M, Browne S, Schenke-Layland K, Pandit A (2014) A Collagen-based Scaffold Delivering Exogenous MicroRNA-29B to Modulate Extracellular Matrix Remodeling. Mol Ther 22: 786-796.

56. Gill SL, O'Neill H, McCoy RJ, Logeswaran S, O'Brien F, et al. (2014) Enhanced delivery of microRNA mimics to cardiomyocytes using ultrasound responsive microbubbles reverses hypertrophy in an in-vitro model. Technol Health Care.

57. Leslie M (2013) Cell Biology. NIH effort gambles on mysterious extracellular RNAs. Science 341: 947.

58. Burnett JC, Rossi JJ (2012) RNA-based therapeutics: current progress and future prospects. Chem Biol 19: 60-71.

59. Wang YZ, Tian FF, Yan M, Zhang JM, Liu Q, et al. (2014) Delivery of an miR155 inhibitor by anti-CD20 single-chain antibody into B cells reduces the acetylcholine receptor-specific autoantibodies and ameliorates experimental autoimmune myasthenia gravis. Clin Exp Immunol 176: 207-221.

60. Momen-Heravi F, Bala S, Bukong T, Szabo G (2014) Exosome-mediated delivery of functionally active miRNA-155 inhibitor to macrophages. Nanomedicine.

61. Hydbring P, Badalian-Very G (2013) Clinical applications of microRNAs. F1000Res 2: 136.

62. Theofilopoulos AN (2012) TLRs and IFNs: critical pieces of the autoimmunity puzzle. J Clin Invest 122: 3464-3466.

63. Saal JG, Krimmel M, Steidle M, Gerneth F, Wagner S, et al. (1999) Synovial Epstein-Barr virus infection increases the risk of rheumatoid arthritis in individuals with the shared HLA-DR4 epitope. Arthritis Rheum 42: 1485-1496.

64. Saal JG, Steidle M, Einsele H, Muller CA, Fritz P, et al. (1992) Persistence of B19 parvovirus in synovial membranes of patients with rheumatoid arthritis. Rheumatol Int 12: 147-151.

65. Thwaites R, Chamberlain G, Sacre S (2014) Emerging Role of Endosomal Toll-Like Receptors in Rheumatoid Arthritis. Front Immunol 5: 1.

66. Park Y, Park S, Yoo E, Kim D, Shin H (2004) Association of the polymorphism for Toll-like receptor 2 with type 1 diabetes susceptibility. Ann N Y Acad Sci 1037: 170-174.

67. Serafini B, Rosicarelli B, Franciotta D, Magliozzi R, Reynolds R, et al. (2007) Dysregulated Epstein-Barr virus infection in the multiple sclerosis brain. J Exp Med 204: 2899-2912.

68. Wu HJ, Ivanov, II, Darce J, Hattori K, Shima T, et al. (2010) Gut-residing segmented filamentous bacteria drive autoimmune arthritis via T helper 17 cells. Immunity 32: 815-827.

69. Wasmoen TL, Sebring RW, Blumer BM, Chavez LG, Jr., Chu HJ, et al. (1992) Examination of Koch's postulates for Borrelia burgdorferi as the causative agent of limb/joint dysfunction in dogs with borreliosis. J Am Vet Med Assoc 201: 412-418.

70. Strle K, Shin JJ, Glickstein LJ, Steere AC (2012) Association of a Toll-like receptor 1 polymorphism with heightened Th1 inflammatory responses and antibiotic-refractory Lyme arthritis. Arthritis Rheum 64: 1497-1507.

71. Alexopoulou L, Thomas V, Schnare M, Lobet Y, Anguita J, et al. (2002) Hyporesponsiveness to vaccination with Borrelia burgdorferi OspA in humans and in TLR1- and TLR2-deficient mice. Nat Med 8: 878-884.

72. Han TU, Cho SK, Kim T, Joo YB, Bae SC, et al. (2013) Association of an activity-enhancing variant of IRAK1 and an MECP2-IRAK1 haplotype with increased susceptibility to rheumatoid arthritis. Arthritis Rheum 65: 590-598.

73. Kaufman KM, Zhao J, Kelly JA, Hughes T, Adler A, et al. (2013) Fine mapping of Xq28: both MECP2 and IRAK1 contribute to risk for systemic lupus erythematosus in multiple ancestral groups. Ann Rheum Dis 72: 437-444.

74. Raychaudhuri S, Thomson BP, Remmers EF, Eyre S, Hinks A, et al. (2009) Genetic variants at CD28, PRDM1 and CD2/CD58 are associated with rheumatoid arthritis risk. Nat Genet 41: 1313-1318.

75. Namjou B, Choi CB, Harley IT, Alarcon-Riquelme ME, Network B, et al. (2012) Evaluation of TRAF6 in a large multiancestral lupus cohort. Arthritis Rheum 64: 1960-1969.

76. Luo X, Yang W, Ye DQ, Cui H, Zhang Y, et al. (2011) A functional variant in microRNA-146a promoter modulates its expression and confers disease risk for systemic lupus erythematosus. PLoS Genet 7: e1002128.

77. Chatzikyriakidou A, Voulgari PV, Georgiou I, Drosos AA (2010) The role of microRNA-146a (miR-146a) and its target IL-1R-associated kinase (IRAK1) in psoriatic arthritis susceptibility. Scand J Immunol 71: 382-385.

78. Nakasa T, Shibuya H, Nagata Y, Niimoto T, Ochi M (2011) The inhibitory effect of microRNA-146a expression on bone destruction in collagen-induced arthritis. Arthritis Rheum 63: 1582-1590.

APPENDIX A

ROLE OF MICRORNA-155 REGULATION BY IL-10 DURING INNATE AND ADAPTIVE IMMUNE RESPONSE TO *BORRELIA BURGDORFERI* AND LYME ARTHRITIS DEVELOPMENT

Figure A.1. Generation of B6 IL10$^{-/-}$ miR-155$^{-/-}$ double knockout mouse. B6 IL10$^{-/-}$ and B6 miR-155$^{-/-}$ mice (generously provided by Dr. Ryan O'Connell) were mated to create a IL10$^{-/-}$ miR-155$^{-/-}$ double knockout (DKO) on the B6 background. Shown is an agarose gel loaded with PCR product using primers specific for wild-type (WT) and knockout (KO) copies of miR-155/*Bic* (top) and *Il10* (bottom), with predicted product size indicated on left. First two lanes are from IL10$^{-/-}$ or miR-155$^{-/-}$ single knockout mice as controls. Third and last lanes are from the founder DKO female and male, respectively. Other lanes (4-8) are from litter of DKO founders.

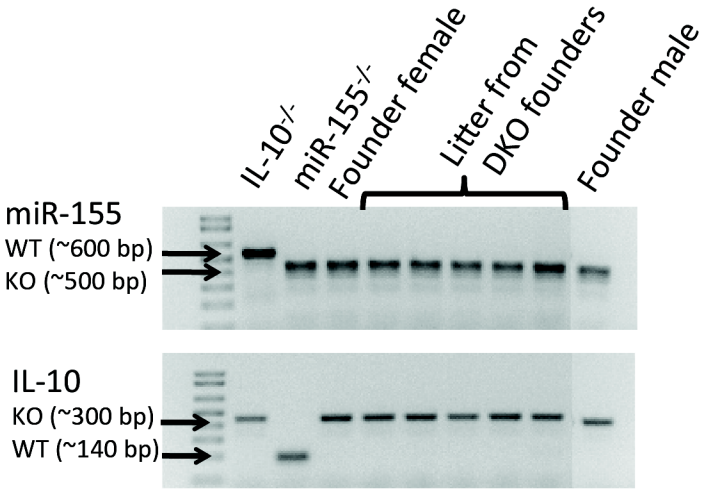
IL-10-/-
miR-155-/-
Founder female
Litter from DKO founders
Founder male
miR-155
WT (~600 bp)
KO (~500 bp)
IL-10
KO (~300 bp)
WT (~140 bp)

Figure A.2. Effect of mR-155 on arthritis, host defense, and IFNγ response following a 4-week infection with *B. burgdorferi.* (A) Rear ankles were measured in a blinded fashion before and after 4 weeks postinfection, and change in ankle measurement is shown for B6, miR-155$^{-/-}$, IL10$^{-/-}$, and IL10$^{-/-}$ miR-155$^{-/-}$ DKO mice bacterial burden (B) and IFNγ profile (C, represented by *Ifng* and *Cxcl10*) in joint tissue was assessed by qRT-PCR analysis of *B. burgdorferi 16SrRNA* in joints, normalized to *βactin.* (D) Serum levels of IFNγ and IL-12 were measured by ELISA in the 4 strains indicated. Statistical significant difference between groups was determined by ANOVA followed by Tukey's post-hoc analysis (* $p<0.05$, $n \geq 7$ mice per group).

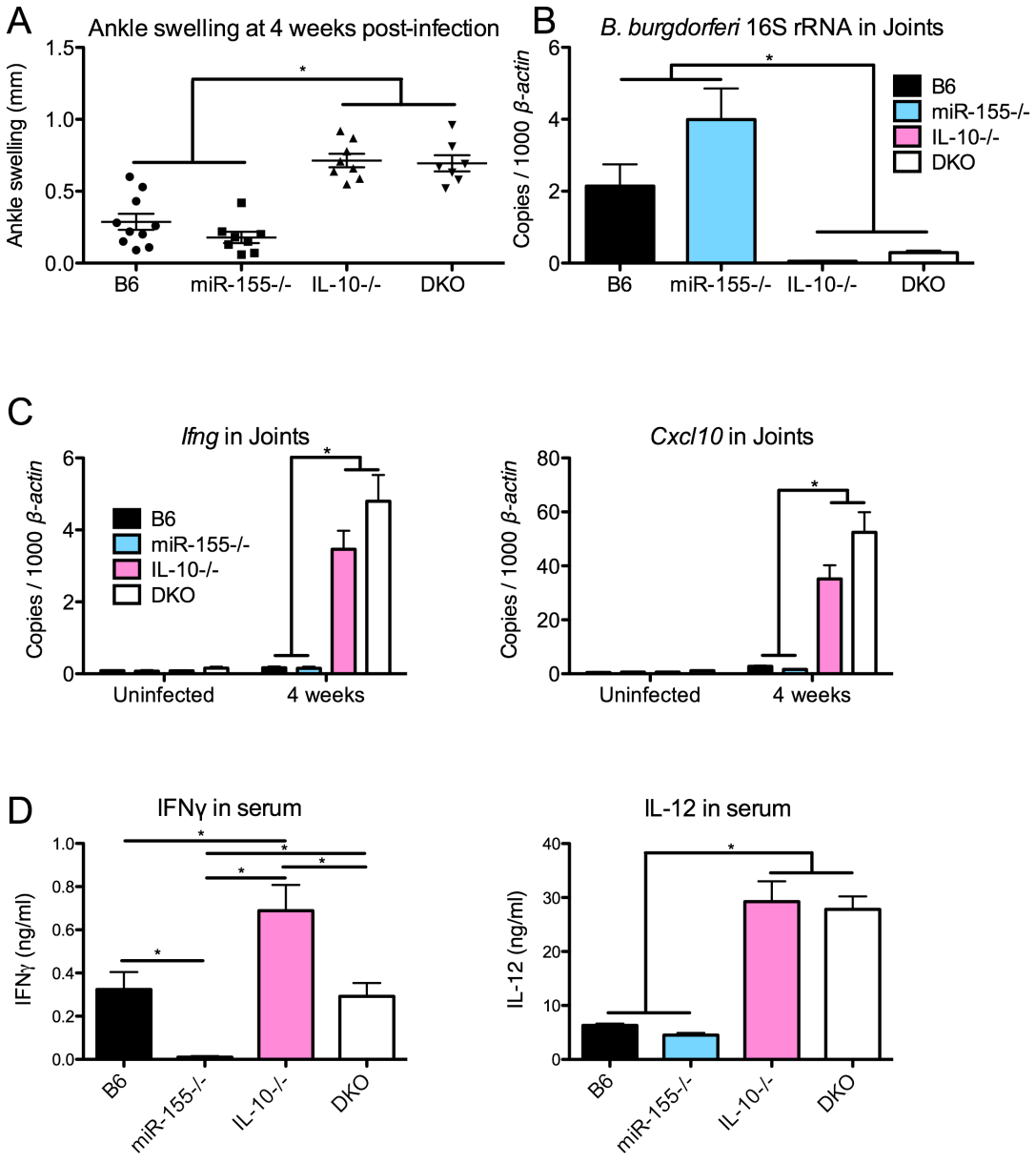
A
Ankle swelling at 4 weeks post-infection
Ankle swelling (mm)
1.5
1.0
0.5
0.0
*
B6
miR-155-/-
IL-10-/-
DKO
B
B. burgdorferi 16S rRNA in Joints
Copies / 1000 β-actin
6
4
2
0
*
B6
miR-155-/-
IL-10-/-
DKO
C
Ifng in Joints
Copies / 1000 β-actin
6
4
2
0
*
B6
miR-155-/-
IL-10-/-
DKO
Uninfected
4 weeks
Cxcl10 in Joints
Copies / 1000 β-actin
80
60
40
20
0
*
Uninfected
4 weeks
D
IFNγ in serum
IFNγ (ng/ml)
1.0
0.8
0.6
0.4
0.2
0.0
*
*
*
*
*
B6
miR-155-/-
IL-10-/-
DKO
IL-12 in serum
IL-12 (ng/ml)
40
30
20
10
0
*
B6
miR-155-/-
IL-10-/-
DKO

Figure A.3. Antibody response to *B. burgdorferi* is negatively regulated by IL-10 and positively regulated by miR-155 at 4 weeks postinfection, and miR-155 is required for IgG1 isotype switching. *B. burgdorferi*-specific antibody levels were measured by ELISA in 2-fold serial dilutions in sera collected from B6 (black circles), B6 miR-155$^{-/-}$ (blue squares), B6 IL10$^{-/-}$ (pink triangles), and DKO (gray diamonds) mice infected for 4 weeks. Total IgG, IgM, IgG1, IgG2c, and IgG3 were measured (n=≥7 mice per strain).

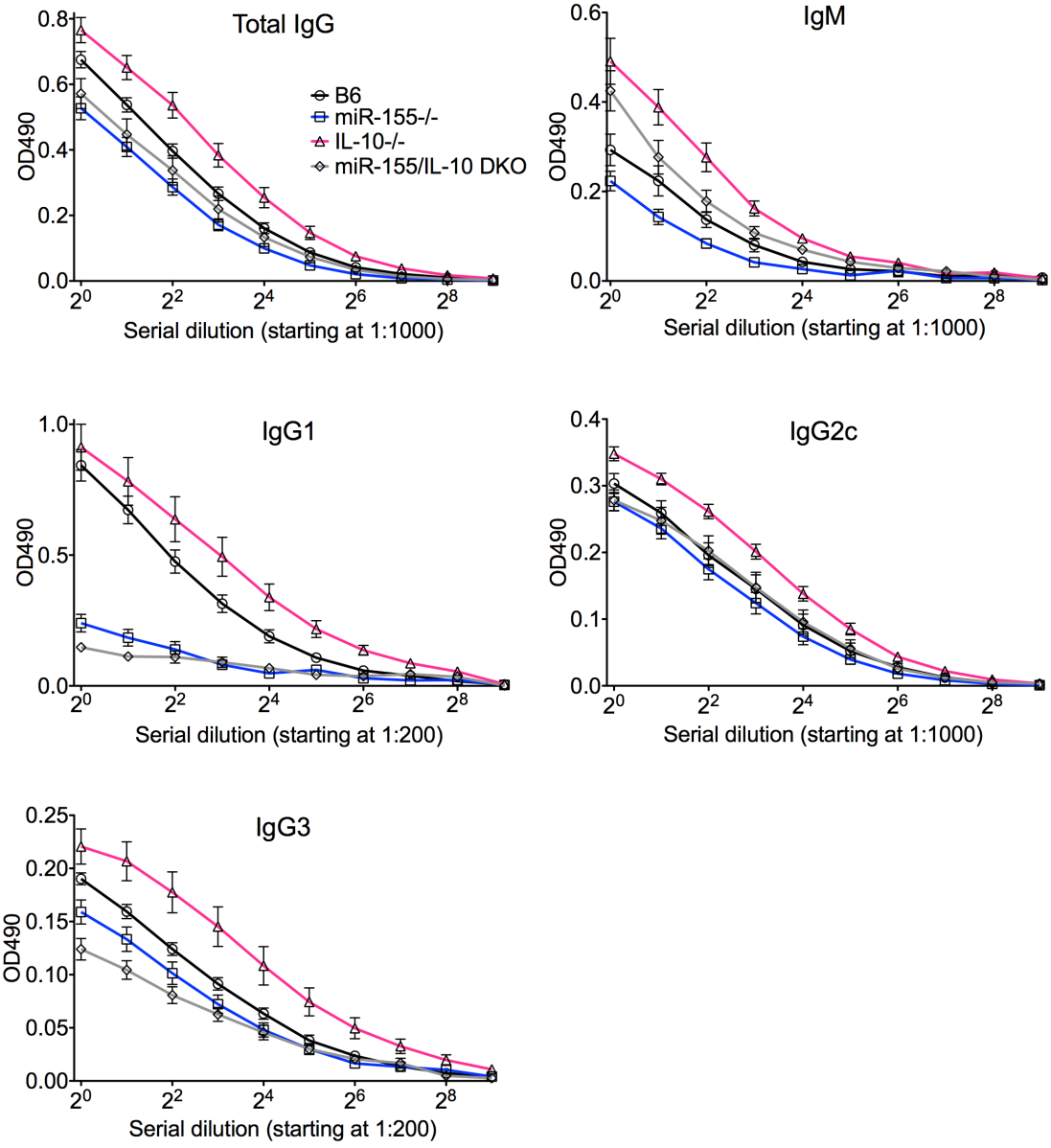
Total IgG
B6
miR-155-/-
IL-10-/-
miR-155/IL-10 DKO
OD490
Serial dilution (starting at 1:1000)
IgM
OD490
Serial dilution (starting at 1:1000)
IgG1
OD490
Serial dilution (starting at 1:200)
IgG2c
OD490
Serial dilution (starting at 1:1000)
IgG3
OD490
Serial dilution (starting at 1:200)

Figure A.4. Macrophage *B. burgdorferi*-induced cytokine production and IFNγ profile are negatively regulated by IL-10 and positively regulated by miR-155. Bone marrow-derived macrophages were cultured from B6, B6 miR-155$^{-/-}$, B6 IL10$^{-/-}$, and DKO mice, and were stimulated with *B. burgdorferi* for 24 hours (MOI 10:1). (A) Supernatant was collected and IL-10, IL-1β, IL-6, and IL-12 cytokine levels were measured by ELISA. (B) RNA was extracted from cells and transcripts quantified by qRT-PCR. Shown are transcripts levels of miR-155, *Tnfa, Cxcl9,* and *Cxcl10*. Statistical significant difference between groups was determined by ANOVA followed by Tukey's post-hoc analysis (*$p<0.05$, n=3 per strain, n.d.=none detected).

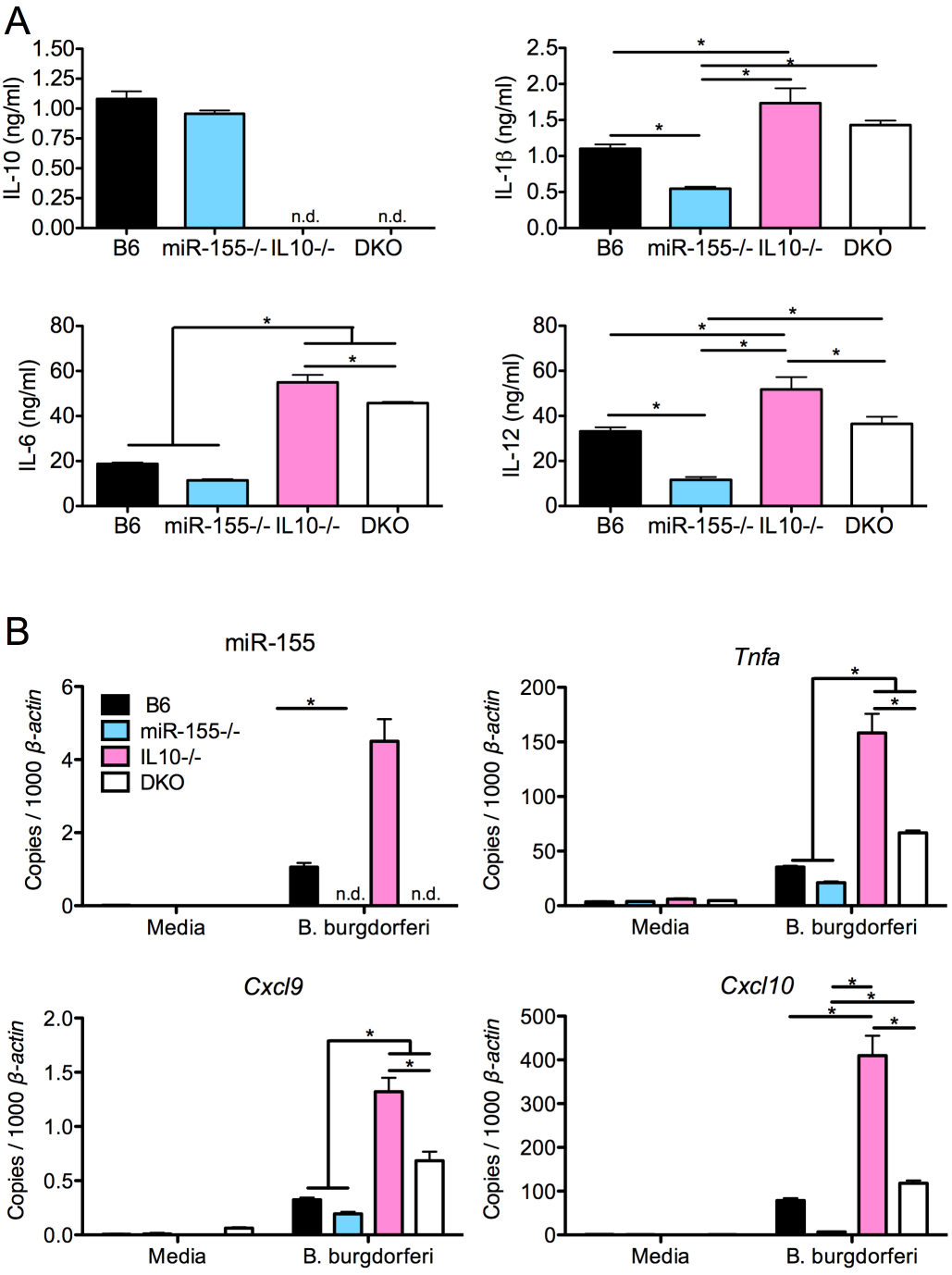
A
IL-10 (ng/ml)
1.50
1.25
1.00
0.75
0.50
0.25
0.00
n.d.
n.d.
B6
miR-155-/-
IL10-/-
DKO
IL-1β (ng/ml)
2.5
2.0
1.5
1.0
0.5
0.0
IL-6 (ng/ml)
80
60
40
20
0
IL-12 (ng/ml)
B
miR-155
B6
miR-155-/-
IL10-/-
DKO
Copies / 1000 β-actin
6
4
2
0
Media
B. burgdorferi
Tnfa
200
150
100
50
Cxcl9
2.0
1.5
1.0
0.5
Cxcl10
500
400
300

Figure A.5. B cells from draining lymph nodes are major producers of IFNγ when stimulated with *B. burgdorferi*, which is independent of IL-10 and miR-155. Inguinal and popliteal lymph nodes were collected from B6, B6 miR-155$^{-/-}$, B6 IL10$^{-/-}$, and DKO mice and cells were stimulated with *B. burgorferi in vitro* (MOI 10:1). At 3 and 5 days poststimulation, cytokine production was measured in cells by intracellular cytokine staining followed by flow cytometry. Shown is mean fluorescence intensity for IFNγ and TNFα in B220+ cells (n=3 per group).

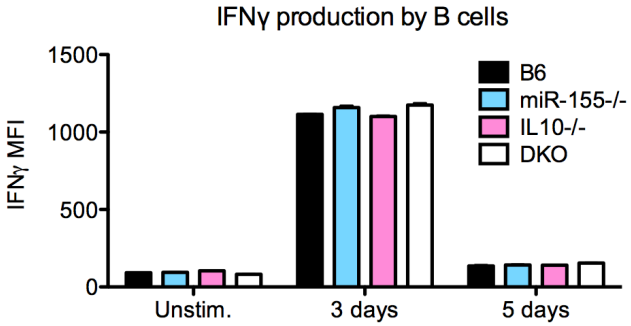
IFNγ production by B cells
IFNγ MFI
1500
1000
500
0
Unstim.
3 days
5 days
B6
miR-155-/-
IL10-/-
DKO

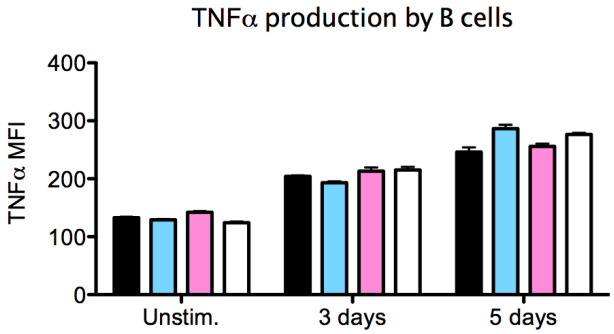
TNFα production by B cells
TNFα MFI
400
300
200
100
0
Unstim.
3 days
5 days

APPENDIX B

EFFECT OF IL-10 ON T AND B CELL PROLIFERATION IN LYMPH NODES, AND IMPACT OF ANTIBIOTIC TREATMENT ON ARTHRITIS, IFNγ RESPONSE, AND T CELL ACTIVATION

Figure B.1. B6 IL10$^{-/-}$ mice contain greater numbers of B and T cells in draining lymph nodes than wild-type B6 mice after infection with *B. burgdorferi* for 4 weeks. Inguinal and popliteal lymph nodes were collected from B6 and B6 IL10$^{-/-}$ mice infected with *B. burgdorferi* for 4 weeks and analyzed by FACS. (A) Representative FACS plot of CD4+ T cells labeled with T cell activation markers CD44 (y-axis) and CD62L (x-axis). Top row are cells from uninfected B6 and IL10$^{-/-}$ mice, and bottom row are cells from B6 and IL10$^{-/-}$ mice infected for 4 weeks. (B) Total cells collected from uninfected and infected B6 and IL10$^{-/-}$ lymph nodes, categorized by B220+ (B cells), B220+ CD62Llo (activated B cells), CD4+ T cells, CD4+ CD62Llo CD44hi (activated CD4+ T cells), and CD8+ T cells. Statistical significant difference between groups was determined by ANOVA followed by Tukey's post-hoc analysis (*$p<0.05$, n=3 mice for each group, representative of 2 independent experiments).

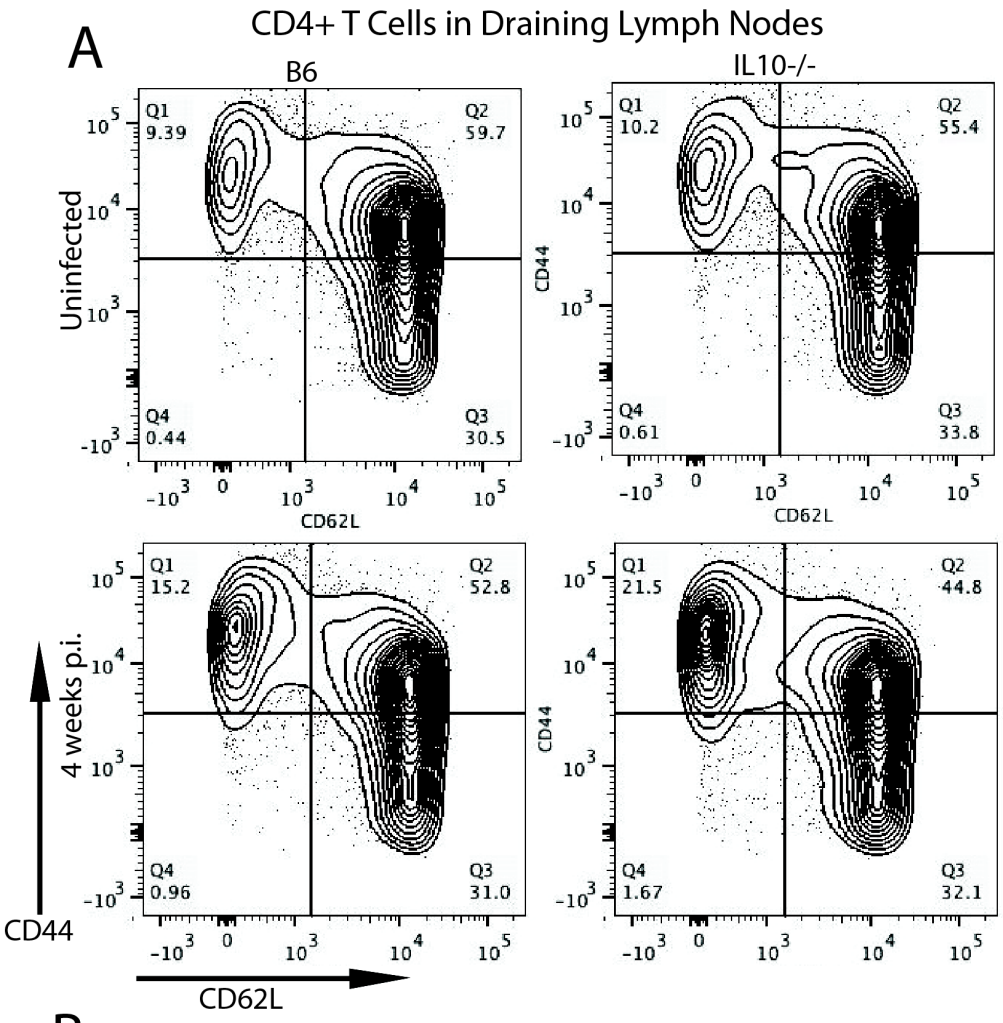
A
CD4+ T Cells in Draining Lymph Nodes
B6
IL10-/-
Uninfected
4 weeks p.i.
CD44
CD62L
Q1 9.39
Q2 59.7
Q4 0.44
Q3 30.5
Q1 10.2
Q2 55.4
Q4 0.61
Q3 33.8
Q1 15.2
Q2 52.8
Q4 0.96
Q3 31.0
Q1 21.5
Q2 44.8
Q4 1.67
Q3 32.1

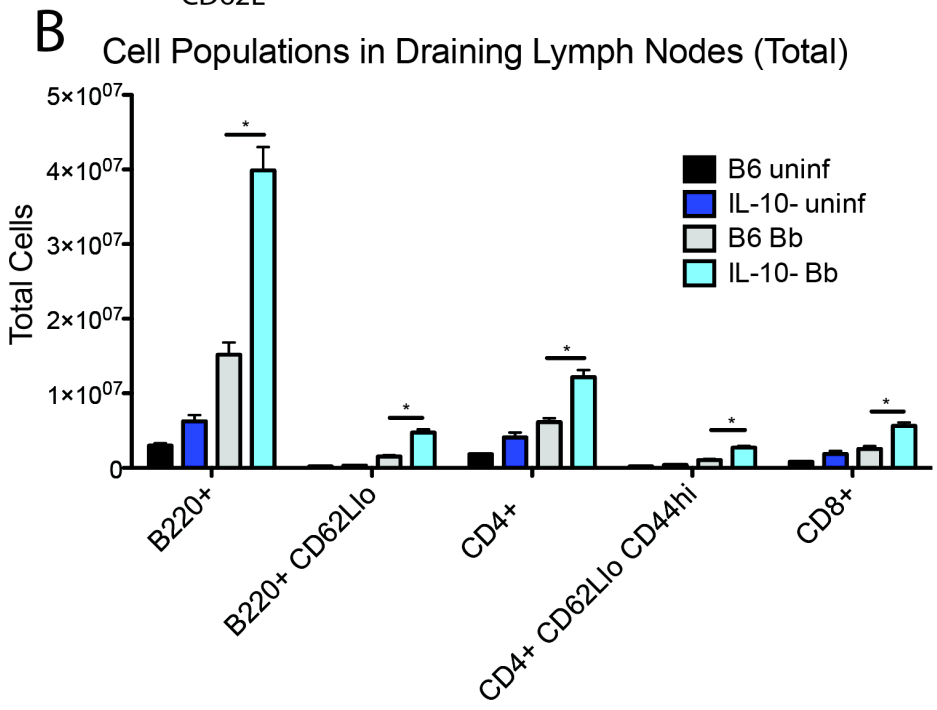
B
Cell Populations in Draining Lymph Nodes (Total)
Total Cells
B6 uninf
IL-10- uninf
B6 Bb
IL-10- Bb
B220+
B220+ CD62Llo
CD4+
CD4+ CD62Llo CD44hi
CD8+

Figure B.2. Effect of antibiotic treatment on arthritis severity, IFNγ profile, and T cell activation in B6 IL10$^{-/-}$ mice. (A) B6 IL10$^{-/-}$ mice were infected with *B. burgdorferi* for 3 weeks followed by daily administration of ceftriaxone (or PBS) by i.p. injection for 4 weeks. Mice were assessed for arthritis, *Ifng* expression, and T cell activation at 9 weeks postinfection. (B) Arthritis was assessed by ankle measurement. *Ifng* expression was measured by qRT-PCR in joint, back skin (site of inoculation), and ankle skin in mice with or without ceftriaxone treatment at 3 and 9 weeks postinfection (+ BSK negative controls). Statistical significant difference between groups was determined by ANOVA followed by Tukey's post-hoc analysis (*$p<0.05$, ***$p<0.001$, $n\geq5$ mice per group). (C) Representative FACS plot of CD4+ (top) and CD8+ (bottom) T cells labeled with T cell activation markers CD44 (y-axis) and CD62L (x-axis) from uninfected, infected (no antibiotic treatment), and infected + antibiotic treated mouse inguinal and popliteal lymph nodes collected at 9 weeks postinfection. Representative of at least 5 mice per group.

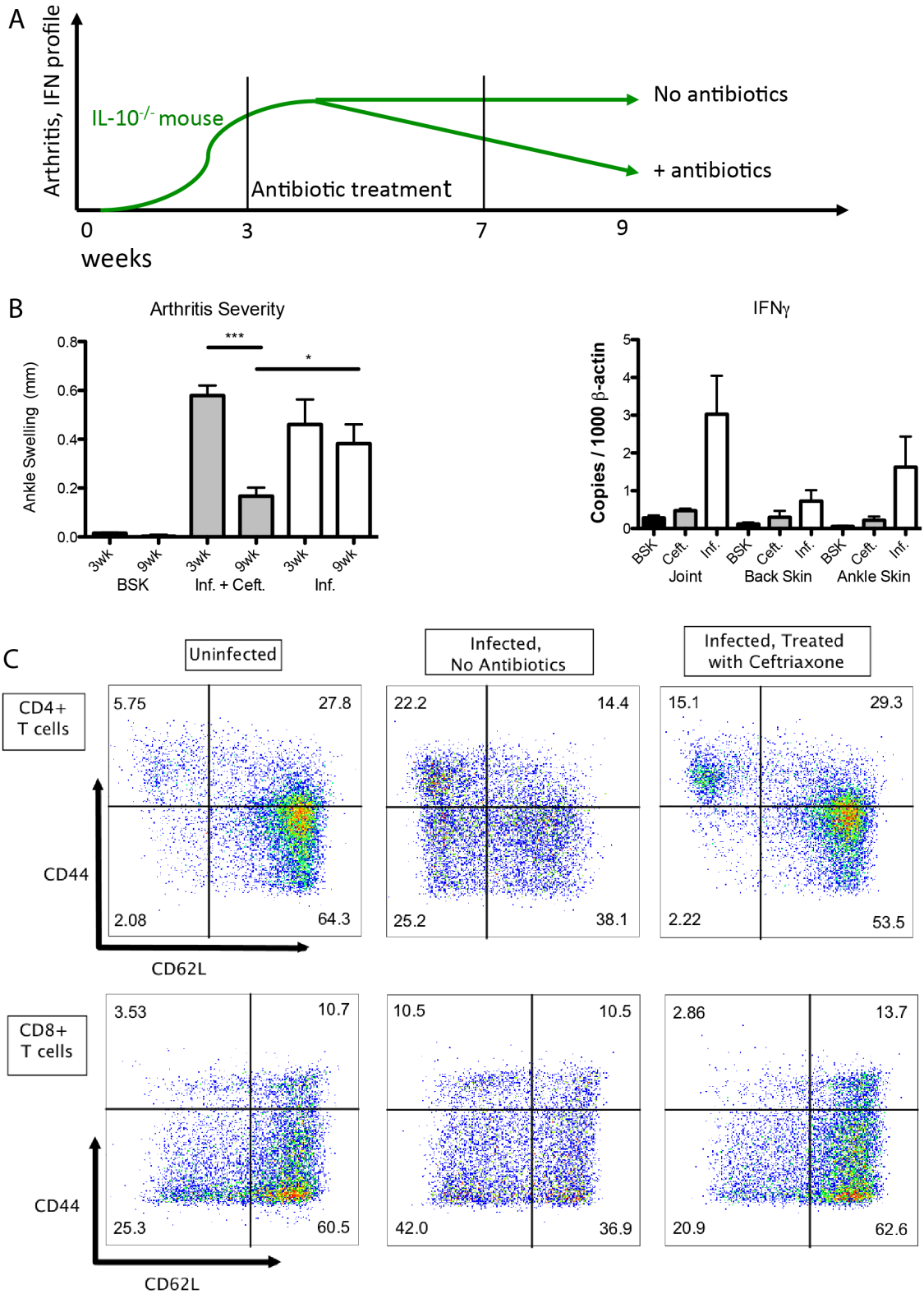
A
Arthritis, IFN profile
IL-10-/- mouse
No antibiotics
+ antibiotics
Antibiotic treatment
0
3
7
9
weeks
B
Arthritis Severity
Ankle Swelling (mm)
***
*
3wk
9wk
BSK
Inf. + Ceft.
Inf.
IFNγ
Copies / 1000 β-actin
BSK
Ceft.
Inf.
Joint
Back Skin
Ankle Skin
C
Uninfected
Infected, No Antibiotics
Infected, Treated with Ceftriaxone
CD4+ T cells
CD8+ T cells
CD44
CD62L
5.75
27.8
2.08
64.3
22.2
14.4
25.2
38.1
15.1
29.3
2.22
53.5
3.53
10.7
25.3
60.5
10.5
10.5
42.0
36.9
2.86
13.7
20.9
62.6

APPENDIX C

EFFECT OF MICRORNA-146a ON ARTHRITIS IN THE K/BxN SERUM TRANSFER MODEL OF RHEUMATOID ARTHRITIS

Figure C.1. B6 miR-146a$^{-/-}$ mice have increased K/BxN serum-induced arthritis. B6 and B6 miR-146a$^{-/-}$ mice were administered 2 doses (day 0 and day 2) of 100 µl K/BxN serum by i.p. injection. Ankle swelling and histopathology scoring was determined at day 7 following administration of first dose. Statistical significant difference in ankle swelling was determined by ANOVA followed by Tukey's post-hoc analysis (*$p<0.05$, n=10 mice per group). Increased trend in histopathology score was not statistically significant between groups by Mann-Whitney u-test (cutoff p value=0.05).

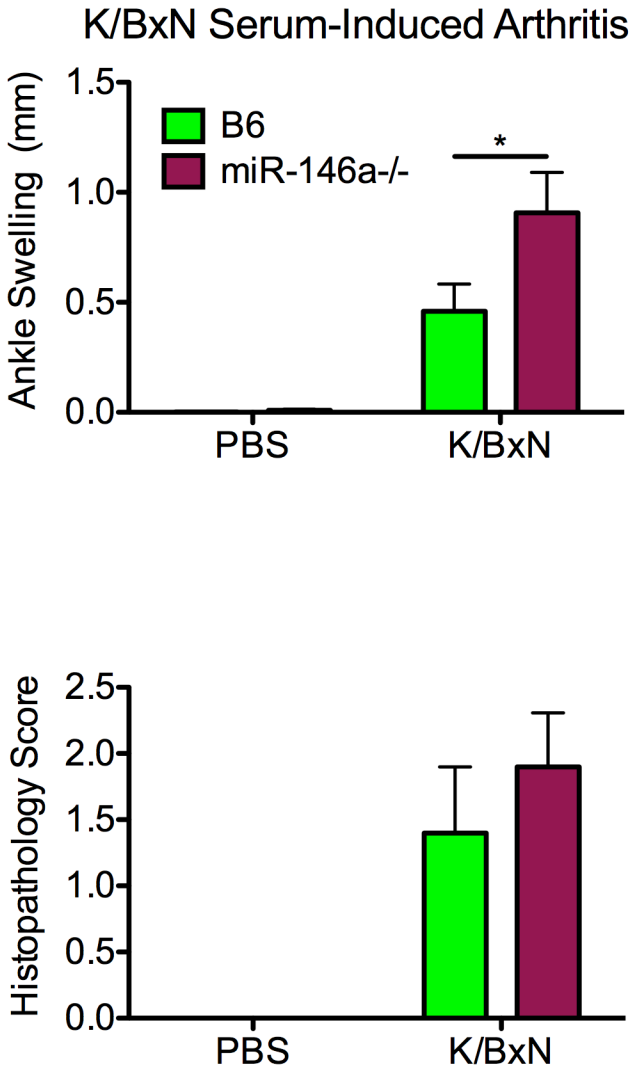
K/BxN Serum-Induced Arthritis
Ankle Swelling (mm)
1.5
1.0
0.5
0.0
B6
miR-146a-/-
*
PBS
K/BxN
Histopathology Score
2.5
2.0
1.5
1.0
0.5
0.0
PBS
K/BxN